






Organocatalysis with carbon nitrides

Sujanya Maria Ruban ^a, Kavitha Ramadass ^a, Gurwinder Singh ^a, Siddulu Naidu Talapaneni ^b,
Gunda Kamalakar ^{c*}, Chandrakanth Rajanna Gadipelly ^d, Lakshmi Kantham Mannepalli ^e,
Yoshihiro Sugi ^{a,f} and Ajayan Vinu ^a

^aGlobal Innovative Centre for Advanced Nanomaterials (GICAN), College of Engineering, Science and Environment (CESE), School of Engineering, The University of Newcastle, Callaghan, Australia;

^bSchool of Chemical Engineering, University of New South Wales, Sydney, NSW, Australia;

^cDepartment of Chemical Engineering, University of Waterloo, Waterloo, Ontario, Canada;

^dFlow Chemistry Division, Amar Equipment Pvt. Ltd, Mumbai, India;

^eDepartment of Chemical Engineering, Institute of Chemical Technology, Mumbai, India;

^fFaculty of Engineering, Gifu University, Gifu, Japan

ABSTRACT

Carbon nitrides, a distinguished class of metal-free catalytic materials, have presented a good potential for chemical transformations and are expected to become prominent materials for organocatalysis. This is largely possible due to their low cost, exceptional thermal and chemical stability, non-toxicity, ease of functionalization, porosity development, etc. Especially, the carbon nitrides with increased porosity and nitrogen contents are more versatile than their bulk counterparts for catalysis. These N-rich carbon nitrides are discussed in the earlier parts of the review. Later, the review highlights the role of such carbon nitride materials for the various organic catalytic reactions including Knoevenagel condensation, oxidation, hydrogenation, esterification, transesterification, cycloaddition, and hydrolysis. The recently emerging concepts in carbon nitride-based organocatalysis have been given special attention. In each of the sections, the structure–property relationship of the materials was discussed and related to their catalysis action. Relevant comparisons with other catalytic materials are also discussed to realize their real potential value. The perspective, challenges, and future directions are also discussed. The overall objective of this review is to provide up-to-date information on new developments in carbon nitride-based organic catalysis reactions that could see them rising as prominent catalytic materials in the future.

ARTICLE HISTORY

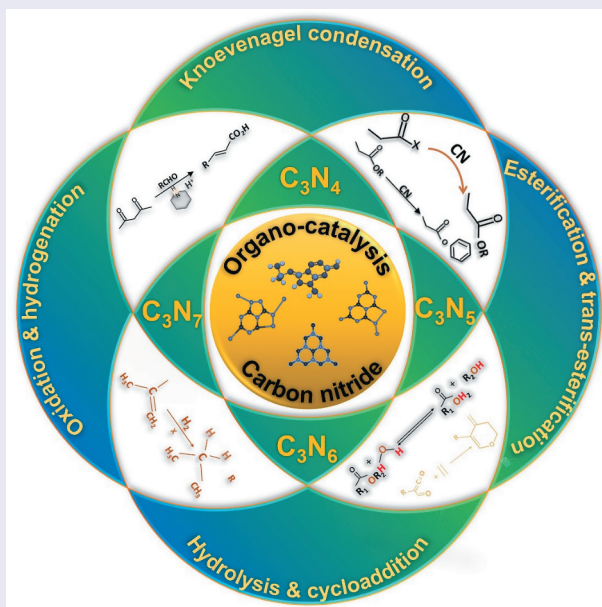
Received 15 February 2023

Revised 2 March 2023

Accepted 5 March 2023

KEYWORDS

Carbon nitride;
organocatalysis;
Knoevenagel condensation;
esterification; cycloaddition;
hydrolysis



CONTACT Ajayan Vinu  Ajayan.Vinu@newcastle.edu.au; Gurwinder Singh  Gurwinder.singh@newcastle.edu.au; Yoshihiro Sugi  sugiyoshihiro@gmail.com  Global Innovative Centre for Advanced Nanomaterials (GICAN), College of Engineering, Science and Environment (CESE), School of Engineering, The University of Newcastle, Callaghan 2308, Australia

*Author was previously affiliated with this institution.

© 2023 The Author(s). Published by National Institute for Materials Science in partnership with Taylor & Francis Group.

This is an Open Access article distributed under the terms of the Creative Commons Attribution-NonCommercial License (<http://creativecommons.org/licenses/by-nc/4.0/>), which permits unrestricted non-commercial use, distribution, and reproduction in any medium, provided the original work is properly cited. The terms on which this article has been published allow the posting of the Accepted Manuscript in a repository by the author(s) or with their consent.

1. Introduction

Global warming due to the increase in the consumption of fossil energy is one of the biggest issues to be addressed by chemical scientists and engineers. The technologies for the minimalization of energy consumption for various domains, such as chemical, fuel, and polymer industries, transportation, biology, medicine, pharmaceuticals, agriculture, *etc.* must be quickly established. Particularly, the decrease in energy consumption of chemical processes is an urgent issue for catalytic technologies. Nanotechnology is the most important research area for the development of new catalytic technologies [1–4].

One of the targets is a catalyst technology of chemical processes based on microporous and mesoporous materials such as carbons [5], carbon nanotubes [6,7], graphene [8], carbon nitrides (CNs) and their engineered counterparts [9–12], metallosilicates and metallophosphates including zeolites [13], metal oxides [14,15] for the catalysts and/or catalytic support to minimize consumption of energy for the reaction and separation of products. Particularly, carbon nitrides including nitrogen-doped carbons are metal-free solid bases to attain maximizing the merits of heterogeneous catalysis [16,17]. One of the major advantages of using them for catalysis is their excellent activity in mild conditions and the easy separation of the products from reaction mixtures [18]. In addition, their combined functionalities of carbon and nitrogen make them attractive as catalysts and/or catalyst supports for various organic transformations [19–23]. However, classical carbon nitrides have some drawbacks of low surface area due to the synthesis at high temperatures, which significantly limits their performances in the catalysis of organic reactions. Recently, the introduction of ordered or disordered mesoporous structures to carbon nitrides through nano-hard templating approach using ordered or non-ordered mesoporous materials and/or by the post-treatment of originally prepared materials expands the catalytic application possibilities of these unique materials [21,24–26]. Mesoporous carbon nitrides (MCNs) with ordered arrays are expected to improve their catalytic properties due to the increase of the reaction sites in the materials.

The catalysis of carbon nitrides including nitrogen-doped carbons works principally based on their aromaticity and amino moiety [27]. The π -electron pools of aromatic nuclei work for photo-redox catalysis through the excitation of illumination, and amino moieties, primary, secondary, and tertiary, work for base catalysis [28]. These properties are the unique features of carbon nitrides as they cooperatively work in photo-redox and base catalyses [29,30]. However, these properties are mainly controlled by the nature of the synthesis approaches used for their synthesis. The

preparation of carbon nitrides generally involves the calcination of different CN precursors with or without hard or soft templates under non-aero conditions. The calcination temperature, nature of the precursors and their nitrogen contents, and polymerization strategies of the precursors decide the final physico-chemical properties of these carbon nitride materials [31]. Particularly, the nature of the basicity is determined by the number of primary and secondary amino moieties that remained during the calcination process. Hence, choosing the appropriate calcination temperature is the key for the high catalyst performances of these materials.

Several reviews on the catalysis of carbon nitrides, especially in photocatalytic water splitting and in organic synthesis, have appeared in the literature that contributed to enhancing the research in the catalysis of carbon nitrides [19,32–36]. In this review, we discuss primarily the base and photo-redox catalyses of these materials in organic synthesis with a focus on Knoevenagel condensation, the cycloaddition of carbon dioxide (CO_2) on epoxides, oxidation, hydrogenation, esterification, trans-esterification and hydrolysis as the typical catalysis examples. The use of carbon nitrides for tandem catalysis and the basic catalyst support combined with the other functional catalysts are also considered with and without illumination. The metal-free catalysis of the carbon nitrides involving hydrogenation and oxidation is also discussed. Further, we discuss the use of carbon nitride catalysis for application in organic synthesis and biomimetic catalysis.

2. Types and the characteristics of carbon nitrides

2.1. C_3N_4

Carbon nitride materials gathered massive attraction owing to their excellent catalytic, electronic, and electrical properties. Based on their structures, carbon nitrides are classified into five different forms which include graphitic carbon nitride ($\text{g-C}_3\text{N}_4$), $\alpha\text{-C}_3\text{N}_4$, $\beta\text{-C}_3\text{N}_4$, cubic C_3N_4 and pseudocubic C_3N_4 . The synthesis of these carbon nitrides except $\text{g-C}_3\text{N}_4$ requires high pressure and high temperature which limit the progression of bulk production of these materials. However, $\text{g-C}_3\text{N}_4$, whose structure closely resembles graphene, can be prepared by using chemical or molecular precursors and require only mild synthesis conditions [37–40]. Interestingly, $\text{g-C}_3\text{N}_4$ possesses the properties of a medium-band gap semiconductor having a graphite-like structure with the CN framework attached with amine functionalities which mainly contributes to the catalysis of chemical reactions [41]. However, $\text{g-C}_3\text{N}_4$ has low electronic conductivity and less specific surface area; therefore, cannot be used in electro-chemical hydrolysis reactions (1.4–2.8 eV) but it

has been widely used in photocatalytic applications owing to its unique band structure. In addition, the electro and thermal catalytic application of these materials are also quite rare [42,43].

Various methods including physical vapor deposition, chemical vapor deposition, thermal polymerization-condensation, and hydrothermal or solvothermal methods are available for the synthesis of g-C₃N₄ [44]. Among these methods, thermal polymerization-condensation is the most used synthesis technique for preparing carbon nitrides and the widely used precursors are urea, melamine, dicyandiamide, cyanamide thiourea, and cyanuric acid [45,46]. Polyaddition and polycondensation are the processes involved in carbon nitride synthesis, which are temperature dependent. Polyaddition is the polymerization process to convert precursors into melamine whereas polycondensation is the condensation of the melamine by the loss of ammonia to form a g-C₃N₄ polymer [42,44]. The carbon nitrides derived from the traditional thermal condensation method have a low surface area (>20 m²/g), highly conjugated stacking of nitrogen atoms in the heptazine structure, and nitrogen atoms with less basicity, less bridging nitrogen atoms and less defective sites at the edges for the graphitic structure. The structure of the g-C₃N₄ may contain the molecular units of s-heptazine (tri-s-triazine) and triazine [47]. Triazine is not as stable as the tri-s-triazine (s-heptazine) structure. For catalytic applications, g-C₃N₄ with tri-s-triazine units may be more beneficial as it has more nitrogen atoms, providing more anchoring and active sites for catalytic reactions. Owing to the stability and other benefits of the tri-s-triazine structure, synthesizing carbon nitrides with tri-s-triazine molecular units is given more attention [48,49].

In the development of carbon nitride materials, the synthesis method plays a critical role since it manipulates the properties of materials including morphology, structure, surface area, active sites, the density of the nitrogen atoms, stability, and size, which are all essential for improving the catalytic activity [50]. However, the key parameter required for the catalysis of carbon nitride is the specific surface area, which is directly linked to the number of active sites connected with the nitrogen atoms. Unfortunately, bulk carbon nitride material exhibits a low surface area, low stability, less nitrogen content, and less accessible active sites which are not useful for catalytic applications. Therefore, researchers tried to modify the structure and framework of carbon nitrides to enhance the catalytic activity of these materials. Various approaches like optimizing precursor ratio, varying calcination process, templating and non-templating techniques, nano modification, doping strategy, and

introduction of terminal amine groups/defect sites have been adopted to tune the properties of the carbon nitride materials [24,45,51,52]. Researchers have successfully modified the properties of the C₃N₄ by employing one or two of these strategies and improved the catalytic activity of the CN materials. For example, Su and his co-workers [53] combined the hydrothermal and deprotonation approaches to synthesize MCN with high basicity. Deprotonated MCN was used as a base catalyst for the reactions between the different aldehydes and malonic derivatives, and these materials exhibited high catalytic activity.

The g-C₃N₄ was oxidized by Krishnan and his co-workers [54] with the help of oxidants such as potassium permanganate (KMnO₄), potassium dichromate (K₂Cr₂O₇), and hydrogen peroxide (H₂O₂) and used as a catalyst for the hydrogen transfer reaction of carbonyl compounds. The oxygenated moieties were added to the CN surface, and when the base was added, the hydrogen donor and the carbonyl compound attached to the modified carbon nitride helped to enhance the rate of catalysis reaction. Recently, Gentile et al. [55] also used the concept of protonation and deprotonation to increase the catalytic activity of carbon nitride materials. Herein, strong acids like sulphuric acid (H₂SO₄) and nitric acid (HNO₃) were chosen for the oxidation treatment and alkali compounds like sodium hydroxide, potassium carbonate, and potassium tert-butoxide (t-BuOK) were used for deprotonation to introduce the basic active sites for the reaction. The oxidation treatment with an acidic mixture introduced the acidic oxygenated functional groups on the surface of the CN materials. The intense oxidation process before the deprotonation enhanced the surface area and thus significantly improved the catalytic activity towards the Knoevenagel reaction.

Another interesting approach to modifying the surface properties of the carbon nitride is to introduce porosity within the CN framework. This was realized by Vinu et al. [56], who reported a new family of CN materials with mesoporous structure (MCN series) by combining the simple polymerization of CN precursors, ethylenediamine – (EDA) and carbon tetrachloride (CTC). The same group also reported MCN with a 3D mesoporous structure and a body-centered cubic *Ia3d* framework using mesoporous silica, KIT-6, and cyanamide as a template and precursor, respectively. The structure of the synthesized materials was found to be heptazine units coordinated by the covalent bonding of CN atoms. The materials were active at room temperature and showed high conversion toward benzaldehyde and malononitrile. The increased activity was achieved due to the large surface area and pore volume, and strong basic sites from the amino groups of the MCN materials.

Another series of g-C₃N₄ with a 3D mesoporous structure was prepared by Vinu et al [26]. through a hard templating strategy with guanidine hydrochloride

as a novel precursor and KIT-6 silica template. The interaction between the silanol groups of the KIT-6 template and the amino group of guanidine is facilitated through hydrogen bonding, which helps to get the replicated structure of the KIT-6 in the final MCN material. MCN from this study was highly porous and had a specific surface area of $303 \text{ m}^2 \text{ g}^{-1}$ and a pore volume of $0.71 \text{ cm}^3 \text{ g}^{-1}$, which was achieved through tuning the pore diameter of the mesoporous silica such as KIT-6. The material synthesized in this study was far better than the previously reported MCN derived from cyanamide ($208 \text{ m}^2 \text{ g}^{-1}$), which explains the important role of the amino groups present in the guanidine hydrochloride which is used as a precursor in this study. These amino groups can be effectively utilized for the reduction and the formation of noble metal nanoparticles onto the surface of MCN and the metal functionalized MCN are found to be excellent catalysts for Suzuki coupling reaction, revealing the importance of synthesis methods and functionalization of MCN for catalytic applications.

2.2. New family of carbon nitrides

2.2.1. C_3N_5 , C_3N_6 and C_3N_7

It is believed that the properties of the materials can be further enhanced by tuning the porosity, structure, and nitrogen contents. Vinu and his co-workers also explored the synthesis of the carbon nitrides with high nitrogen contents and ordered porosity and discovered a new series of MCNs with ordered structure and new stoichiometries (C_3N_5 , C_3N_6 , and C_3N_7) from various high nitrogen-containing cyclic or aromatic precursors. Single molecular precursors such as 5-amino-1*H*-tetrazole, 3-amino-1,2,4-triazole, and aminoguanidine were used to prepare MCNs with different carbon and nitrogen configurations such as C_3N_5 , C_3N_6 , C_3N_7 , and $\text{g-C}_3\text{N}_4$ through varying the calcination temperatures [57–60]. Interestingly, the MCN with C_3N_5 stoichiometry was unique and offer peculiar catalytic properties owing to its triazole moieties which offer strong basicity due to the strain exerted by the 5-membered aromatic ring. These new materials with 1-amino/imino-1,2,4-triazole moieties are highly basic compared with 2-amino/imino-1,3,5-triazine moieties of C_3N_4 . The C_3N_5 stoichiometry with azo linkage synthesized via the thermal deamination of melem hydrazine shows a reduced band gap of 1.76 eV [39].

A recent study by Ruban and her co-workers [51] demonstrated the relation between the nitrogen species, MCN structures, different calcination temperatures, and the catalysis performance with the help of Knoevenagel condensation. The triazole moieties in the MCN structure primarily decide the basicity of the materials, which in turn helps to enhance the catalytic activity of the material for the Knoevenagel condensation reactions. Furthermore, it was found

that MCN structure also controls the catalytic activity; the 3D structure is preferred over the 1D structure, owing to the high specific surface area and pore volume and many active sites which suppress pore blocking. In addition, MCN with a 3D structure helped to transfer the reactant molecules in the porous channels effectively and facilitated the accessibility of the other molecules involved in the reactions. In this study, the nitrogen content, and the textural parameters of MCN structures were finely tuned by using different mesoporous silica templates with varying pore diameters, morphology and structure, and calcination temperature from 350 to 550°C.

The catalytic activity of novel nitrogen-rich carbon nitrides such as C_3N_5 , C_3N_6 , and C_3N_7 with a uniformly ordered mesoporous structure was tested for the reaction between benzaldehyde and malononitrile under different conditions such as pressure, temperature, catalysts dosage. Weak bases like potassium fluoride, piperidine, or other ammonium salts ethylenediamine amino acids, such as glycine, alanine, and proline, or triphenylphosphine, are the conventional catalysts for these reactions. These catalysts are homogenous and suffer many drawbacks such as being expensive, complicated product separation process, and recyclability. The newly synthesized N-rich MCN materials with large surface area, pore volume, and abundant basic sites are highly active and showed a high yield within a short period for Knoevenagel condensation. This study also confirmed that MCN with moieties of 1-amino/imino-1,2,4-triazole is more stable and basic than other moieties such as amino/imino-1,3,5-triazine, revealing the importance of the nitrogen content and pore structure for the organic catalytic transformation.

2.2.2. PHI-based ionic carbon nitrides

Stability and crystallinity are the two major issues associated with conventional polymeric carbon nitrides (PCNs). Therefore, researchers have developed a new type of carbon nitrides with poly heptazine imide (PHI) structure, which are highly stable and crystalline. PHIs are generally synthesized from nitrogen-rich compounds through solid-state reactions with alkali metal chlorides or thermal condensation of CN precursors in eutectic salt melts [61,62]. Post-modification is another way to prepare PHI-based CNs by treating the condensed CNs with alkali metal salts. PHI-based carbon nitrides are reported to have excellent stability, high crystallinity, and electronic conductivity which are all often missed in conventional tri-s-triazine or heptazine-based carbon nitrides [63]. The ionothermal approach is the best feasible method to prepare alkali-metal PHIs with the help of Na, K, and Cs-based salts [64]. K-PHI is the widely reported ionic carbon nitride which can be prepared through 1) a combination of mechanical and chemical treatment of the CN

precursor such as 5-amino tetrazole with KCl/LiCl eutectic mixture and polymerization at 550°C; 2) mixing potassium thiocyanate, potassium malonate pentahydrate, and dicyanamide and calcined at 500°C; 3) mixing potassium thiocyanate and LiCl and condensation-polymerization at 550°C. Savateev et al. 2017 adopted a thermal condensation method to synthesize highly crystalline K-PHI with 1,2,4-triazoles in eutectic metal salts and this new carbon nitride material is presented with staggered ions arranged as crystal packs in the channels and showed excellent performance in the photocatalytic splitting of water with the hydrogen production of 14.7 $\mu\text{mol H}_2$ per h [65]. Schlomberg et al. [66] adopted the ionothermal synthesis strategy and prepared a new type of highly crystalline potassium containing PHI (K-PHI) and its counterpart through the proton exchange (H-PHI). The out-of-plane structure present in K-PHI showed unidirectional layer offset, due to the presence of the hydrated potassium ions, whereas the H-PHI has a larger degree of faulty stackings because of the weaker structure (Figure 1). The improved structure in PHI due to the loss of in-plane coherence, optimizing the smaller and lateral platelet dimensions, and the presence of abundant terminal cyanamide groups, helped in enhancing the photocatalytic performance. Another interesting study [67] reported K-PHI as an efficient material for the oxidative coupling reaction with the help of light. Lithium chloride, potassium chloride, and amino tetrazole were mixed in a ball mill and calcined at a temperature of 550°C. The synthesized materials performed well as a photocatalyst for the conversion of benzyl amines due to the continuous push-pull mechanism of electrons in the K-PHI which mediated the two benzylamine molecules coupling. Very recently, Wu and his co-workers [68] fabricated a new composite material such as potassium doped on carbon nitride

and silica support. The newly developed material showed a mesoporous structure with rod-shaped morphology. The introduction of K atoms into the CN-SBA-15 structure improved the basicity of the materials and thus enhanced the Knoevenagel condensation reaction activity. In addition, the calcination temperature played an important role in the chemical bonding between the potassium and CN/SBA15. At 550°C heating, potassium species were uniformly dispersed on CN/SBA15 support with the help of nitrogen atoms, and the covalent bonding between the potassium and nitrogen is responsible for the stabilization of K on the support. Therefore, the synthesis approach for the design of carbon nitride with different functionalities and the porous structure is crucial in developing them as catalysts for different chemical reactions.

2.2.3. Microporous carbon nitrides

Microporous carbon nitrides are another type in the CN family that appeals to be promising in terms of their unique porous structure and CN framework within the nanochannels. Vinu et al. [69] realized this opportunity and reported the first microporous carbon nitride with a high specific surface area using MCM-22 as a template through a simple polymerization reaction between EDA and CTC. Later, Xu et al. [70] used the same strategy to prepare microporous carbon nitride and applied them for Knoevenagel condensation and further found that the microporous CN materials are better in performance due to their abundant active sites and nitrogen functional groups (Lewis's base) in the CN framework. The pore dimension of the microporous carbon nitrides can also be controlled using the microporous template with different structures (1 and 3D). For example, Stegmann et al. [71] prepared zeolite templated microporous carbon nitrides with 1D and 3D structures using three different zeolites like zeolite

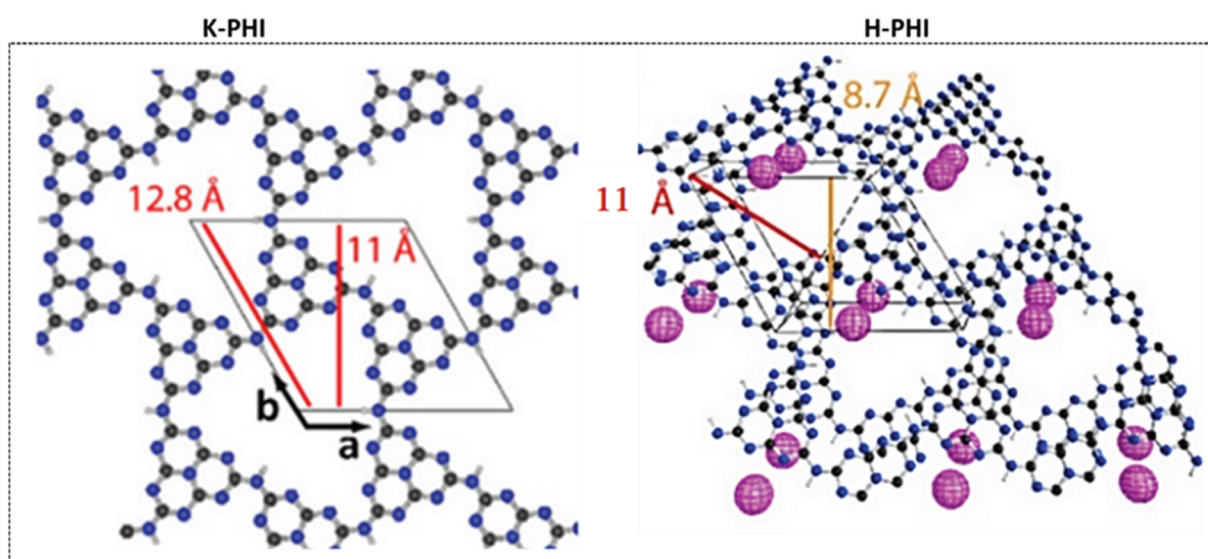


Figure 1. Predicted theoretical structure of K-PHI and its counterpart H-PHI (metal free), reproduced with permission from [66].

Y, ETS-10, and ZSM-5. CNs were found with heptazine structure and microporosity. Zeolite Y and ETS-10 were found to be better templates for the formation of the carbon nitride structure as compared to ZSM-5 since it is hard to deposit the CN precursors in the narrow pores of the ZSM-5 due to the sterical restrictions. Recently, Vinu et al. extended this strategy for the fabrication of microporous carbon nitride with C_3N_5 stoichiometry and a lot of free NH_2 groups using high nitrogen-containing precursor, aminoguanidine hydrochloride and ultra-stable zeolite Y as the template. The unique carbon nitride exhibits two tetrazines and one triazine rings in the unit cell in their CN framework and a high specific surface area of $130.4\text{ m}^2\text{ g}^{-1}$. The availability of free NH_2 groups together with the high surface area and unique microporous structure makes it an excellent adsorbent for CO_2 molecules and a basic catalyst for organic transformations [72].

2.2.4. Other new carbon nitrides

Although C_3N_5 , C_3N_6 , and C_3N_7 are prevalent stoichiometries of carbon nitrides of interest, various other forms have also been reported recently with promising results in catalytic applications. The C_5N_2 with conjugated $C=N$ linkage with a reduced band gap is suitable for H_2O_2 production [73]. The C_3N_2 containing a five-membered ring synthesized from the zeolitic imidazole framework possesses a narrow optical band gap of 0.81 eV and is efficient for photoelectrochemical biosensing [74]. Low-cost C_3N_3 from cyanuric chloride can be synthesized on a copper surface for photoelectrochemical water splitting [75]. Similarly, C_2N [76], C_3N [77], and $C(CN)_3$ [78] have been synthesized from different precursors and utilized for various catalytic and other applications.

3. Active centers of catalysis of carbon nitrides

Graphitic carbon nitrides are prepared by thermal treatments of various nitrogen precursors usually under non-aerial atmospheres as discussed in the previous section. For example, carbon nitride with C_3N_4 compositions exhibits a structure with triazine and/or tris-triazine nuclei connecting each other through tri-substituted nitrogen. There is another type of nitrogen with mono-, di-, and tri-substitution attached to triazine and tri-s-triazine nuclei [3]. These properties make them multifunctional due to the different types of nitrogen in the materials. For example, C_3N_4 has two types of nitrogen moieties with aromatic and aliphatic characteristics. Aromatic moieties of tris-triazine (heptazine) nuclei are fundamental structures of carbon nitrides with semiconductor and Lewis basic character properties due to their hetero-aromaticity. The other nitrogen moieties are mono-, di-, and tri-substituted with non-aromatic character.

Tri-substituted nitrogen works as a connector of tris-triazine nuclei; However, the former two types of nitrogen moieties are remained by incomplete formation of tri-s-triazine nuclei. The bonding energies of the bonds are estimated around 290 eV and 400 eV, respectively, [27]. The aliphatic nitrogen moieties have strong basic characteristics, particularly for di- and mono-substituted nitrogen in carbon nitride.

Triazine and tri-s-triazine moieties, principal constituents of $g-C_3N_4$ can also be activated by visible illumination to form electron-hole [79,80]. The electron-hole formed by visible illumination separates free electrons and holes, and resulting electrons and holes move to the surface and work towards redox reactions. These holes can work for the oxidation of organic chemicals under visible illumination. Particularly, radical anion $\bullet O^{2-}$ will work as an oxidant in photocatalyzed oxidative reactions. Some radical precursors assist hydrogen atom transfer abstract (HAT) from -C-H- with the cooperation of $\bullet O^{2-}$ to form $\bullet CH$, and accelerate the total chemical reactions [81,82]. Typical HAT compounds involve N-hydroxyphthalimide (NHPI), N-hydroxytetrachlorophthalimide (Cl_4NOPI), hydroxyl perfluorobenziodoxole (PFBI-OH), and 4-benoylpyridine (4-BzPY). They work effectively with hydrogen atom transfer chemicals in photocatalyzed organic reactions. Some of them work as HAT for the acceleration of hydrogen atom abstraction in the combination of peroxides, such as hydrogen peroxide and t-butyl hydrogen peroxide to accelerate oxidative catalysis under thermocatalysis [83].

4. Prominent catalysis using carbon nitride

4.1. Knoevenagel condensation

Knoevenagel condensation of carbonyls with active methylene compounds occurs normally by the base catalysis. It is a typical model reaction to know the catalytic properties of the newly found catalyst. In this section, the catalysis of carbon nitrides with different structures and nitrogen contents in the Knoevenagel condensation is discussed [84–87].

4.1.1. Metal-free carbon nitride for Knoevenagel condensation

The presence of nitrogen functionalities in the carbon nitrides offers basic catalytic properties which make them available for Knoevenagel condensation. As discussed previously, these functionalities can be controlled with the simple adjustment of the nature of the CN precursors and the calcination temperatures. For example, Vinu and his co-workers have synthesized MCN-11 from 5-amino tetrazole using KIT-6 as templates at 350–550°C under an Ar atmosphere [51,58]. They applied this catalyst for the Knoevenagel

condensation of benzaldehydes with malononitrile. The catalytic activities decrease gradually with the increasing calcination temperature as shown in Figure 2(a). The samples prepared at 350 and 400°C have excellent catalytic performances with high yield and selectivity for benzylidene malononitrile. The differences in the catalysis are possibly due to the change of structures from C₃N₅ to C₃N₄ by the increase in the temperatures. It should be noted that the MCN samples synthesized at 350 and 400°C have a C₃N₅ structure with 1-amino-1,2,4-triazole moieties, and the samples synthesized at 450, 500, and 550°C have g-C₃N₄ structure with the condensed 2-amino-1,3,4-triazine moieties. For all these catalysts, the high basicity originated from the remaining -NH₂ and/or >NH groups formed during the calcination.

In another report, Elamanthi and his co-workers succeeded in controlling the pore diameter of the MCN and further demonstrated the influence of pore diameter on the catalytic activity [88]. Figure 2(b) shows the influence of pore sizes of hexagonal MCN (HMCN) in the condensation of p-hydroxybenzaldehyde and malonic acid to p-hydroxycinnamic acid. Catalytic activities were increased

until 5.9 nm; however, kept almost constant for the MCN with wider pore sizes. The low activities for narrow pore SBA-15 are due to steric hindrances for the diffusion of the reactants in the small pores. Talapaneni and his co-workers prepared 3D mesoporous C₃N₄, with different pore diameters using cyanamide as CN precursor and KIT-6 with different pore diameters as a hard template. It was found that the activity of the materials is significantly enhanced owing to their 3D porous structure and large pore diameter [24]. In another report, Zhang and his co-workers applied MCN-1 for Knoevenagel condensation and demonstrated that the calcination temperature plays a key role in controlling the catalytic activity in the Knoevenagel condensation [89]. Among MCN-1 prepared at different temperatures, MCN-1 prepared at 400°C showed the highest catalytic activity, giving benzaldehyde and acetone conversions of 99% and 92%, respectively, in the reactions of benzaldehyde or acetone and malononitrile. The high activity is due to the presence of the tri-coordinated nitrogen and/or amino groups in the MCN-1 prepared at 400°C (Figure 2(c)). Similarly, Liu and his co-workers also demonstrated the influence of the calcination

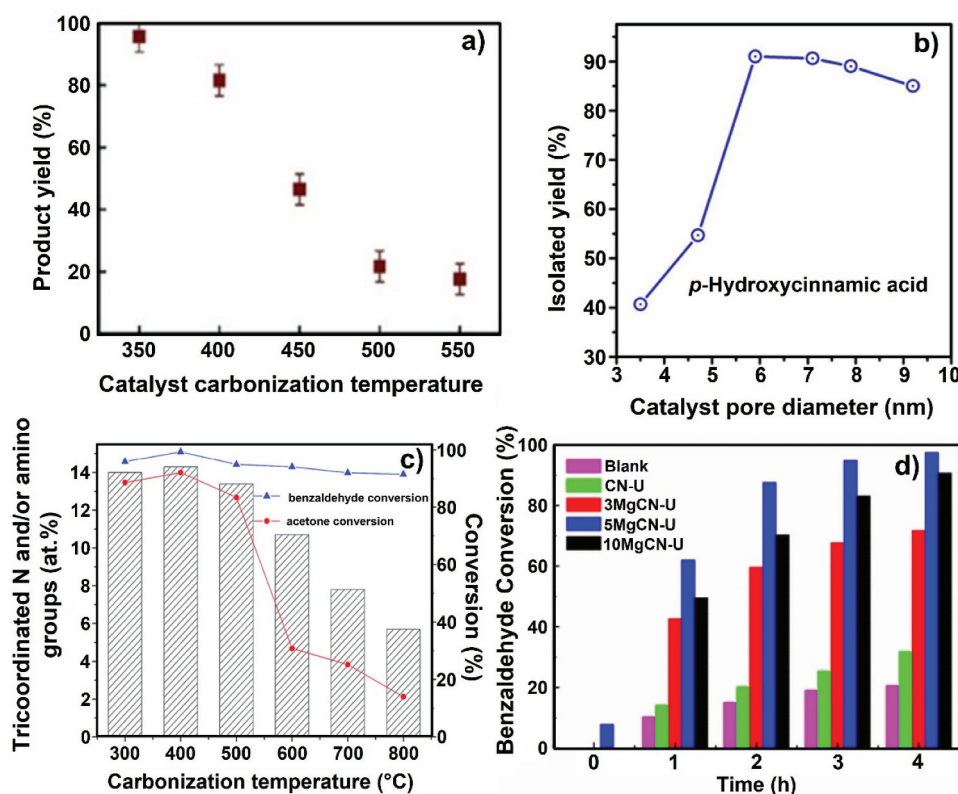


Figure 2. (a) Influence of materials synthesis temperature on the yield of benzylidene malononitrile, reproduced with permission from [51], (b) Effect of pore diameter of different HMCN catalysts on the yield of phydroxycinnamic acid. Reaction conditions: p-hydroxybenzaldehyde (4.00 mmole), malonic acid (8.10 mmole), HMCN catalysts (200 mg), toluene (10 ml), reaction time 60 min, and azeotropic method (105°C), reproduced with permission from [88], (c) Plots for the benzaldehyde and acetone conversions obtained in the Knoevenagel condensations of benzaldehyde or acetone and malononitrile against the surface concentrations of tricoordinated nitrogen and/or amino groups, reproduced with permission from [89], and (d) Catalytic performance for Knoevenagel condensations of xMgCN-U catalysts with different Mg loading amount, reproduced with permission from [90].

Table 1. Catalytic activity in Knoevenagel condensation [90].

Materials	Conversion (%)	Selectivity (%)	Yield (%)
–a	7.3 ± 1.0	7.2 ± 1.1	0.5
SBA-15	8.1 ± 1.2	13.1 ± 1.2	1.1
CN-400	8.8 ± 1.3	26.1 ± 1.4	2.3
CN/SBA15–350	63.7 ± 2.1	95.0 ± 2.0	60.5
CN/SBA15–400	88.6 ± 2.4	95.1 ± 2.3	84.3
CN/SBA15–450	55.5 ± 1.9	91.6 ± 2.2	50.8
CN/SBA15–500	54.6 ± 1.8	94.7 ± 2.2	51.7

Reaction condition: 0.1 g of catalyst, 10 mmol of benzaldehyde, 10 mmol of malononitrile, 5 ml of acetonitrile, 900°C, and 4 h, ^awithout catalyst.

temperature of mesoporous C₃N₄ on the catalytic activity in the Knoevenagel condensation [91]. Again, the catalyst prepared at 400°C showed the highest activity which is linked to the high percentage of bridged nitrogen species on the catalysts. These sites act as a basic site required for the basic catalysis (Table 1).

Su and his co-workers deprotonated mpg-C₃N₄, derived from cyanamide with 12 nm SiO₂ particles through a simple treatment with basic aqueous solutions (K₂CO₃, KOH, t-BuOK) and applied for the Knoevenagel condensation [53]. The deprotonation significantly increases the basicity of the catalyst and also improves the catalytic performance. The catalyst worked well with various aldehydes and active methylene and could be reused and was highly stable without any loss of intrinsic catalyst activity. Xu and his co-workers also reported the NaOH detemplation of MCN (CND-NaOH) fabricated using formaldehyde and urea as a precursor and microcellular silica foam (MCF) as a template [92]. The deprotonation occurred simultaneously with the detemplation of the silica template by NaOH solution (CND-NaOH). NaOH detemplation allowed the mesoporous structures to be retained when compared to detemplated material obtained with HF (CND-HF) (Table 2). CND-NaOH gave excellent catalytic performances with high

Table 2. Catalytic performance of the CND catalysts in Knoevenagel condensation reactions [91].

Entry	Catalyst	Conversion (%)	Selectivity (%)	Yield (%)
1 ^a	—	4.0	80.7	3.2
2 ^b	CND-HF	53.5	96.4	51.6
3 ^b	CND-0.5 M	93.7	98.2	92.0
4 ^c	CND-0.5 M	80.4	93.2	74.9
5 ^b	CND-0.75 M	90.9	97.1	88.3
6 ^b	CND-2.0 M	84.5	96.7	81.7
7 ^d	CND-0.5 M	96.1	91.6	88.0
8 ^e	CND-0.5 M	93.8	80.4	75.4
9 ^f	CND-0.5 M	93.2	93.5	87.1
10 ^g	CND-0.5 M	37.9	97.8	37.1
11 ^h	CND-0.5 M	73.6	93.7	69.0
12 ^c	CND-KOH-0.5 M	96.2	92.3	88.8

^aWithout any catalyst. ^bUnless specified, the reaction conditions were as follows: 10 mmol of benzaldehyde, 10 mmol of malononitrile, 0.4 mL of *n*-decane, and 5 mL of acetonitrile as solvent. $W_{\text{catal.}} = 100$ mg. $T = 70^\circ\text{C}$, $t = 4$ h. In the Knoevenagel condensation reactions of benzaldehyde, the byproducts were solely the corresponding acids originating from self-oxidation of benzaldehyde. ^c20 mmol of benzaldehyde and 20 mmol of malononitrile. ^d10 mmol of pentanal and 10 mmol of malononitrile. ^e10 mmol of *p*-anisaldehyde and 10 mmol of malononitrile. ^f10 mmol of furaldehyde and 10 mmol of malononitrile. ^g10 mmol of benzaldehyde and 10 mmol of ethyl cyanoacetate under 5 mL of acetonitrile. ^h10 mmol of benzaldehyde and 10 mmol of ethyl cyanoacetate under 5 mL of *n*-butanol.

selectivity for benzylidene malononitrile with high conversion of benzaldehyde.

Xu and his co-workers also prepared MCN (CN-MCF) from CTC and EDA using mesocellular silica foam (MCF) at 600°C under an Ar atmosphere and demonstrated its performance in the Knoevenagel condensation [93]. The catalytic performances were significantly enhanced by the introduction of the large mesoporous structure by MCF and further, the CN-MCF showed great catalytic stability and versatility (Table 3). Similarly, different MCN with C₃N₄ stoichiometry were prepared with MCF, SBA-15, and FDU-12 as the templates and showed good activity with high selectivity for Knoevenagel condensation of benzaldehyde and acetone [94,95] (Table 4). The same research group reported the preparation of microporous carbon nitride (CN-Mic) using MCM-22 as a template and CTC and EDA as CN precursors [70]. The resulting CN-Mic has a pore diameter of 0.3 nm and was applied for Knoevenagel condensation after washing with NH₄HF₂. The catalytic activity of CN-Mic was much higher than that of CN-MCF. The material, possibly, has a new type of Lewis base characters due to g-CN compositions in the microporous framework (Table 5). In another report, Ansari and his co-workers prepared MCN from melamine using mesoporous silica, INC-2 as templates [52]. The mixture was calcined finally calcined at 550°C and the silica template was removed by 3% HF solution. The resulting MCN was applied for the Knoevenagel condensation of ethyl cyanoacetate with benzaldehydes under microwave irradiation. The yield of catalyst performance falls in the range of 75%–95% within a short time of 12 min. The catalyst can be readily recovered and reused for up to 5 runs without loss in catalytic activities.

Table 3. Catalytic activity of CN-MCF samples for Knoevenagel condensation reactions [92].

Entry	Catalyst	Conv. (%)	Sel. (%)	Yield (%)
1 ^a	CN-MCF-0.2	81.4	92.7	75.5
2 ^a	CN-MCF-0.4	84.1	93.6	78.7
3 ^a	CN-MCF-0.6	78.1	92.6	72.3
4 ^a	CN-MCF-0.8	76.5	93.5	71.5
5 ^b	CN-MCF-0.4	96.9	94.7	91.8
6 ^a	CN-bulk-0.4	16.5	92.3	15.3

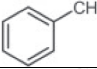
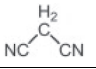
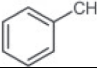
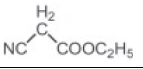
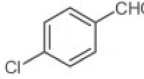
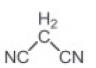
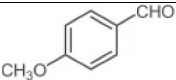
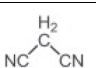
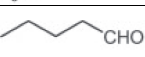
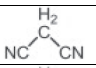
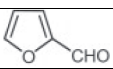
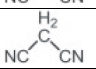
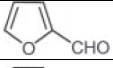
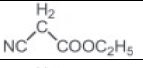
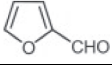
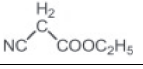
^a5 mmol of benzaldehyde and 5 mmol of malononitrile, ^b3 mmol of benzaldehyde and 3 mmol of malononitrile.

Table 4. Catalytic performances of CND/SBA-15 materials in Knoevenagel condensation [182].

Entry	Catalyst	Conversion (%)	Selectivity (%)	Yield (%)
1	SBA-15	3.6	96.5	3.3
2	0.4CND/SBA-15	11.2	94.1	10.5
3	0.6CND/SBA-15	33.7	95.2	32.1
4	0.8CND/SBA-15	48.0	95.7	45.9
5	1.0CND/SBA-15	62.8	94.9	59.6
6	1.2CND/SBA-15	58.6	94.2	55.2

^aReaction conditions: 10 mmol of benzaldehyde, 10 mmol of malononitrile, 0.5 mL of *n*-decane, 5 mL of CH₃CN, $T = 90^\circ\text{C}$, $t = 5$ h, and $W_{\text{catal.}} = 50$ mg.

Table 5. Various Knoevenagel condensations catalyzed by the CN-Mic catalyst^a [70].

Entry	Aldehyde	Nitrile	Time (h)	Conv. (%)	Sel. (%)
1 ^b			4	87.1	95.1
2 ^c			4	53.6	96.1
3 ^b			3	92.4	96.3
4 ^b			6	82.1	97.4
5 ^b			6	84.5	98.2
6 ^b			4	90.3	96.3
7 ^b			4	41.6	97.1
8 ^c			4	87.8	97.2

^aReaction condition: 10 mmol of aldehyde, 10 mmol of methylene group-containing nitrile, 0.5 mL of *n*-decane as internal standard, 100 mg of CN-Mic. Catalytic tests were performed at 90°C, ^b5 mL of CH₃CN as solvent, and ^c5 mL of *n*-butanol as solvent.

Bahuguna and his co-workers further extended the unique basic properties of the MCN and fabricated a nanocomposite of the potassium-functionalized graphitic carbon nitride (KGCN) and reduced graphene oxide (RGO) [96]. Nanocomposites, KGCN-RGO, were applied for Knoevenagel condensation of benzaldehydes with malononitrile or ethyl cyanoacetate in ethanol (Table 6). Among the catalysts prepared, K20GCN-RGO gave the best results for the synthesis of corresponding arylidene derivatives at room temperature (Table 7). KGCN not only works as a base catalyst for condensation, but also helps the adsorption of reactant molecules to their surface for condensation catalysis. For example, the nanocomposite K20GCN-RGO was applied for the tandem synthesis of aryl substituted chromenes by the multi-step base catalysis wherein the benzylidenemalononitrile, Knoevenagel product, from the aldehyde and malononitrile sequentially condensed with dimedone, resulting in high yield formation of the 4*H*-chromene. They also synthesized indole-substituted 4*H*-chromens by the Knoevenagel reaction

Table 6. Optimization for the Knoevenagel condensation of benzaldehyde and malononitrile [95].

Entry	Catalyst	Catalyst (wt%)	Time (min)	Yield (%)
1	-	-	60	trace
2	GCN	10	60	45
3	RGO	10	60	30
4	K10-GCN	10	25	90
5	K20-GCN	10	12	97
6	KGCN-RGO	2	30	51
5	KGCN-RGO	5	30	69
8	KGCN-RGO	10	10	98
9	KGCN-RGO	20	10	97
10	KGCN-RGO	30	20	90

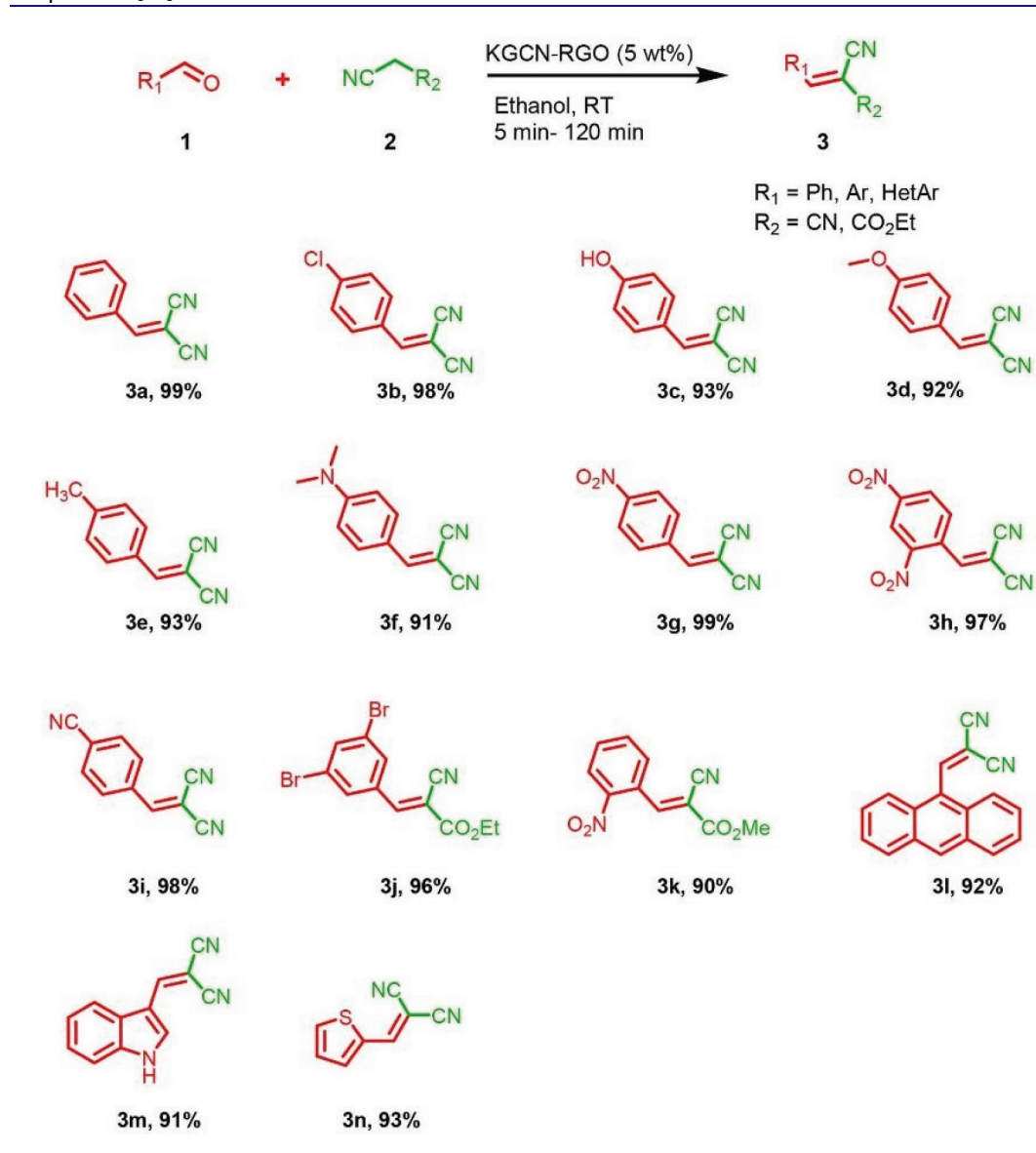
Reaction conditions: benzaldehyde, 1 mmol; malononitrile, 1 mmol, solvent, ethanol at room temperature.

of salicylaldehydes and active methylene compounds, following the condensation of indoles over polyaniline modified carbon nitride (NPGCN), where aniline modification of the nitrile can prevent from the formation of undesired bis-indole formation [97]. The one-pot tandem reactions involving Knoevenagel condensation have also been examined by the combination of oxidation and hydrogenation by using modified carbon nitriles as the catalysts [98,99].

In another interesting work, a unique approach to oxidation and deprotonation was introduced to enhance the basic properties of carbon nitride. For example, Gentile and his co-workers synthesized graphitic carbon nitride (g-CN) that was first strongly oxidized by an acid mixture (H₂SO₄/HNO₃) [55]. The oxidized carbon nitride (CNO) shows a large number of surface acidic moieties and can easily be deprotonated by washing with strong bases (NaOH, K₂CO₃, *t*-BuOK) to introduce the basic sites. The resulting carbon nitride, CNO-M, was applied for the Knoevenagel condensation of benzaldehyde and malononitrile. Oxidized C₃N₄ enhanced catalytic performances by the treatment of bases although no enhancement occurred for unoxidized C₃N₄. Among the bases used, the treatment with NaOH was found to be the best as it was able to deprotonate even less acidic hydrogen. In this case, the prepared catalyst showed excellent performance in the condensation of malononitrile with various benzaldehydes over CNO-NaOH and yielded corresponding arylidene malononitriles over 99% at 90°C for 2 h.

Not only the porous carbon nitride but even the catalytic properties of the bulk carbon nitriles can also be tuned with the simple modification of the synthesis procedure. For example, Zhang and his co-workers

Table 7. Substrate scope for the synthesis of Arylidene derivatives of malononitrile and ethyl cyanoacetate. Reaction conditions: Aldehyde, 1 mmol; active methylene, 1 mmol; KGCN-RGO 5 wt%; ethanol, 3 ml at room temperature [95].



prepared $g\text{-C}_3\text{N}_4$ by thermal condensation of urea with the addition of a small amount of dicyandiamide (DCDA) followed by the treatment with KOH for deprotonation to increase the basicity of the catalysts [100]. This method provides a much higher high product yield compared to the direct thermal decomposition of urea alone. It was demonstrated that the addition of the small amount of DCDA significantly enhanced the catalytic activity of $g\text{-C}_3\text{N}_4$ in the Knoevenagel condensation of benzaldehyde with malononitrile, acetone, and malononitriles and benzaldehyde with ethyl cyanoacetate (Table 8). It was found that although four types of nitrogen species, primary amine ($-\text{NH}_2$), secondary amine, ($>\text{NH}$), tertiary amine ($>\text{N}-$), and pyridinic nitrogen ($\text{C}=\text{N}-\text{C}$), were present in the $g\text{-C}_3\text{N}_4$, the addition of DCDA increased the amount of $-\text{NH}_2$ which is key for enhancing the catalytic activity. The catalytic activity of these four types of

Table 8. Knoevenagel condensation of benzaldehyde and malononitrile over $g\text{-C}_3\text{N}_4$ [99].

Entry	Catalyst	X (%) ^a	S (%) ^b	TON _{bulk} ^c	TON _{surf} ^c
1	None	9.8	89.5	–	–
2	DCDA	14.8	91.1	–	–
3	DCN	17.4	97.4	0.20	37.00
4	DUCN-4	26.9	98.5	0.31	31.62
5	DUCN-2	33.1	98.9	0.37	30.60
6	DUCN-1	98.2	99.2	–	–
7	DUCN-0.5	98.9	99.3	–	–
8	DUCN-0.25	99.0	99.6	–	–
9	UCN	99.2	99.7	–	–
10	UREA	92.4	99.3	–	–
11	DUCN-4-KOH	75.5	99.1	–	–

^aX: the conversion of benzaldehyde or acetone, ^bS: the selectivity to benzylidene malononitrile (I), isopropylidene malononitrile (II), or ethyl α -cyanocinnamate (III). Reaction conditions: 40°C, 1 mmol benzaldehyde or acetone, 3 mmol malononitrile or ethyl cyanoacetate, 20 mg catalyst, 2 h for reactions (I) and (II) and 6 h for reaction (III), and ^cTON_{bulk} and TON_{surf} are calculated on the basis of the content of nitrogen species in the catalyst and on the surface of the catalyst, respectively.

nitrogen species decreases in the order: of $-\text{NH}_2 > >\text{NH} > >\text{N}- > \text{C}=\text{N}-\text{C}$ in the base catalysis of $g\text{-C}_3\text{N}_4$. The

catalytic activity of different types of nitrogen species is determined not only by the structure of the nitrogen species but also by the stability of the organic substrates. The $-NH_2$ and $>NH$ groups have similar catalytic capabilities, but they offer a much higher base catalytic activity than that of $C=N-C$.

Sharma and his co-workers integrated the phase transfer catalyst of 18Crown ether6 with $g-C_3N_4$, derived from urea, for the Knoevenagel condensation at room temperature [101,102]. Particularly, $g-C_3N_4$ enhanced the condensation with up to 99% within ~ 30 min in the presence of 18Crown ether6. The coexistence of $g-C_3N_4$ is essential for catalysis (Table 9).

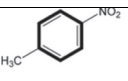
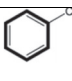
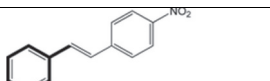
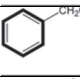
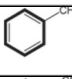
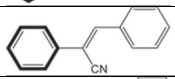
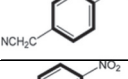
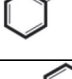
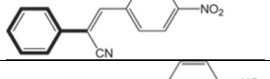
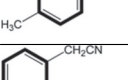
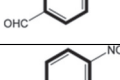
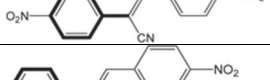
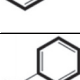
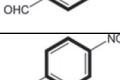
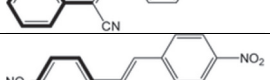
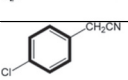
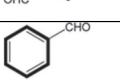
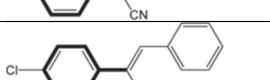
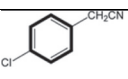
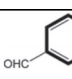
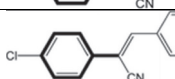
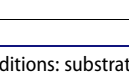
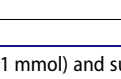
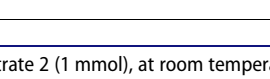
Knoevenagel condensation of aldehydes with active methylene compounds can also occur over acidic modified C_3N_4 . Choudhary and his co-worker examined the sulfonation of $g-C_3N_4$, derived by the calcination of DCDA at $550^\circ C$, by using $ClSO_3H$ as a sulfonating agent [103]. The resulting $S-g-C_3N_4$ was applied for the Knoevenagel condensation of benzaldehydes with malononitrile to corresponding benzylidene malononitriles in high yields for 30 min at $50^\circ C$. They also tried tandem condensation based on acid-base bifunctional natures of $S-g-C_3N_4$ and obtained naphthopyrone derivatives in high TON. Sadjadi and his co-workers also introduced acidic and ionic-liquid functions in graphitic carbon nitride which was prepared by the calcination of Zinnia grandiflora petals and urea, followed by the polymerization of 2-acrylamido-2-methyl-1-propane-sulfonic acid, acrylic acid and the as-prepared 1-vinyl-3-butylimidazolium chloride [104]. The resulting

carbon nitrides have high catalytic activities for the Knoevenagel condensation of a series of benzaldehyde with malononitrile. The high catalytic activities come from the benefits of acidic and ionic liquid functions. The catalysts were also applied for the one-pot, three-component Biginelli reaction under a very mild reaction condition in an aqueous solvent for the synthesis of dihydropyrimidinones. The presence of both acidic and ionic liquid functions helped to achieve 100% yield dihydropyrimidinones and also worked well with the various substrates having different electronic properties.

To increase the basicity of the CN catalysts, a doping strategy has been adopted. For example, Deng introduced Mg within the $g-C_3N_4$ through simple mixing of urea and $MgCl_2$ under an air atmosphere and investigated them for Knoevenagel condensation of benzaldehyde with malononitrile [90]. Mg-doping improved catalytic performance as shown in Figure 2(d). The 5MgCN-U catalyst with 5% Mg doping wt. exhibited the highest conversion of 97% at $70^\circ C$ with good recycling stability for four cycles: 88% benzaldehyde conversion and nearly 100% benzylidene malononitrile selectivity. These results show Mg-doping improved the basic property of $g-C_3N_4$ for the acceleration of the base catalysis.

Wei and his co-workers reported the preparation of boron-doped $g-C_3N_4$ materials (CNBF) by thermal copolymerization of dicyandiamide and imidazole ionic liquid, BmimBF₄ [105]. CNBF enhanced catalytic activity in Knoevenagel condensation of an

Table 9. Screening of $g-C_3N_4$ catalyst using PTC for Knoevenagel condensation with different substrates^a [100].

Entry	Substrate 1	Substrate 2	Product	Time (min)	Yield (%)
1				30	99
2				30	99
3				30	99
4				30	99
5				30	85
6				30	88
7				30	80
8				30	85

^aReaction conditions: substrate 1 (1 mmol) and substrate 2 (1 mmol), at room temperature ($25^\circ C$), 18Crown ether 6 (PTC) (0.1 mmol), solvent toluene (5 mL) and $g-C_3N_4$ basic catalyst (30 mg).

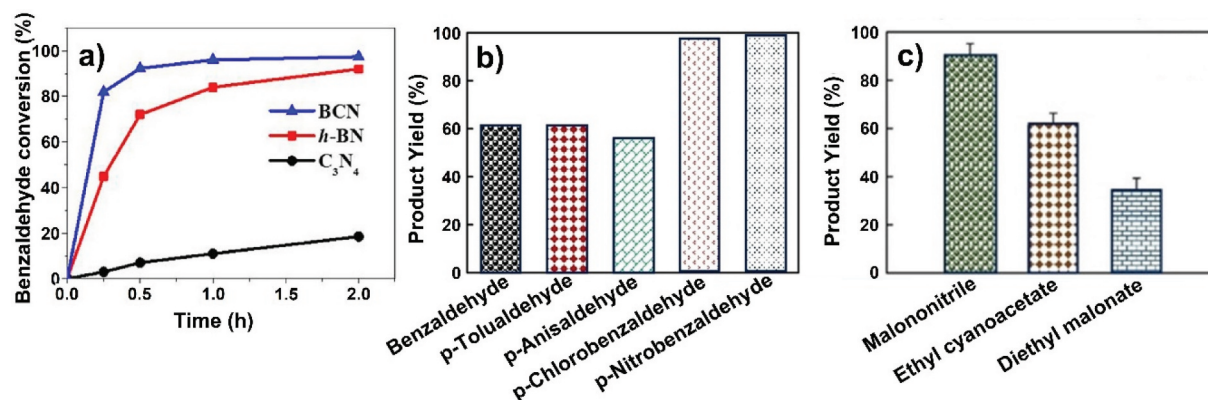


Figure 3. (a) Conversion of benzaldehyde over BCN, h-BN and C_3N_4 . Reaction conditions: 2.5 mmol of benzaldehyde, 2.5 mmol of malononitrile, 15 ml of toluene, 100 mg catalyst, 80°C oil bath under N_2 as the protection atmosphere, reproduced with permission from [106], (b) Reactivity for p-substituted benzaldehydes with malononitrile, reproduced with permission from [51], (c) Influences of active methylene compounds on the yield of benzylidene malononitrile, reproduced with permission from [51].

aldehyde with malononitrile as shown in Figure 3(a) [106]. The catalytic activity of CNBF increased with the amounts of boron doping: $CNBF-0.1 < CNBF-0.3 < CNBF-0.7$, which is the same order as the basic site concentration observed from CO_2 -TPD. The MAS NMR showed that the boron was evenly doped in tri-s-triazine rings of g- C_3N_4 . Boron doping causes reduced electron conjugation in the tri-s-triazine rings which leads to enhanced basicity at nitrogen sites (Table 10).

4.1.2. Mechanism of Knoevenagel condensation

Base catalysis in organic chemistry is highly dependent on the electronic properties of reactants [107]. There are many works on the Knoevenagel catalysis of benzaldehydes with malononitrile over carbon nitride-related materials as discussed in the previous section. Many of these papers are written from their aspects and the catalytic activity of the carbon nitride catalysts is also influenced by the substituents of benzaldehyde and active methylene compounds and the common reaction conditions, such as temperature, period, catalyst amount, solvent, etc. Figure 3(b) shows some results chosen from our papers to know the influences of substituents on the Knoevenagel catalysis of

benzaldehydes with malononitrile by using MCN-11 calcined at 400°C [51]. The yields of condensate and benzylidene malononitriles have increased by the electron-withdrawing substituents: $MeO- > Me- > -H > -Cl > -NO_2$. Figure 3(c) shows the condensation of benzaldehyde with dimethyl malonate, cyanoacetate, and malononitrile over the MCN-11. The electron-withdrawing properties of methylene moieties accelerate the catalysis in the order: malononitrile > ethyl cyanoacetate > diethyl malonate. Generally, the yields were influenced by the substituents: electron-withdrawing groups enhance the Knoevenagel condensation. These features of the catalysis show that the activation of both reactants, aldehyde and active methylene, are important parameters and that the condensation over carbon nitride, C_3N_4 , occurred by the typical-based catalyzed condensation of the nucleophile [108].

These properties of the condensation can summarize as follows: lower density of electron of benzene ring favors the interaction with tri-s-triazine moieties of carbon nitrides, and lower densities of methylene moieties: negatively charged methylene moieties attack the positive aldehyde moieties for the condensation. These results reveal that the carbon nitride works as a proton absorber and interacts with the positively charged aldehyde carbon. The mechanism for the condensation is shown in Figure 4 [70]. Usually, the Knoevenagel condensations are applied for the condensation of aldehyde and active methylene compounds, such as malononitrile, ethyl cyanoacetate, and dimethylmalonate as discussed above [109]. However, it is possible to apply for toluene with strong electron-withdrawing groups and benzyl cyanide with appropriate substituents. For example, nitrotoluene with benzyl cyanides gave their condensation product, p-substituted stilbene with high efficiency over g- C_3N_4 in the presence of 18-crown-6 as the phase transfer reagents. The results exemplify that an effective combination of the accepting substrates and active methylene compounds can condensate by the carbon nitrides with appropriate reaction conditions [110].

Table 10. Catalytic performances of b-doped g- C_3N_4 ^a [105].

Entry	Catalyst	Conversion BA ^b (%)	Selectivity BMN ^c (%)	S_{BET} of catalyst (m ² /g)	Catalytic activity $\mu mol_{BA}/m^2_{catalyst}\cdot h$
1	-	0.2	-	-	-
2	g- C_3N_4	5.6	98.8	8.6	27.1
3	g- C_3N_4 (U)	25.2	99.8	77.6	13.5
4	mpg- C_3N_4	34.3	99.9	85.7	16.7
5	CNBF-0.1	19.7	99.1	13.3	61.7
6	CNBF-0.3	38.0	99.3	21.3	74.5
7	CNBF-0.5	78.6	99.8	42.9	76.3
8	CNBF-0.7	63.6	99.8	25.3	104.9

^a S_{BET} —Surface area measured by the Brunauer–Emmett–Teller method, ^bThe catalyst was prepared using cyanamide as a precursor and nano-sized silica particles as hard templates. Reaction performed at 70°C for 2 h using CH_3CN (10 ml) as the solvent, 1 mmol benzaldehyde, 2 mmol malononitrile, ^bbenzaldehyde, ^cbenzylidene malononitrile, and S_{BET} is surface area of materials.

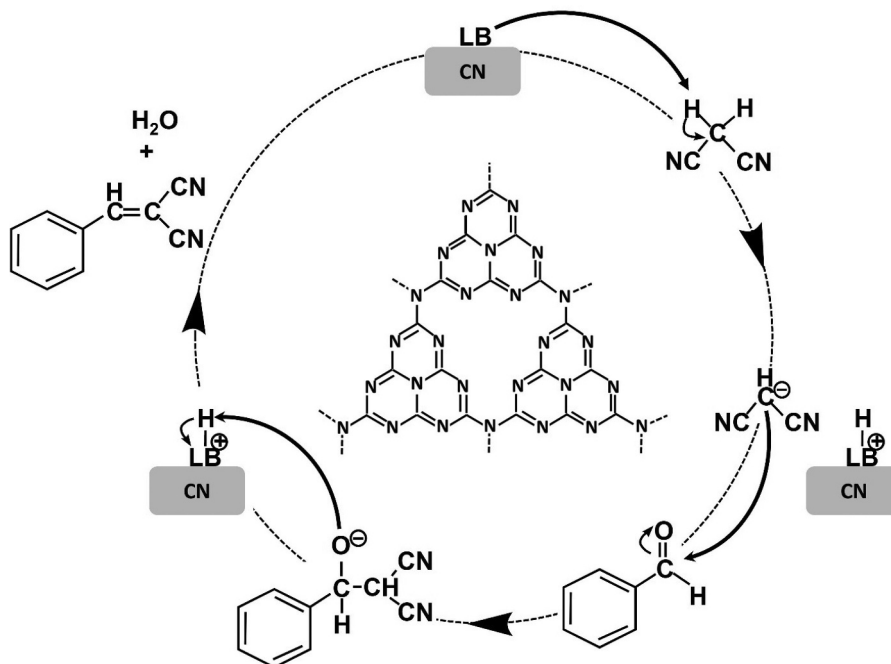


Figure 4. Mechanism of Knoevenagel condensation of benzaldehyde and malononitrile, reproduced with permission from [70].

4.2. Oxidation by g-CN_s and their modified forms

Through the oxidative pathway, various fine and pharmaceutical compounds can be synthesized using metal or metal oxide substituted porous zeolite or zeolite-based catalysts and expensive oxidants including dichromates. However, these catalysts suffer from serious stability issues owing to the release of metals from the catalysts. g-C₃N₄ can replace these less stable catalysts as they are metal-free and have the ability to activate oxidizing agents such as oxygen into corresponding radical molecular O₂ species. The visible-light-induced photocatalytic reaction mechanism is depicted clearly in Figure 5(a). Oxidation processes employing the family of g-CN_s as catalysts can be categorized into two types: (1) metal-free g-CN_s and (2) anchored metal complexes or impregnated hetero

atoms on the surface of the g-CN framework. Various oxidation of alkanes, alkenes, and aromatics conducted over graphitic carbon nitrides (g-CN_s) and their mesoporous counterparts, metal oxide hetero-junction of g-CN_s either in photocatalytic or conventional liquid/gaseous phase pathways.

4.2.1. Metal free g-CN_s in oxidation

Metal-free catalytic processes must avoid contamination by either substrates or products, particularly in the field of pharmaceutical and agricultural purposes. Here, we summarize the important research in the oxidation of organic compounds by g-CN_s. Catalytic processes by metal-free g-CN_s can be carried out by thermal or photocatalysis methodologies [111]. Thermal oxidation usually employs O₂ or H₂O₂ as an oxidant in the

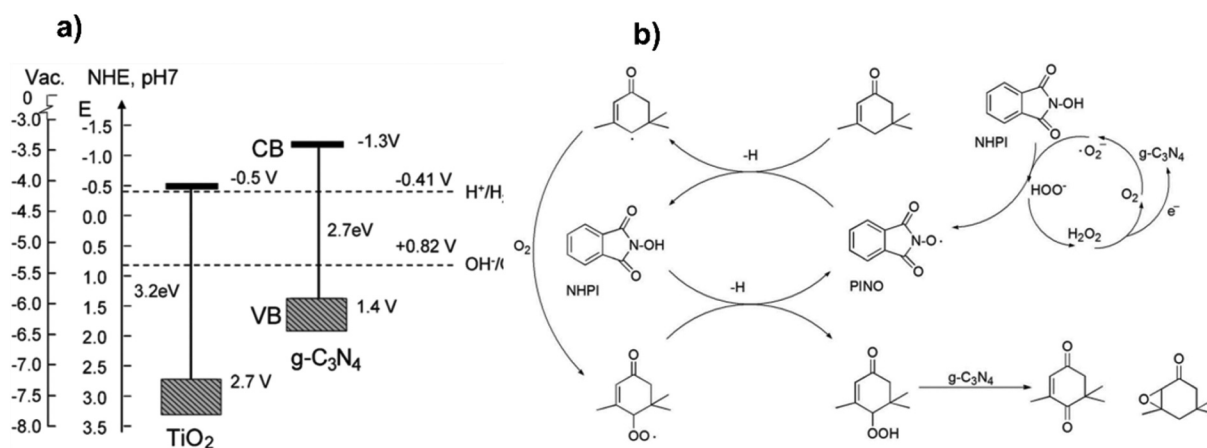


Figure 5. (a) Visible light-induced photocatalytic reaction mechanism of g-C₃N₄, and (b) reaction mechanism for the oxidation of α -isophorone to keto-isophorone, reproduced with permission from [83].

absence of light. Thermal, chemical, and mechanical etching of the g-C₃N₄s generate new active sites compared to their parent forms and were found to be useful in the oxidation by photoredox processes such as the conversion of benzyl alcohol to benzaldehyde [112]. The catalytic activities of the g-C₃N₄s were also found to be enhanced by in-situ synthesis of hetero junctions from the g-C₃N₄s and other carbon allotropes such as carbon nano tubes [113]. α -isophorone was transformed to keto-isophorone with molecular O₂ employing N-hydroxyphthalimide (NHPI) anchored to metal-free g-C₃N₄. According to the authors, the reaction mechanism involved the formation of a superoxide radical anion resulting from the abstraction of electrons from the g-C₃N₄, the capture of atomic hydrogen with a simultaneous formation of a peroxy radical anion (Figure 5(b)) [83]. Nitrogen-rich MCNs were successfully employed for the CO₂ activation in the epoxidation of cyclic alkenes and the simultaneous formation of phenol from benzene using molecular oxygen (Figure 6) [114]. A high-temperature oxidative thermal etching of metal-free g-C₃N₄ forming the corresponding nano-sheets was used in the selective epoxidation of styrene. The time length of the etching process had a remarkable impact on the exfoliation process, lamellar thickness, morphology, and chemical state of nitrogen in the parent g-C₃N₄ [115].

Selective partial oxidation of ethanol to acetaldehyde was achieved in the gaseous phase using metal-free g-C₃N₄s. It was observed that the greater presence of -C-N=C- active sites favored selective aldehyde formation [116]. A structural transition of g-C₃N₄ to nonstoichiometric carbon nitride during the reaction and the formation of newer tertiary nitrogen active site concentration leads to the formation of side products thus decreasing the selectivity of the desired product. This clear change in the product selectivity and yield indicates the influence of the -C-N=C- active site in determining the formation of aldehyde [117]. Oxidation of activated aliphatic C-H bonds of aryl hydrocarbon

(such as toluene) was successfully achieved in the liquid phase by the boron-doped metal-free g-C₃N₄. Compared to traditional metal catalysts, the metal-free, boron-doped g-C₃N₄s displayed greater selectivity towards the benzaldehyde product. Besides being stable, these catalytic materials exhibited remarkable activity for C-H bond activation with environmentally benign oxidant O₂ [118]. In a similar attempt, mesoporous g-C₃N₄ was successfully used as a catalyst in the presence of O₂ as an oxidizing agent in a high-pressure semi-liquid phase reaction to transform the C-H bond of the methyl group in toluene to benzaldehyde. During the catalysis, the free radical anions of oxygen were effectively arrested by the g-C₃N₄ surface, causing a boost in the selectivity of the product aldehydes [119].

Boron and Fluorine-enriched mesoporous metal-free g-C₃N₄s were also employed as catalysts for the oxidation of cyclohexane in the liquid phase to cyclohexanone. An ionic-liquid mediated methodology was adopted for the synthesis of g-C₃N₄ catalysts and claimed that the procedure can be extended for the incorporation of heteroatoms into the g-C₃N₄ morphology to conveniently tune the surface properties according to the requirement [120]. Metal-free PCN was also used for the gram-scale synthesis of *tert*-benzylic alcohols in a photocatalytic oxidation reaction [121]. In another report, Geng et al. have successfully developed a metal-free g-C₃N₄ catalyst for the synthesis of biologically valued isochromanones, phthalides, isoquinolinones, isoindolinones and xanthenes from readily accessible alkyl aromatic precursors in good yields mediated by visible light. These g-C₃N₄ catalysts were highly competitive and yielded comparative amounts as that of homogeneous metal catalysts. The reaction mechanism involves a single electron transfer (SET) with the substrate to afford the benzylic radical. This reaction triggers the formation of nitrogen radical cation, followed by base-promoted deprotonation to generate benzylic radical subsequently by the formation of peroxide radical

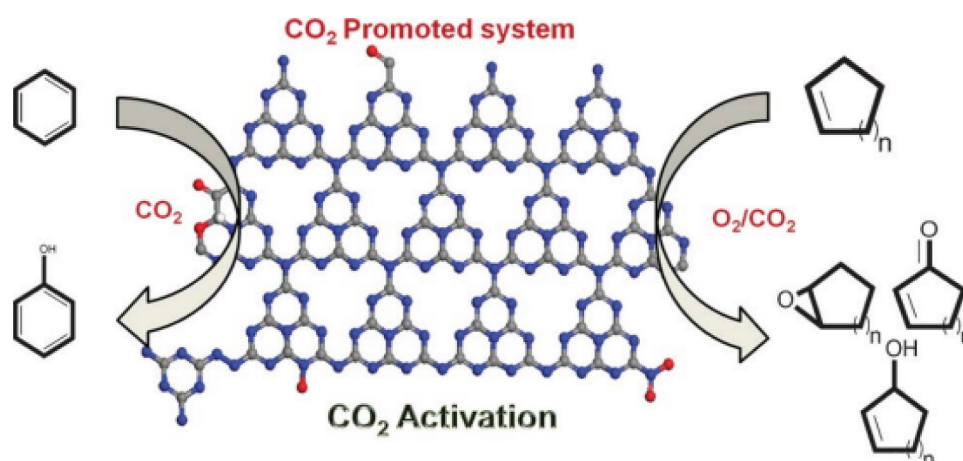


Figure 6. Oxidation of benzene to phenol over mesoporous g-C₃N₄, reproduced with permission from [114].

•OOH from superoxide anions. Finally, the intermediates formed transformed into the products with the simultaneous formation of water as the side product (Figure 7) [122]. In another innovative approach, Mazzanti et al. have successfully prepared g-CN thin films for the visible light-mediated conversion of benzyl alcohols to corresponding benzaldehydes [123]. In this case, the oxidation of benzyl alcohols mediated by the g-CN thin films involves singlet oxygen, which is sensitized via energy transfer (EnT) from triplet excited states.

Aerobic oxidative coupling of resveratrol and its analogs by mesoporous g-CN was also accomplished. The metal-free reaction environment, visible-illumination, and the use of molecular O₂, make this photocatalytic aerobic oxidative coupling reaction an environmentally benign process. The reaction mechanism involves: the generation of superoxide radical anion (O₂^{•-}), hydrogen abstraction/proton transfer from the substrate, and simultaneous formation of hydrogen peroxide. Parallely, holes generated in the valence band of the catalyst, assist the formation of the quinone methide radical and benzyl radical which further undergo coupling and tautomerization to yield δ-viniferin [124].

4.2.2. Modified carbon nitrides in oxidation

Modification of g-CN materials through deformation [125], hydrolysis [126], doping [127], and conjugation [128] was widely employed to enhance their catalytic performance. Incorporation of heteroatom into the g-CN, coupling of metal oxide and carbon nitride forming heterojunction, and metal complex anchoring onto the mesoporous g-CN surface impart additional functionality to the parent g-CN. These formed hybrid materials find important catalytic applications in chemical transformations [113,129,130]. For example, Ru nanoparticles were deposited on graphitic CN and N-doped MCN, and they were studied in the oxidation of betulin to betulone. It was observed that Ru supported on a hard-templated carbon nitride exhibited higher catalytic activity compared to Ru/N-carbon

nitride composites, and the high catalytic activity in the former case was attributed to the higher concentration of weak basic sites [131]. Thomas et al. found a linear correlation between the population of weakly basic nitrogen atoms on the g-CN surface and the quantity of Pd incorporation, which again exhibited an excellent correlation in the oxidation activity of benzyl alcohol and selectivity towards the formation of benzaldehyde. These nitrogen-enriched g-CN displayed comparable activity with polymeric C-N materials [132]. Zou et al. have successfully demonstrated non-noble metal oxide V₂O₅ deposited onto the g-CN in the reaction of styrene to benzaldehyde. The aldehyde formation was linked to the hydroxy radical-mediated mechanism when hydrogen peroxide was employed as an oxidant (Figure 8(a)). The reaction was carried out in a thermo photocatalytic system. Several analogues of styrene were also tested for oxidation to yield corresponding aldehydes in high yields [133].

Carbon nitride can also have the ability to accelerate the oxidation of organic chemicals through the photo-redox process under the irradiation of sunlight. Gand his co-workers examined aerobic oxygenation of the benzylic methylene for the generation of synthetically and biologically valued isochromanones, phthalides, isoquinolinones, isoindolinones, and xanthenes using g-CN as a catalyst under sun illumination. g-CN can oxidize tertiary C-H bond to tertiary alcohols by O₂ using PCN, a carbon nitride from Urea and formalin, under blue LED irradiation in the presence of N-hydroxytetrachlorophthalimide (Cl₄NHPI) [122,136], and activated O₂^{•-} radical transferred to Cl₄PINO, resulting in the oxygenation of the tertiary C-H to alcohols, where Cl₄PINO works for HAT reagent in photocatalysis. The oxidative cleavage of vicinal diols was examined by CN620, prepared from DCDA in a micellar medium under air, which gave ketone or aldehyde in good to high yields. PCN can also be used for the oxidative cleavage of C=C in aryl olefins to corresponding carbonyls in the presence of N-hydroxysuccinimide (NHSI) under visible illumination [137]. Fenofibrate, a pharmaceutical drug

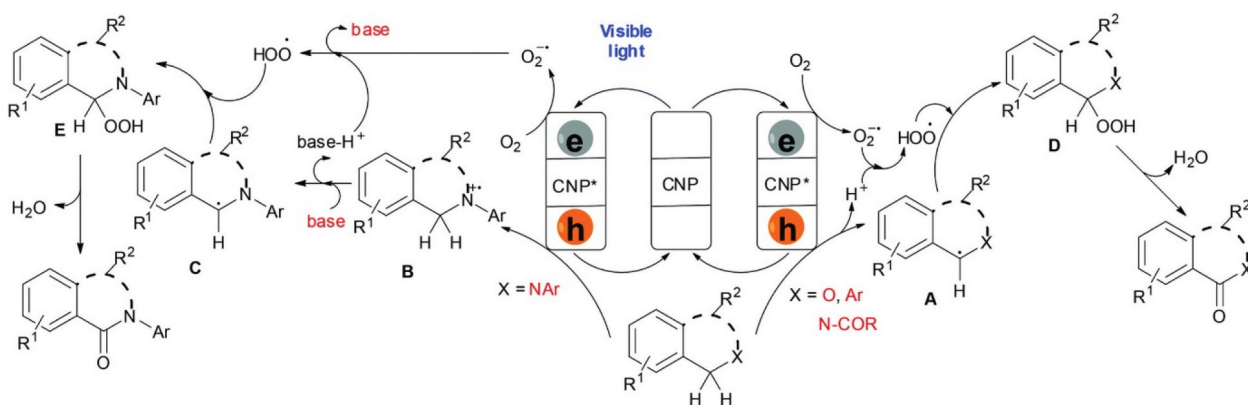


Figure 7. Plausible reaction mechanism for the synthesis of isochromanones, phthalides, isoquinolinones, isoindolinones and xanthenes from readily accessible alkyl aromatic precursors, reproduced with permission from [122].

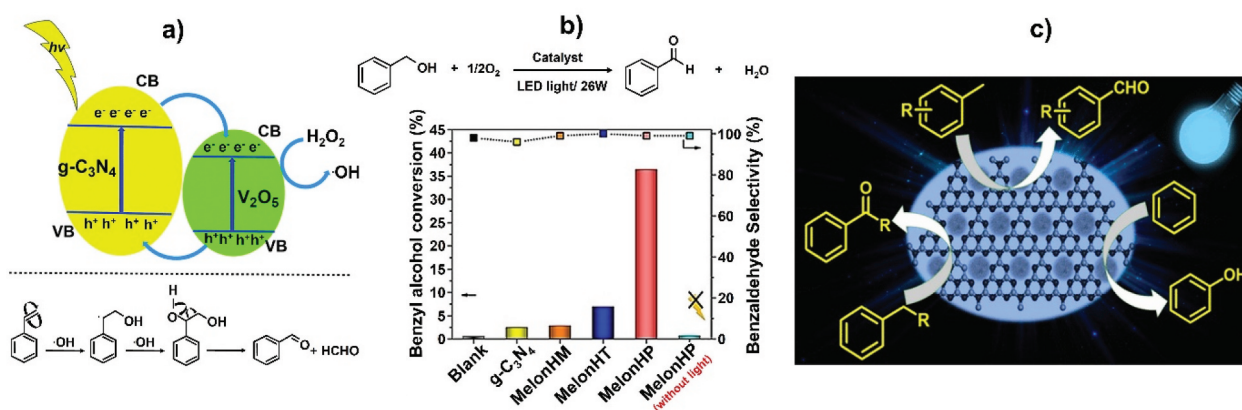


Figure 8. (a) Oxidation employing non-noble metal oxide incorporated on g-CN surface, reproduced with permission from [133], (b) Comparisons of benzyl alcohol conversion and benzaldehyde selectivity over various photocatalysts for visible-light-induced photocatalytic aerobic oxidation to benzaldehyde, reproduced with permission from [134], and (c) Oxidation of methyl arenes and their analogues, reproduced with permission from [135].

for the treatment of abnormal lipid levels, was also synthesized from the corresponding olefin without metal contamination. Cyanamide-functionalized carbon nitride (MCNCN_x) was also employed for the oxidation of sulfinates to vinyl sulfone and the resultant catalyst showed excellent activity with a high yield to vinyl sulfones [138].

Wang and his co-workers carried out the in situ formation of azo-methine ylides from aldehyde and N-methyl alanine and applied for the oxidation of β -IP to KIP and its precursor, 4-hydroxy-3,5,5-trimethyl-2-cyclohexen-2-one (HIP) with oxygen under visible illumination [130]. The oxidation was enhanced by the functionalization of g-CN with ylides with ferrocene moiety and in the addition of NHPI under photoredox catalysis, resulting in KIP 88% conversion with 93% selectivity at a mild temperature of 25°C. Photoinduced catalysis of g-CN with NHDI also worked well for the allylic oxidation of cholesteryl acetate to 7-keto-cholesteryl acetate. The oxidation of allylic C-H bonds enhanced by redox properties of g-CN coupled with nitrosyl radical from NHPI using O₂ as oxidant.

Cu-incorporated g-CN was successfully employed for the simultaneous oxidation and amidation in one reaction step in the liquid phase with excellent activity, reusability, and a simple workup method [139]. The reaction proceeds through a free radical mechanism in the presence of a Cu/g-CN catalyst and *tert*-butyl hydroperoxide as an oxidizing agent. In similar research work, Gafuri et al. have studied the oxidative amidation tandem reaction employing the Cu(II)- β -cyclodextrin immobilized on g-CN nanosheets as a highly effective catalyst. The oxidative amidation was accomplished in a single step. The reaction proceeds through a free radical mechanism with hemiaminal intermediate in the presence of activated *tert*-butyl peroxy radical [140]. Epoxidation of trans-stilbene to trans-stilbene oxide was also effectively catalyzed by bimetallic clusters

(Fe, Pd, and Ir) supported on the mesoporous g-CN catalysts in the liquid phase. These catalysts showed superior conversion of the substrate and selective formation of the epoxide which was attributed to the formation of active oxygen species [141]. Han and colleagues have also reported the oxidation of toluene to benzaldehyde catalyzed by Cu and B doped g-CN by *tert*-butyl hydroperoxide (TBHP) oxidizing agent [142]. The presence of the redox cycle created by these metal ions facilitates free-radical oxidation which helps in achieving excellent catalytic performance.

Benzyl alcohol was converted to benzaldehyde employing thiophene-anchored g-CN in a photocatalytic reaction under visible light. The reason for the selective oxidation of the substrate was an effective modification of π -conjugated system of the substrate, causing a change in the intrinsic properties of the semiconductor. The formation of singlet oxygen (¹O₂) observed by electron spin resonance (ESR) analysis further confirms the oxidation capability of the functionalized CN [143]. Zheng et al. have reported the conversion of α -hydroxy ketones to 1,2-diketones catalyzed by mesoporous g-CN by irradiation of visible light [117]. The prepared catalyst promoted the activated O₂ to generate the superoxide radical anion ($\bullet O_2^-$) which reacted with the substrate to form an intermediate alkoxide anion.

A photocatalytic oxidation reaction was carried out using cobalt ion-impregnated mesoporous g-CN prepared via a simple sonication technique. Ghafuri et al performed one-pot photo-oxidation of alcohol and Knoevenagel condensation using a mesoporous g-C₃N₄ catalyst. The reaction mechanism involves the excitation of electrons from the valence band to the conduction band with simultaneous production of holes which facilitate the oxidation of Co⁺² to Co⁺³ species. The generation of photo electrons during this process helps in the formation of oxygen anionic radicals. The existence of O₂⁻ species and the presence of

the basic sites on the ordered mesoporous graphitic CN further facilitates the deprotonation of benzyl alcohol to produce anion, which reacts with the holes (h^+) to produce the carbon radical. In the end, the recombination of the radical with the superoxide radical lead to the formation of aromatic aldehydes. Due to the presence of the amine groups on the surface of g-CN, deprotonation of malononitrile occurs. Subsequently, the catalyst activates the C=O bond of aldehyde followed by the nucleophilic addition of carbanion and the dehydration to afford benzylidenemalononitrile [98].

Igor Krivtsov et al. studied the effect of phenyl substituents on the partial oxidation of benzyl alcohols employing thermally etched and H_2O_2 -treated polymeric graphitic carbon nitrides (g-CN). Based on the results obtained (Table 11), authors have concluded that electron donating (ED) substituents in para- and ortho-position to the CH_2OH -group promote the reactivity of the substrate without compromising the selectivity towards benzaldehyde formation, compared to the unsubstituted substrate. Similar results were noticed in the case of meta-substituted benzyl alcohol with electron (EW) group. On the other hand,

Table 11. Initial reaction rate of methoxy-substituted alcohols to aldehydes, conversion of the reaction after 4 h of irradiation and selectivity at 20% of conversion in the presence of the TE and TEO photocatalysts [142].

Substrate	Product	Initial reaction rate 10^4 [mM min ⁻¹]		Conversion [%]		Selectivity [%]	
		TE	TEO	TE	TEO	TE	TEO
		16	8	50	29	82	88
		91	19	100	82	90 ^a	89 ^a
		77	18	100	100	98	96
		30	13	76	47	72	85
		109	48	100	100	84	89
		40	41	100	100	80	92
		20	19	63	58	40	78
		27	19	54	50	25	46
		11	7	33	22	55	58
		28	22	78	64	94	94

[a] Selectivity at 60% of conversion.

the presence of ED-group in meta-position or EW-group in para position reduced the reactivity as well as the selectivity towards the product. Theoretical (Quantum mechanical) studies implied that the reactivity correlates with the positive charge on the benzylic carbon in the benzyl alcohol cation intermediate, while the selectivity, most probably, was impacted by a negative charge on the phenyl ring. The H₂O₂ treatment of the catalyst enhanced the product selectivity [144]. Along similar lines, Zhang et al. synthesized the carbon-nanodot doped g-CNs and tested them in the aerobic oxidation of BA, and substituted BA in the photocatalytic pathway. Studies are conducted employing EW and ED functional groups substituted on the benzyl alcohol. The reaction mechanism was not established. Authors have also carried out E-factor parametric analysis (Table 12) at the laboratory scale to establish the feasibility of commercialization of these catalytic materials [145]. In another interesting report, Garcia et al. also employed g-CN photocatalysts derived from the polycondensation of melamine, cyanuric, and barbituric acids for the selective oxidation of aromatic alcohols [146]. The hydrazone-linked heptazine-based PCNs were tested in the aerobic oxidation of benzyl alcohol to benzaldehyde in a photocatalytic pathway under mild reaction conditions and the results are presented in Figure 8(b). It was seen that hydrazone linkages in the PCNs played a vital role in the photocatalytic reaction, making MelonHP which is 17 times more active than parent g-CN. This synergistic effect between hydrazone linkages and heptazine units was further established by the much lower photocatalytic activity of an analogous heptazine-based porous polymer without the hydrazone moiety (MelonP) [134].

Bellardita et al. have studied the phosphorous-doped g-CNs in the photocatalytic oxidation of BA. Photocatalytic oxidation under UV and visible illumination of BA, 4-methoxy BA and piperonyl alcohol exhibited improved selectivity towards the benzaldehyde. The presence of cyanuric acid during the synthesis of g-CN did not significantly alter the oxidizing ability, nevertheless increased the conversion of the alcohol and the selectivity of the aldehyde product and was attributed to the higher specific surface area of the modified sample compared to the parent g-CN [147].

Table 12. Estimation of the waste generated in the photocatalytic oxidation of carveol to carveone [143].

Contributor	E-factor contribution [kg kg ⁻¹]
Reaction	
Water	38.8
CD-C ₃ N ₄	0.26
CO ₂ from a light source	12.800
DSP	
CH ₂ Cl ₂	102.8
MgSO ₄	1.9

Verma et al. developed VO@g-CN catalysts for the oxidation of methyl arenes and their analogues photochemical pathway employing H₂O₂ as an oxidant. Schematics of the types of oxidations achieved are presented in Figure 8(c) [135]. Huang et al. fabricated a ship-in-the-bottle type nano photocatalyst thiophen-incorporated covalent triazine framework (CTF) for the selective oxidation of alcohols to the corresponding aldehydes and ketones, with molecular oxygen. Interestingly, the activity of the CTF was comparable to that of metal oxide catalysts [148]. Shvalagin et al. synthesized molten potassium and lithium salts treated g-CNs by post-synthetic treatment. These materials were employed as photocatalysts in BA oxidation to benzaldehyde in the presence of Air/O₂ at room temperature. The modified catalysts improved the product yield by sixfolds [149]. On the other hand, Wu et al. synthesized Co₃O₄-impregnated g-CN catalysts and successfully used them in the aerobic oxidation of BA to benzaldehyde in the liquid phase at 80°C. The enhanced activity is a result of a synergistic effect between Co₃O₄ and g-CN [150]. Pahari and Puravankara synthesized a hybrid catalyst consisting of layered phosphorene and layered carbon nitride for the selective conversion of toluene and benzyl alcohol to benzaldehyde, photocatalytically in the presence of O₂. The superior catalytic activity is ascribed to the synergistic electronic coupling at the interfacial layers of the phosphorene and carbon nitrides. It was demonstrated that the active oxidation species are photogenerated electron-hole pairs and superoxide anion radicals [151]. Zhang et al. successfully synthesized non-metal P/S doped g-CN hierarchical mesoporous spheres. These S-doped g-CN meso spheres successfully acted as a catalyst in the H₂ production coupled with benzyl alcohol oxidation to benzaldehyde in the presence of TEOA sacrificial agent in a photocatalytic pathway. Sulfur doping created a synergistic effect and an electronic structure modulation of hybrid material resulting in more trapping centers and broader visible light absorption [152].

Gu and co-workers studied the impact of g-CN morphology and their specific surface area on the photocatalytic oxidation of BA to benzaldehyde. Bulk, lamellar, and coralloid g-CNs were synthesized employing chemical and annelation procedures. It was found that coralloid-derived g-CN formed a higher specific surface area (123.7 m²g⁻¹) g-CN compared to the bulk (5.4 m²g⁻¹) and lamellar g-CNs (2.8 m²g⁻¹) resulting in a higher photocatalytic efficiency. The improved efficiency of coralloid g-CN was the effective capture of electrons and acceleration of carrier separation, due to the presence of a higher number of nitrogen vacancies. Improved catalytic activity was also due to the formation of superoxide radicals ($\cdot\text{O}_2^-$) and holes (h^+) in the oxidation process and the higher

surface area of the coralloid g-CN that is responsible for the improved active collision of the substrate. The results of different catalysts prepared in this study and benzyl alcohol oxidation reaction results are summarized in Figure 9(a,b) [153].

In another interesting report, Lima et al. employed chemical, thermal and mechanical procedures to introduce the defects in the structure of parent g-CN. These materials were tested in the benzyl alcohol aerobic oxidation employing an LED light source in a photocatalytic pathway in aqueous media. Thermal treatments have reduced the band gap energy while mechanical treatments widened the same. Specific surface area (SSA) was also significantly increased in the case of the thermally treated samples, whereas very little increase in SSA was observed in the case of mechanically and chemically treated g-CN's (Figure 9(c,d)). The benzaldehyde yield was 3–4 times higher using a thermally treated catalyst, compared to bulk g-CN. Mechanically and chemically treated g-CN's have exhibited a fall in the yield of benzaldehyde due to a very low increase in the band gap [112].

The same group also studied the reduced graphene oxide(r-GO)/carbon nitride (CN) hybrid photocatalyst for the BA oxidation to benzaldehyde. Employing UV light as the energy source in photocatalysis all the photons were absorbed by the CN phase. In thermally treated g-C₃N₄ catalysts (CN_T) due to the exfoliation,

the behavior of the photocatalyst was very similar and most of the photo-generated holes (h⁺) were efficiently used in the oxidation reaction. The reduced graphene oxide (0.1 wt% r-GO) plays the role of electron sink, promoting effective charge separation between the photogenerated e⁻/h⁺ pairs (Figure 10(a)). As the loading of rGO increased the surface electric charge of the CN_T surface rises, promoting the electronic transition between excited CN and rGO (Figure 10(b)), however with further increase in the rGO loading photocatalytic performance fell as photons absorption faced competition from CN_T. In the visible light range, absorption by CN_T was low. The CN_T phase gets activated by a small part of the visible spectrum and rGO played the role of electron quencher preventing the electron-hole recombination (Figure 10(c)). The conversion of BA and product selectivity was considerably low due to the overlap between LED emission and photocatalyst absorption being smaller. On the other hand, the remaining visible irradiation (450–700 nm) can photo-excite the rGO phase, and as the energy levels of the CN_T conduction band and rGO excited state are similar, the thermodynamic barrier to e⁻ transfer was negligible and the photogenerated e⁻/h⁺ pairs were stabilized by back electron donation (from rGO to CN_T conduction band), thus creating reactive holes on the rGO surface which was available for the selective oxidation of BA [154]. Fernandes et al. synthesized

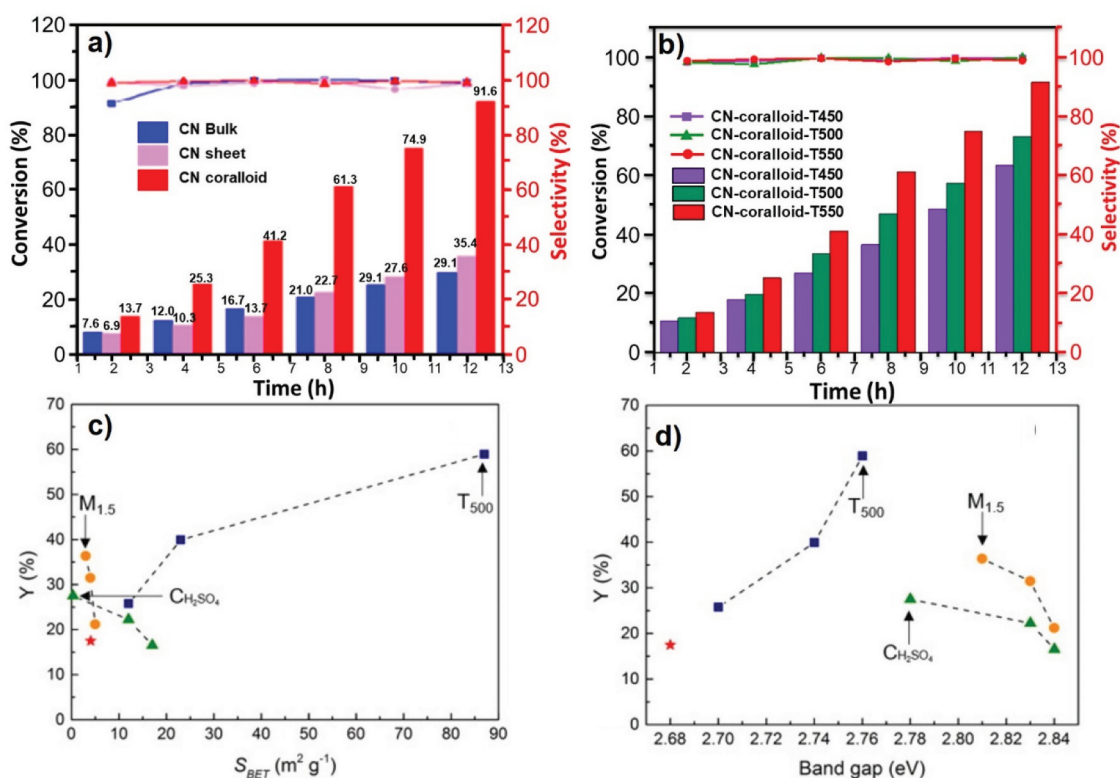


Figure 9. Photocatalytic oxidation of benzyl alcohol over (a) various forms of CN, and (b) various coralloid CNs annealed at different temperatures, reproduced with permission from [153], and (c & d) Yield of BAL production using bulk g-C₃N₄, and post-treated photocatalysts by chemical, mechanical and thermal methods as a function of S_{BET} and band gap, reproduced with permission from [112].

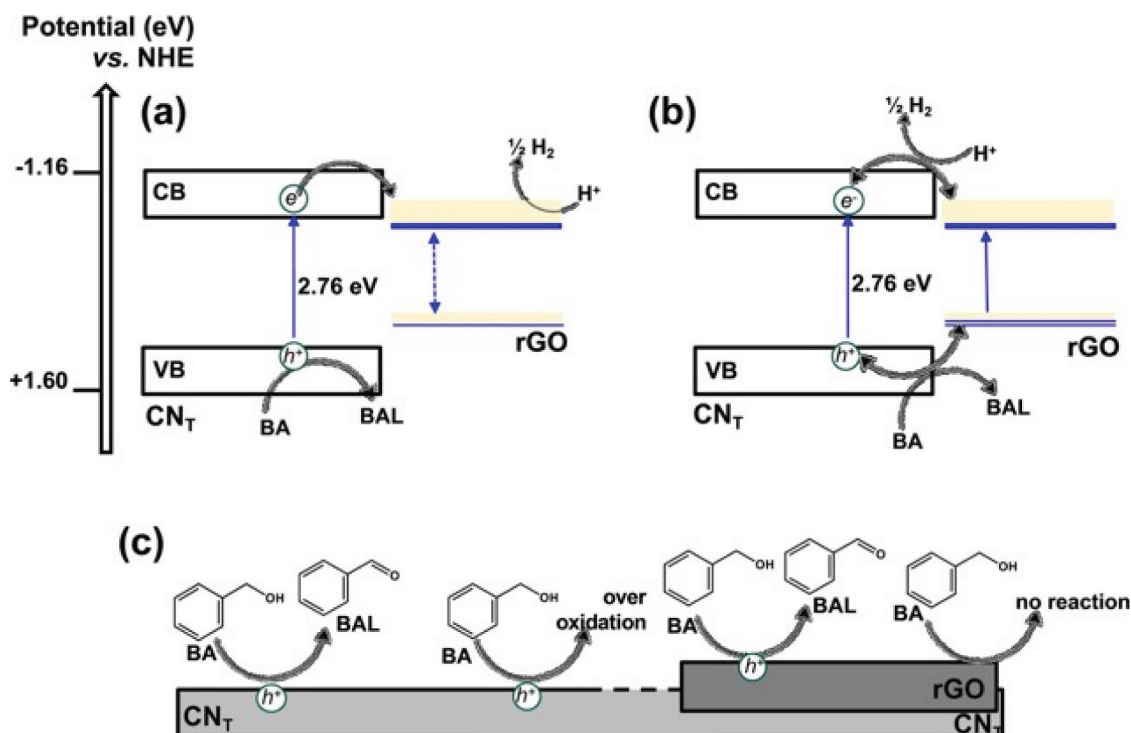


Figure 10. Proposed mechanism for selective oxidation of BA by 0.10 rGO/CNT using a) UV and b) visible irradiation, and c) schematic view of the oxidation of BA to BAL in the catalyst surface of CNT and 0.1% rGO/CNT catalyst, reproduced with permission from [154].

defect-induced 3-dimensional g-CN employing DCDA precursor, silica template via hard-templating route resulting in high specific surface area materials. These catalysts were successfully used in the photocatalytic conversion of p-anisyl alcohol to p-anisaldehyde in deoxygenated aqueous solutions under UV-LED irradiation [155]. In a similar work, Long et al. used g-CN catalysts for the selective photooxidation of aromatic alcohols in aqueous media. It was demonstrated that the unique electronic structure of carbon nitrides avoids the direct formation of hydroxyl radicals that typically cause the total oxidation of organics [156]. In another report, Ding et al. demonstrated the synthesis of defect-induced g-CN, employing nitric acid-pre-treated melamine as a precursor. The prepared material showed excellent photocatalytic aerobic oxidation activity for the conversion of BA to benzaldehyde owing to the greater SSA and the presence of nitrogen vacancies that resulted in the enhancement of optical absorption of visible light causing the separation efficiency of photogenerated electron-hole pairs [157].

Zhang et al. studied the effect of solvent in the photocatalytic oxidation of glycerol employing oxygen-functionalized g-CN. It was noticed that the nature of the solvent employed has a pronounced impact on the oxidation reaction pathway and the type of the product formed. Figure 11 indicates the reaction pathways over the catalyst surface in acetonitrile and water solvents. Active radical capture experiments and EPR investigation established that singlet oxygen and superoxide radicals were the main reactive species in

the reaction mechanism. Moreover, it was found that the oxidative esterification reaction can occur to generate new ester compounds in the glycerol acetonitrile solution [158].

4.3. Hydrogenation by g-CN and their metal-modified forms

Porous g-CN are excellent supports for the hydrogenation reaction. Pd, Au, Pt, Ni supported on g-CN and mesoporous g-CN were extensively studied for the hydrogenation reaction [159,160]. For example, the selective hydrogenation of phenol and its derivatives over a Pd/g-CN catalyst in aqueous media was carried out by Wang et al. The catalysts showed very high conversion of phenol and selectivity towards hexanone. This was attributed to the structure of the catalytic semiconductor-metal heterojunction, resulting in stable and uniform dispersion of Pd. The resulting morphology, crystal structure, and electronic configuration of the catalyst surface facilitated the adsorption of the substrate in an energetically favorable mode, offering the highest conversion and product selectivity [161]. Dodangeh et al. also carried out the hydrogenation of acetylene over Ni-supported mesoporous g-CN catalyst. Careful manipulation of the feed composition ratio (mole ratio H_2/C_2) and optimization of reaction temperature yielded greater conversion of acetylene and higher selectivity of ethylene when compared to the commercial catalyst [159]. The selective hydrogenation of nitroarenes to their corresponding aryl amines has

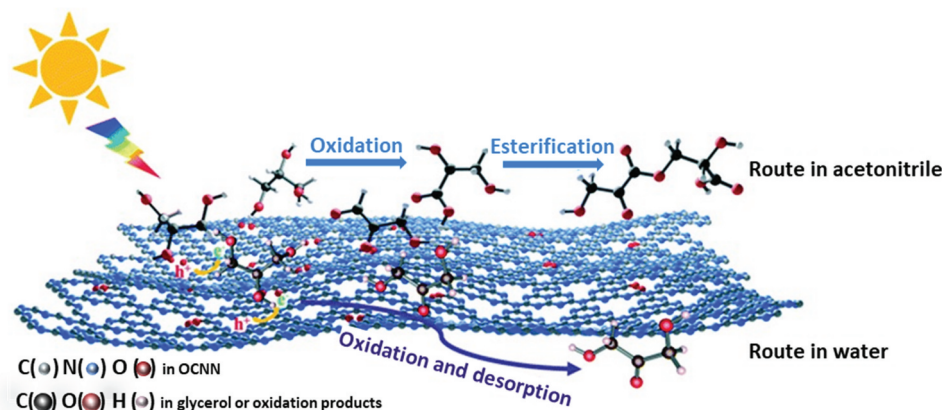


Figure 11. Possible photocatalytic reaction routes for glycerol oxidation over OCNN-2 in water and acetonitrile, reproduced with permission from [158].

been achieved by mesoporous g-CN (Ni-W₂C/g-CN) in the presence of Lewis acid tungsten carbide. Greater than 92% yield and 100% selectivity were achieved for phenylamine. It was demonstrated that Ni-W₂C component acts as a catalyst for the generation of active hydrogen, whereas g-CN plays the role of the base, weakening the N-O bond [162].

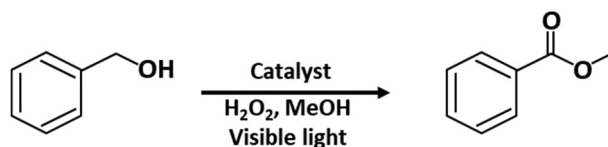
Pd, Pt, Ag, and Au supported on g-CN catalysts were also employed in the styrene hydrogenation to ethyl benzene at room temperature. Excellent conversion of styrene (99%) and more than 99% selectivity were observed using Pd/g-CN. The highly reusable nature of the catalyst was attributed to Mott-Schottky effect between the metal nanoparticles and the carbon nitride support [163]. In another interesting report, Coulson et al. demonstrated the synthesis of inorganic Ir complex ($[(\eta^5\text{-C}_5\text{Me}_5)\text{IrCl}(\text{g-CN-k}2\text{N,N}')]\text{Cl}$) anchored to the g-CN, which is highly active in the hydrogenation of terminal alkenes. The remarkable selectivity of the catalyst for the desired product is due to the restricted steric environment of the outer coordination sphere at the edge sites of g-CN [164]. Pd supported on to the ordered mesoporous graphitic carbon nitrides (ompg-C₃N₄) was also tested for the chemoselective hydrogenation of quinoline. It was learned that Pd (0) nanoparticles were stabilized by the active amino groups present on the support surface coupled with the synergistic effect. Mass transfer limitations were minimized by the ordered cylindrical mesoporous structure providing the higher selectivity of the hydrogenated product [165].

4.4. Esterification and transesterification

Direct esterification from an acid and an alcohol, transesterification from an ester and alcohol, and the ester exchange reaction between two esters are all essential economic processes in producing renewable chemicals [166]. Both these reactions have been

studied by acid and base catalysis, involving homogeneous and heterogeneous counterparts. Esterification and transesterification are industrially performed using homogenous strong base catalysts like NaOH or KOH [166]. On an industrial scale, however, this results in time-consuming and costly purification operations and the inability to replenish the catalyst. As a result, the search for an appropriate and efficient heterogeneous catalyst continues. While various heterogeneous catalyst alternatives have been offered, these catalysts frequently contain metals to make them catalytically efficient, which makes their synthesis expensive and the catalyst susceptible to metal leaching [167]. Carbon nanotubes (CNTs), graphene, carbon quantum dots, graphitic carbon nitride (g-C₃N₄), and other carbon-based materials have received attention in recent years due to their exciting properties [168]. Among these catalysts, g-C₃N₄ has demonstrated a varied variety of possible applications, particularly in the semiconducting application, namely, in photochemical esterification reactions. The structural characteristics underline that g-C₃N₄ possesses both basic and semiconducting capabilities [129]. The triazine moiety governs the semiconducting nature (electronic property), whereas the surface uncondensed amine groups and the edge-positioned C-N-C motif rule the multifunctional property (Brønsted and Lewis basicity). Surprisingly, the catalytic activity can be controlled by tuning the edge terminations with a less ordered structure, increasing the surface area, and incorporating suitable acidic properties via functionalization or intrinsic surface modification with heteroatoms such as B, O, F, P, S, and so on [167,169,170].

Verma and his colleagues demonstrated direct esterification of alcohols by C-H activation utilizing several transition metal-impregnated g-C₃N₄ materials [171]. It was observed that even after a 24-h reaction, the reaction with Fe₃O₄@g-C₃N₄ produced no ester but just benzaldehyde. The copper (Cu@g-C₃N₄)

Table 13. Oxidative esterification of alcohols over various transition metal-based g-C₃N₄ catalysts [173].

Entry	Catalyst	Time	Yield ^{a,b}
1 ^c	Fe ₃ O ₄ @g-C ₃ N ₄	24 h	-
2 ^c	Cu@g-C ₃ N ₄	24 h	-
3 ^c	Ag@g-C ₃ N ₄	24 h	-
4 ^c	Pd@g-C ₃ N ₄	12 h	35%
5	V ₂ O ₅ @g-C ₃ N ₄	12 h	64%
6	V(II)@g-C ₃ N ₄	12 h	37%
7	VO@g-C ₃ N ₄	3 h	98%
8 ^{c,d}	VO@g-C ₃ N ₄	12 h	-

^aReaction condition: 1 mmol of benzyl alcohol; methanol 2 mL; 1.5 mmol H₂O₂; Catalyst 25 mg; 40-watt domestic bulb; ^bisolated yield; ^cBenzaldehyde formation was observed; ^dReaction performed under dark.

and silver (Ag@g-C₃N₄) impregnated g-C₃N₄ materials do not affect the reaction. Pd@g-C₃N₄ gave a 35% yield of methyl benzoate since the reaction did not complete; the remaining benzyl alcohol was transformed into aldehyde and the corresponding acid. Further, vanadium-based g-C₃N₄ catalysts gave better results under photochemical circumstances owing to their semiconductor behavior (Table 13) [172]. The VO@g-C₃N₄ was prepared by calcining urea at 500°C for 3 h and then dispersing it in a methanolic solution of vanadyl acetylacetonate [VO(acac)₂] under sonication. It was demonstrated that 98% methyl benzoate yield was obtained by oxidative esterification via photocatalytic C-H activation of benzyl alcohol with methanol utilizing H₂O₂ as an oxidant and VO@g-C₃N₄ in methanolic medium and under visible illumination. Only a trace quantity of oxidative esterification product was produced during the control reaction

using pure V₂O₅, demonstrating that g-C₃N₄ is not only hydrogenizing the V₂O₅ but also functioning as a promoter under photochemical conditions. The g-C₃N₄ operates as a basic surface to speed up C-H activation and esterification. The built-in photoactive chromophore would absorb energy and help to cross the activation energy barrier, allowing esterification to occur [173].

In another study, the highest activity in the photocatalyst screening was demonstrated by the g-C₃N₄ derivative prepared by co-condensation of urea and oxamide followed by post-calcination in a molten salt (CN-OA-m) [174], presumably due to its enhanced optical absorption in the visible region compared to most other known CN materials. Pieber et al. investigated the use of g-C₃N₄ materials in semi-heterogeneous catalytic systems for dual nickel/photocatalysis (Figure 12(a)) [175]. Under the

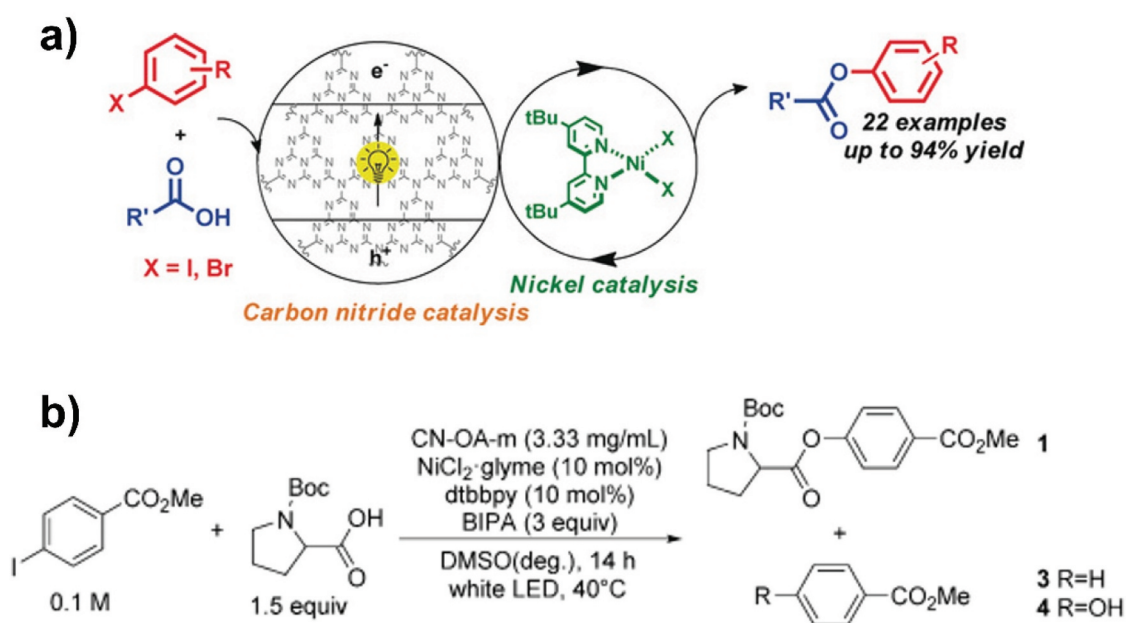


Figure 12. (a) Semi-heterogeneous dual nickel/photo catalysis using carbon nitriles for esterification of carboxylic acids with aryl halides, reproduced with permission from [175], and (b) CN-OA-m in the dual nickel/photocatalytic esterification of methyl 4-iodobenzoate with Boc-Pro-OH, reproduced with permission from [175].

influence of white-LED (RGB) irradiation, carbon nitride materials can catalyze the esterification of *N*-(tert-butoxycarbonyl)-proline (BocPro-OH) and methyl 4-iodobenzoate. A comprehensive analysis of all other reaction parameters revealed that a cocktail of CN-OA-m (3.33 mg mL^{-1}), NiCl_2 glyme, 4,4-di-tert-butyl-2,2-dipyridyl (dtbbpy), and *N*-tert-butylisopropylamine (BIPA) in dimethyl sulfoxide (DMSO) is particularly suitable, delivering the desired ester 1 in 96% yield after 14 h of irradiation (Figure 12(b)). The catalyst gave excellent yields for a broad range of aryl iodides and carboxylic acids [175].

For a conventional esterification reaction, Samanta and Srivastava prepared a series of g- C_3N_4 (CN) catalysts using urea(U), thiourea(T), and a mixture of urea-thiourea(UTU) [176]. Functional carbon nitride was prepared by the reaction of g- C_3N_4 with aqueous H_2SO_4 . Characterizations revealed that bi-functional, acidic ($-\text{SO}_3\text{H}$), and basic ($-\text{NH}_2$) sites were introduced after the aqueous H_2SO_4 treatment. The esterification of oleic acid with methanol using the most active catalyst S-CN(UTU)-60 gave a methyl oleate yield of more than 90% in 4.5 h. Similarly, S-CN(UTU)-60 gave 98% dialkyl carbonate yield from the transesterification of cyclic carbonate with methanol. The high yield of di-alkyl carbonate in the case of S-CN(UTU)-60 correlates well with the CO_2 TPD studies showing high basicity in the CN framework. Mesoporous graphitic carbon nitride (CN-MCF) demonstrated 16.2% propylene carbonate (PC) conversion and 83.4% dimethyl carbonate (DMC) selectivity in a typical transesterification operation at 160°C [177]. The catalytic activity was derived from its high surface area and a large number of N-containing species, which were considered as the catalytic active sites in the transesterification, according to N_2 adsorption-desorption and XPS characterization. In another study carried out for biodiesel production, bulk carbon nitride (b-CNMs) catalysts were created by pyrolyzing melamine and then post-modified with thermal (t-CNMs) or acid (a-CNMs) treatments. The nanofibers (f-CNMs) were made by pyrolyzing melamine with a molten salt technique, which resulted in the formation of basic oxygen-rich functional groups on the surface of the f-CNMs [178]. Transesterification of canola oil to biodiesel was then performed, yielding 96% conversion using a 1 wt% catalyst loading, a low oil-to-methanol ratio of 1:24, and reaction temperatures and times of 150°C and 3 h, respectively.

Deprotonated mesoporous g- C_3N_4 was achieved by a simple method of treatment of g- C_3N_4 material with a basic aqueous solution of t-BuOK. The prepared mpg- C_3N_4 -tBu is an active base catalyst in transesterification processes. Using mpg- C_3N_4 -tBu at 110°C , several primary, allylic, cyclic, and aliphatic alcohols were subjected to reactions with ethyl acetoacetate. Transesterification of allylic alcohols is difficult since

the product readily undergoes decarboxylative rearrangement. But in the present condition, unsaturated allylic alcohol such as cinnamyl alcohol underwent transesterification, affording ester in high yield with >85% conversion and 99% selectivity [53].

Vinu and colleagues used a new precursor with a high nitrogen content, aminoguanidine hydrochloride ($\text{NH}_2\text{NHCNHNH}_2\cdot\text{HCl}$), through a hard-templating approach with the mesoporous silica SBA-15 being used as a template to create a highly ordered mesoporous C_3N_6 with an extremely high nitrogen content and tunable pore diameters for the first time [60]. The nitrogen content in the CN nanostructures was higher (1.6–1.8), than usual (0.2, lower than theoretical values), and was tunable via a simple adjustment of the pore diameter of the templates. Such materials with a high N/C ratio showed high activity for the metal-free Friedel–Crafts acylation and transesterification reactions. The same group also proved the basic catalytic performance of MCN for the transesterification of ethyl acetoacetate with various alcohols such as 1-butanol, 1-octanol, cyclohexanol, benzyl alcohol, and furfuryl alcohol under heterogeneous reaction conditions without the use of any solvents at a reaction temperature of 110°C for 6 h. The basic sites in MCN-1, which are formed by free NH_2 groups on the MCN-1 walls and uncondensed terminal NH_2 from ethylenediamine, are the source of its catalytic activity, which promotes the transesterification of ethylacetoacetate as they offer strong Lewis basic sites. The catalytic results demonstrated that MCN-1 was an excellent catalyst in transesterifying long and short-chain primary alcohols, as well as cyclic and aromatic alcohols, to generate high yields of their corresponding β -keto esters. More notably, when 1-butanol was added, the catalyst was extremely active with 69% conversion and 100% butyl acetoacetate selectivity [179]. They also reported for the first time the use of mesoporous ultrasmall silica nanoparticles as a template to create well-ordered mesoporous C_3N_4 nanoparticles with a size smaller than 150 nm (MCN-3) and a high nitrogen content (C_4N_2). MCN-3 has twice the nitrogen content of MCN-1 and MCN-2, which were made from SBA-15 and SBA-16, respectively. MCN-3, a highly ordered, mesoporous, metal-free basic catalyst, was catalytically employed in the transesterification of β -keto esters; MCN-3 showed improved performance in the transesterification of β -keto esters with good conversion and 100% product selectivity Figure 13 [180]. Similar work was reported by Li et al. by preparing SBA-15-supported g- C_3N_4 catalysts, by the dissolution of DCDA into SBA-15, followed by calcination which resulted in CND/SBA-15. This was used to study the transesterification reaction of EC with methanol in a high-pressure autoclave at 0.6 MPa CO_2 at 160°C for 6 h. The CND/SBA-15 material showed a high EC conversion of 81%,

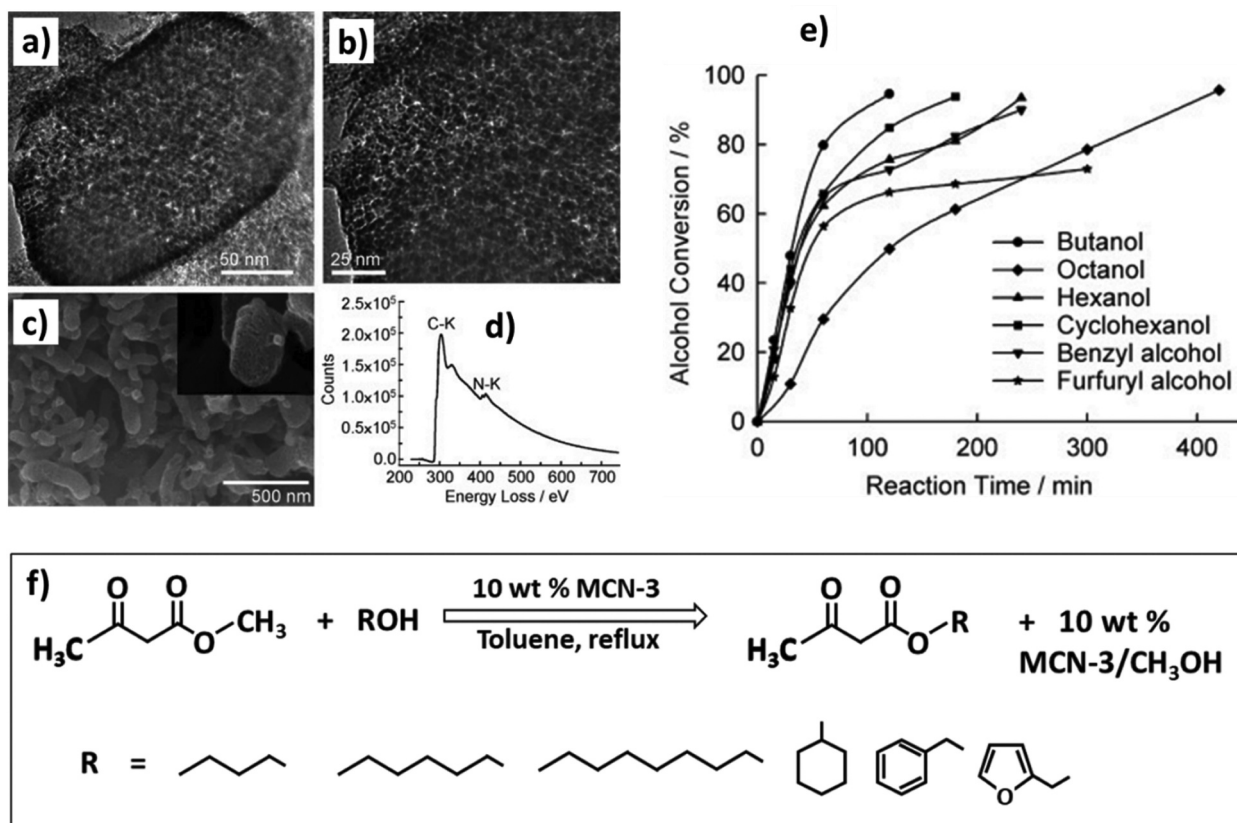


Figure 13. (a & b) Transmission and (c) scanning electron microscopy images and (d) electron energy loss spectrum of MCN-3; (e) Basic catalytic performance of MCN-3 in the transesterification of β -keto esters of different alcohols. Reaction conditions: β -keto ester/alcohol molar ratio 1.2:1, catalyst MCN-3 (10 wt% of total reaction mixture), solvent toluene, reaction temperature 110°C, reproduced with permission from [180].

affording a maximum dimethyl carbonate yield of up to 80%. The chemical compositions of CND/SBA-15 were mainly basic N-containing species in the form of amines [181]. Another important contribution to the transesterification catalysis was a series of mesoporous $g\text{-C}_3\text{N}_4$ materials prepared by DCDA as a precursor by a nanocasting method through a new detemplation. In this, the silica template was removed by an alkaline solution of NaOH, and the material was denoted as CND-NaOH ($g\text{-C}_3\text{N}_4$ detemplated by NaOH). The mesoporous CND material exhibited excellent activity in the transesterification of EC and CH_3OH . After the catalytic test of 6 h at 160°C, the conversion of EC and selectivity to DMC were 91.3% and 99.3%, respectively [92].

By sequential calcination and sulfonation of $g\text{-C}_3\text{N}_4$, Verma et al. reported sulfonated graphitic carbon nitride, ($S\text{-}g\text{-C}_3\text{N}_4$), a polar and strongly acidic catalyst with exceptional reactivity and selectivity in biodiesel synthesis and esterification reactions at room temperature. The acid strength is expected to be higher due to the anticipated positive charge developed on the nitrogenous framework after the attachment of $-\text{SO}_3\text{H}$. During the esterification of oleic acid, a complete conversion to methyl oleate happened in 4 h [182]. The group investigated a wide range of fatty acids and their analogs for esterification and biodiesel

production. All the long-chain fatty acids were converted into corresponding methyl esters, irrespective of the unsaturation in fatty acids. Further, studies with ethyl benzoate and ethyl cinnamate using methanol solvent showed the equilibrium shift to corresponding methyl ester in very high yields (>98%). A larger concentration of methanol, which is utilized as a reaction medium in transesterification, may be the cause of the reaction's rightward solidification.

Esterification/transesterification has been catalyzed by $g\text{-C}_3\text{N}_4$ using either a typical thermally induced approach or a light-assisted pathway [183]. Furthermore, a multi-functional activity can be incorporated in the $g\text{-C}_3\text{N}_4$ materials using selective precursors, surface functionalization, or doping strategies to achieve the required functionality for conventional catalysts and to achieve high visible light absorption capacity with optimum band-edge potentials and excitons lifetime to trigger the desired esterification/transesterification reactions. Thus, there is plenty of room for future $g\text{-C}_3\text{N}_4$ manipulation, such as changes in architecture/morphology and nanostructure (1D/2D/3D) engineering, textural, electrical & optical, and surface properties, to make it an effective heterogeneous catalytic material. Given the economic and environmental benefits of biodiesel or other

essential esters, it is expected that the use of g-C₃N₄ will provide a new sustainable approach for base-catalyzed organic processes [184].

4.5. Cycloaddition of CO₂ to epoxides

CO₂ is a cheap, non-toxic, and readily available carbon source, and utilization of CO₂ as a carbon feedstock for conversion into valuable chemicals is a practical route to reduce global warming. However, CO₂ is both thermodynamically and kinetically inert, and, due to this high stability, its transformation into valuable chemicals is complex [185]. The difficulty of CO₂ activation is the critical limiting factor for its valorization, and very few processes have been commercialized involving large quantities of CO₂, including methanol, salicylic acid, urea, and cyclic carbonates. Cycloaddition reactions using CO₂ is a 100% atom economical process, which involves CO₂ insertion into a 3-membered epoxide ring to yield a 5-membered ring, a cyclic carbonate. To favour this transformation, g-C₃N₄ is considered the favourable catalyst as it can offer both high CO₂ adsorption and basicity with many active centers (Figure 14) [3].

For example, mesoporous g-C₃N₄ synthesized using melamine was used for the conversion of propylene oxide to propylene carbonate using CO₂. The catalyst exhibited 34% propylene oxide conversion and 90% propylene carbonate selectivity with a TOF of 3.4 h⁻¹ under moderate conditions in DMF solvent. Further, g-C₃N₄ supported on SBA-15 was utilized for propylene carbonate synthesis under solvent-free conditions with doped metal ions acting as Lewis's acids sites. Zn²⁺ exhibits the highest cooperativity among the metal salts used for doping, with conversion and selectivity of 98.3% and >99%, respectively (Table 14) [186]. In this reaction, the activated CO₂ is transferred to the epoxide via a transfer mechanism from the g-C₃N₄ nanosphere inside the silica mesopore channel, facilitating cyclic carbonate synthesis

through Zn²⁺ activated epoxide species. In another report, Su et al. demonstrated the synthesis of porous and amino-rich g-C₃N₄ without using a rigid template using urea as the precursor to generate defective and edge-enriched g-C₃N₄ and applied it for the production of a range of cyclic carbonates without a co-catalyst under 100% dry conditions [187]. Edge defects are thought to include primary amines (-NH₂) and secondary amine groups (-C-NH-C), allowing them to activate CO₂. In this case, the epoxide is triggered by the -OH groups on the faulty C₃N₄ edge. The activity of the g-C₃N₄ can be controlled with the adjustment of the carbonization temperature. It was demonstrated that the catalyst prepared at a lower carbonization temperature offered much higher activity than the materials prepared at a higher carbonization temperature. The high activity is attributed to the lower crystallinity and polymerization degree, which resulted in more edge defects, with the incompletely coordinated nitrogen atoms serving as the main active sites in the cycloaddition reaction.

According to Zhao et al., boron-doped carbon nitride (B-CN) is very active and selective for cycloaddition processes. Even under solvent-free circumstances, B-CN supported on mesoporous silica SBA-15 (i.e. B_{0.1}CN/SBA-15) exhibits over 95% conversion and selectivity for cycloaddition of CO₂ and styrene oxide (SO) to generate styrene carbonate (SC). This is mostly owing to the acid-base duality caused by B doping, which allows CO₂ and epoxide to co-activate. A mechanism based on acid-base duality is postulated, in which CO₂ activates the basic >NH sites and SO activates the acidic -B(OH)₂ sites via hydrogen bonding. The SC is formed by the reaction of co-activated CO₂ and SO. Density Functional Theory simulations were performed to support the mechanism, which reveals that the co-adsorption of CO₂ and SO on B-CN is energetically advantageous and follows the Langmuir-Hinshelwood mechanism (Figure 15) [188].

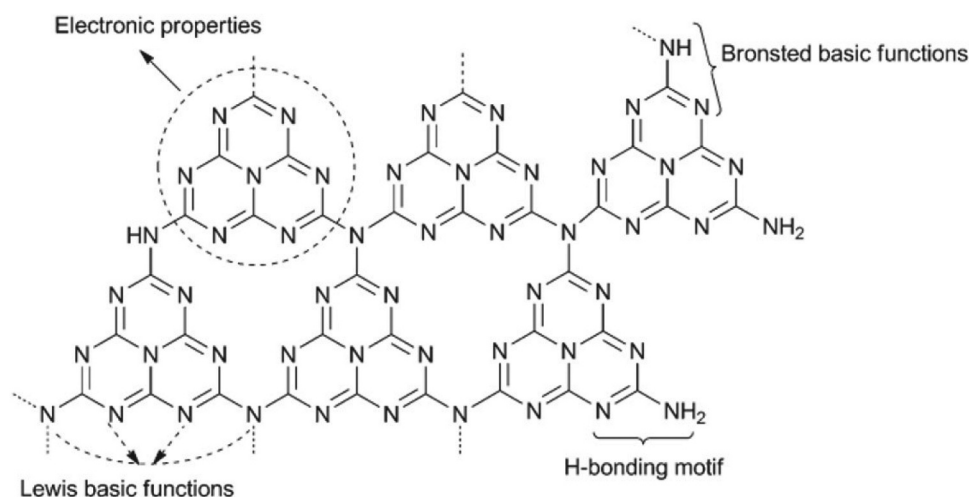


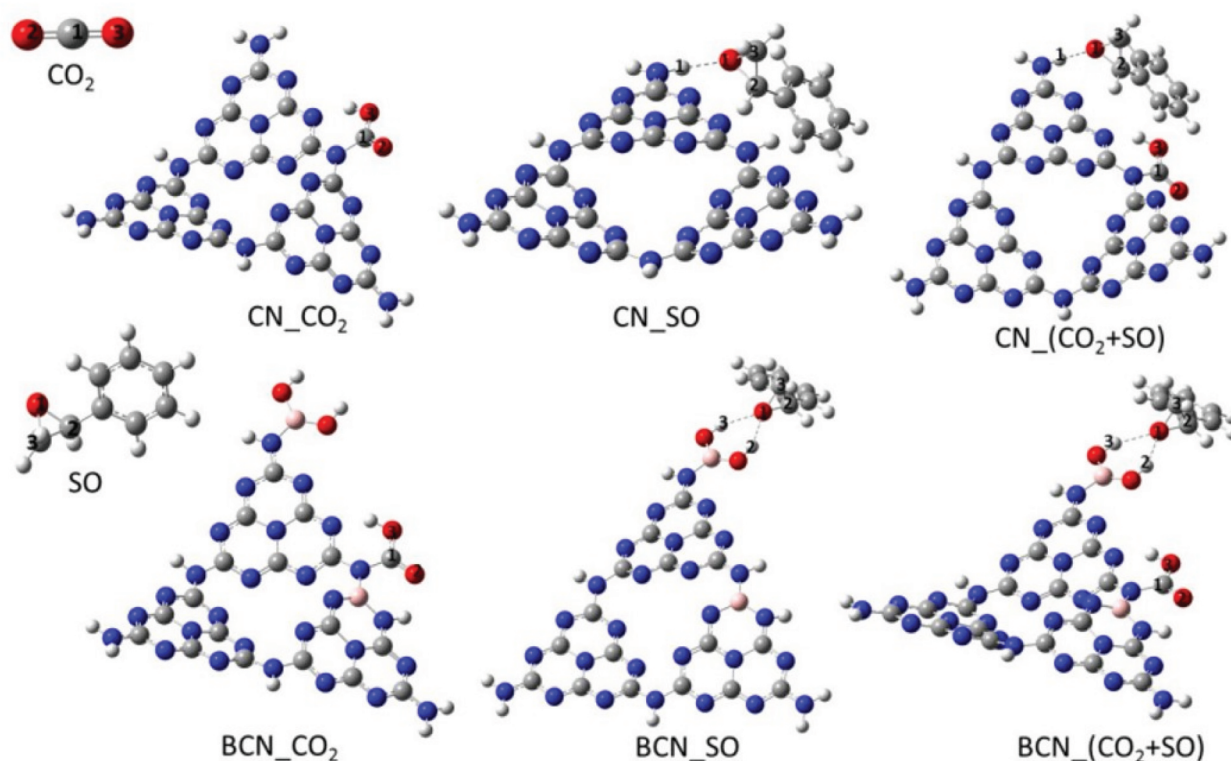
Figure 14. Multiple functional groups in the g-C₃N₄ skeleton, reproduced with permission from [3].

Table 14. Cycloaddition of CO₂ using various metal-doped g-C₃N₄ [187].

Samples	Doped ions (wt%)	Epoxides	Conversion (%)	Selectivity (%)
SBA-15	-	Styrene oxide	0	0
g-C ₃ N ₄ /SBA-15	-	Styrene oxide	28.8	>99
SBA-15	Zn ²⁺ (0.8)	Styrene oxide	7.4	79
g-C ₃ N ₄ /SBA-15	Zn ²⁺ (0.8)	Styrene oxide	94.5	>99
g-C ₃ N ₄ /SBA-15 ^b	Zn ²⁺ (0.8)	Styrene oxide	51.7	92
Porous g-C ₃ N ₄ ^c	Zn ²⁺ (0.8)	Styrene oxide	40.2	94
g-C ₃ N ₄	Zn ²⁺ (0.8)	Styrene oxide	14.1	90
g-C ₃ N ₄ /SBA-15	Cd ²⁺ (0.81)	Styrene oxide	36.7	>99
g-C ₃ N ₄ /SBA-15	Fe ³⁺ (0.82)	Styrene oxide	91.2	>99
g-C ₃ N ₄ /SBA-15	Zn ²⁺ (0.8)	Propylene oxide	97.1	>99
g-C ₃ N ₄ /SBA-15	Zn ²⁺ (0.8)	Ethylene oxide	98.3	>99

^aReaction conditions: epoxides: 3 ml, reaction temperature: 150°C, CO₂ pressure: 3.5MPa, reaction time: 1.5 h, catalyst amount: 0.1 g;

^bThe sample was prepared by the incipient wet impregnation of the precursors; ^cSBA-15 was used the hard template and the silica structures were removed by HF aqueous solution.

**Figure 15.** DFT optimized model for CO₂ and so adsorption/co-adsorption on CN and BCN, reproduced with permission from [188].

In another study, n-bromobutane grafted mesoporous g-C₃N₄ demonstrates higher catalytic activity with 88% conversion and 98% selectivity for solvent-free propylene carbonate production. The in-situ depleted electrophile, Br⁻ activates the epoxide ring, while the defect-rich edge positioned -NH₂ polarizes the CO₂ molecule, resulting in the bi-functional nature. Butane has been examined in conjugation with halides, and it has been discovered that bromide has the best activity due to its superior leaving group ability. The higher catalytic activity is due to the mesoporous nature (15 nm), high surface area (241 m²g⁻¹), and coexistence of terminal -NH₂ groups in g-C₃N₄ and X groups, which is even better than the externally induced n-bromobutane to carbon nitride during the process [189]. Many techniques for increasing g-C₃N₄ activity have been investigated, including increasing surface area,

improving defect sites [187], and immobilizing the functional group [189,190]. The activity of the catalyst for the cycloaddition reaction can be enhanced by the synergetic interaction between acid and basic sites [191]. Therefore, acid-base bifunctional g-C₃N₄ with high efficiency for CO₂ cycloaddition to epoxides is desirable. It should be noted that the bifunctional g-C₃N₄ must be inexpensive, stable, and simple to handle, as well as devoid of metals and solvents during preparation and application. Under metal-free conditions, doping phosphorus (P) is an excellent technique to produce acid sites in g-C₃N₄ [192]. Zhang et al. [192] and Ma et al. [193] both reported that acid sites could be introduced to g-C₃N₄ by replacing C with P at the bay and corner positions, but they employed a costly ionic liquid as a P source, and the amount of P doping was minimal. Furthermore, it is unclear how the doping was carried

out. Hexachlorotriphosphazene (HCCP) has a structure comparable to melamine's tri-s-triazine. Furthermore, during copolymerization, the P-Cl bond is active and readily interacts with the -NH_2 of melamine. The integration of P atoms into the tri-s-triazine network of $g\text{-C}_3\text{N}_4$ is expected to be greatly aided by the usage of HCCP. Direct thermolysis of melamine and hexachlorotriphosphazene yielded a series of P- $g\text{-C}_3\text{N}_4$ with different phosphorous loading, incorporating acid sites into the $g\text{-C}_3\text{N}_4$ framework. In this case, Bu_4NBr served as the nucleophilic anion source to accommodate the basic sites. In the presence of a P- $g\text{-C}_3\text{N}_4$ catalyst and Bu_4NBr as a co-catalyst, the cycloaddition of CO_2 toward PO is higher than when P- $g\text{-C}_3\text{N}_4$ or Bu_4NBr are used alone. Propylene carbonate yield and selectivity are 99.8% and 99.9%, respectively, as compared to Bu_4NBr & P- $g\text{-C}_3\text{N}_4$ alone. The high activity $\text{Bu}_4\text{NBr}/\text{P-}g\text{-C}_3\text{N}_4$ is attributed to the synergetic effect of acid sites and halide anions for the ring-opening of epoxide and the basic sites for adsorption and activation of CO_2 [194].

The cycloaddition of CO_2 with epichlorohydrin for the synthesis of the corresponding carbonate has been achieved solvent-free by Huang et al. using protonated acidic functionality containing carbon nitride treated with H_2SO_4 [195]. As a result of protonation, the surface chemistry and electronic properties of urea-derived carbon nitride have been altered, which has resulted in the incorporation of hydroxyl and amine groups into the bulk carbon nitride resulting in a 17-fold increase in catalytic activity. Surface hydroxyl groups (-OH) and amine groups (-NH_2) are responsible for this improved reactivity. Similarly, Samanta et al. synthesized carbon nitride CN-(UTU) derived from urea and thiourea, which has better catalytic performance than urea/thiourea under cyclic carbonate synthesis from epichlorohydrin without co-catalysts [196]. Furthermore, chemical exfoliation of the resultant materials with H_2SO_4 improves the catalytic activity, resulting in the simultaneous incorporation of $\text{-SO}_3\text{H}$ and -NH_2 groups into the $g\text{-C}_3\text{N}_4$ framework. (Figure 16)

In another interesting report, Biswas and Mahalingan presented the synergistic impact of combining $g\text{-C}_3\text{N}_4$ with tetrabutylammonium bromide (TBAB) to convert epoxides to cyclic carbonates for the first time at 1 atm pressure under solvent-free

conditions [197]. Epichlorohydrin, styrene oxide, phenyl glycidyl ether, and allyl glycidyl ether were all converted to cyclic carbonates using 50 mg of $g\text{-C}_3\text{N}_4$ and 1.8 mol% of TBAB relative to an epoxide (13.7 mmol) at 1 bar of CO_2 at 105°C for 20 hours. However, very modest conversions were found for other epoxides such as 1,2-epoxy hexane, 1,2-epoxy octane, and 1,2-epoxy-9-decene, and no ring-opening of the internal epoxide cyclohexene oxide occurred. The authors have reported only conversions rather than separate yields of the cyclic carbonate products. Catalyst recycling studies revealed no loss of activity after 7 cycles. Tests performed with these reagents separately showed conversion rates below 40%. It is therefore proposed that both $g\text{-C}_3\text{N}_4$ and TBAB work cooperatively. By interacting with the epoxide ring through hydrogen bond formation, the $g\text{-C}_3\text{N}_4$ amino groups increase the electrophilicity of the epoxide carbon. By doing so, the carbon atom becomes more susceptible to nucleophilic attack by the bromide anion of TBAB, ring opening the epoxide and thereby initiating its conversion into cyclic carbonate (Figure 17).

The key hurdles that these catalysts currently face are achieving acceptable conversions for the more difficult branched and substituted epoxides, rather than merely simple, sterically unimpeded terminal epoxides, and obtaining respectable conversions and yields under gentler reaction conditions. Some of these catalytic systems must also be improved in terms of sustainability, such as eliminating the requirement for hazardous and unsustainable solvents. The future of these catalysts, on the other hand, seems bright, and they will remain an essential subject of study for boosting green and sustainable CO_2 consumption.

4.6. Hydrolysis

4.6.1. Hydrolysis of ammonia borane (AB)

Hydrolysis of ammonia borane (AB) is a chemical reaction of high interest as one of the end products is hydrogen which is regarded as the potential fuel for the future [198]. The chemical reaction $\text{NH}_3\text{BH}_3 + 2 \text{H}_2\text{O} \rightarrow \text{NH}_4\text{BO}_2 + 3 \text{H}_2$ generally requires a catalyst to proceed and most often heterogeneous catalysts with high efficiency and durability are

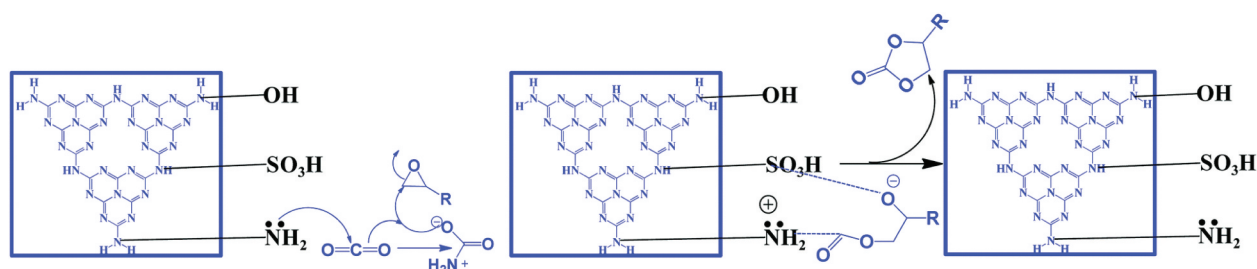


Figure 16. Synthesis of cyclic carbonates assisted by a bi-functional $g\text{-C}_3\text{N}_4$ catalyst, reproduced with permission from [196].

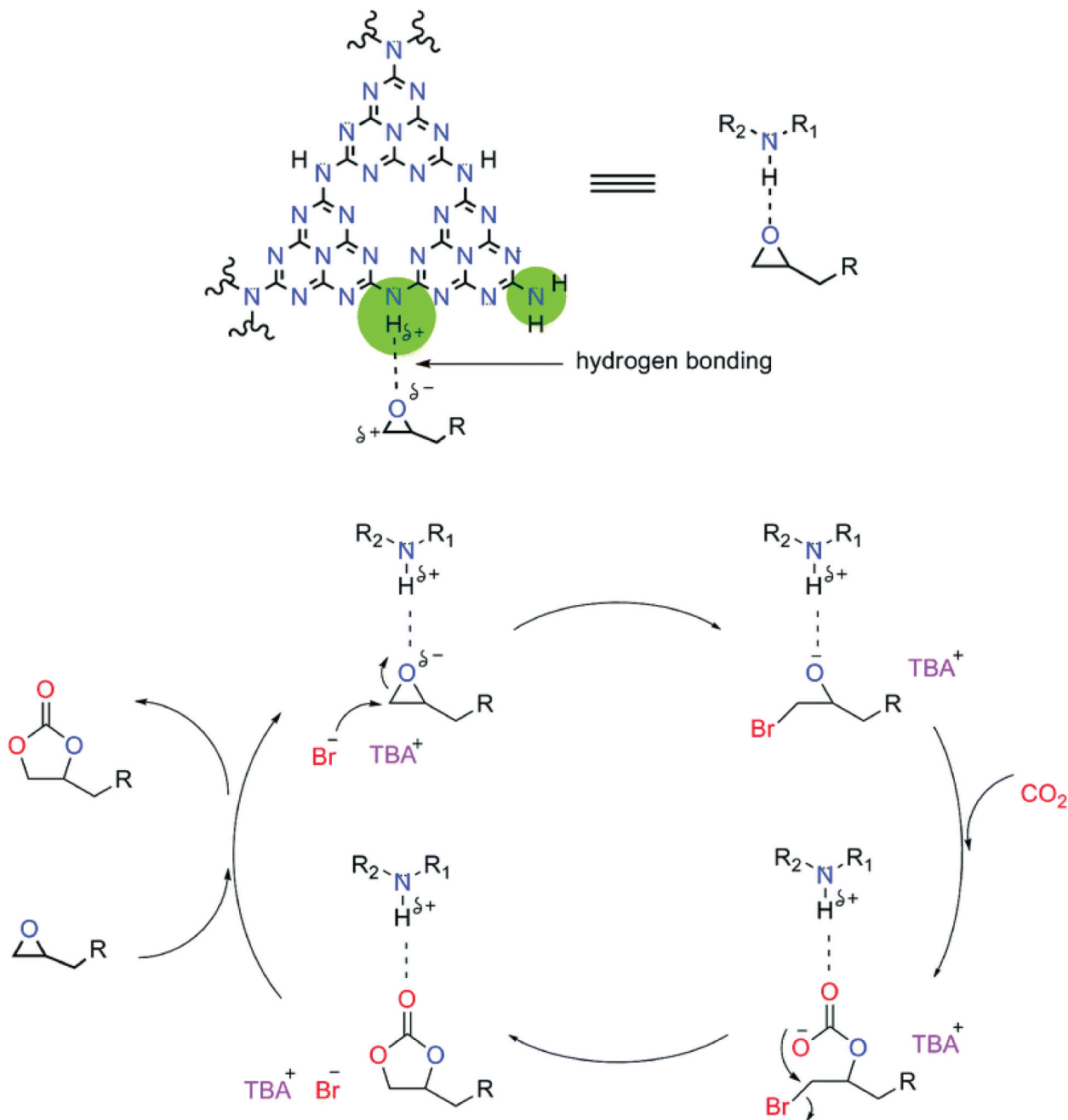


Figure 17. Proposed mechanism for the $g\text{-C}_3\text{N}_4$ and TBAB catalyzed conversion of epoxides and CO_2 into cyclic carbonates, reproduced with permission from [197].

required. Metal-based nanoparticles are deemed to be highly effective for the hydrolysis of AB; however, their agglomeration is a primary drawback. This drawback could be addressed by dispersing such metal nanoparticles on porous supports such as carbon nitride. For example, exfoliated mesoporous $g\text{-C}_3\text{N}_4$ synthesized from guanidine hydrochloride via carbonization at 550°C could be used as porous support for platinum nanoparticles (Pt NPs) generated from chloroplatinic acid hexahydrate ($\text{H}_2\text{PtCl}_6 \cdot 6 \text{H}_2\text{O}$) (Figure 18(a)) [199]. The heterojunction created by Pt NPs and mesoporous $g\text{-C}_3\text{N}_4$ results in better separation and increased lifetime of the charge carriers which contributed to a 2.25 times higher photocatalytic activity for hydrolysis of AB under

white light (Figure 18(b)). It was also revealed that the loading of Pt has a significant effect on the hydrolysis reaction (Figure 18(c)). The mechanism revealed a formation of the midgap interface (Schottky barrier) between conduction and valence bands which reduced the recombination of charge carriers thereby extending their lifetime and enhancing the hydrolysis of AB (Figure 18(d)). Another instance reports monometallic metal (Pd) based MCN as a highly active catalyst for the hydrolysis of AB [201]. A co-reduction approach was used to disperse Pd nanoparticles (Pd NPs) on the surface of MCN and the catalyst showed a high turnover frequency of $122 \text{ mol H}_2 \text{ mol metal}^{-1} \text{ min}^{-1}$ at room temperature for hydrolysis of AB in an aqueous

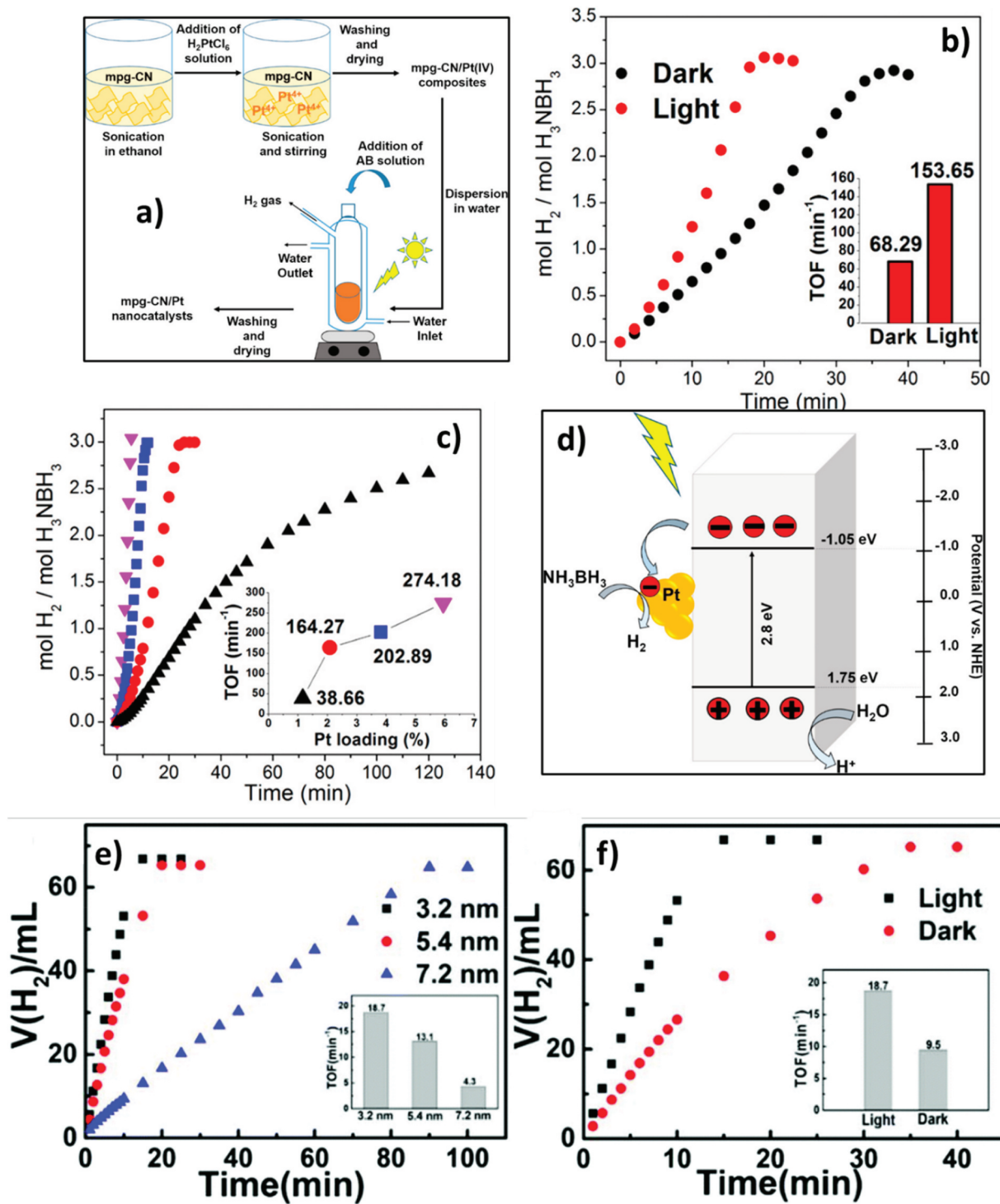


Figure 18. (a) Synthesis of platinum nanoparticles (Pt NPs) supported on mesoporous graphitic carbon nitride (mpg-CN), (b) Time vs molH₂/mol NH₃BH₃ plots for mpg-CN/Pt with 2.95% Pt loading, (c) Effect of different loading of Pt on the hydrolysis of ammonia borane, and (d) Mechanism of photocatalytic hydrolysis of AB using mpg-CN/Pt, reproduced with permission from [199], (e) Hydrolysis of AB in aqueous solution under white illumination using nickel-loaded graphitic carbon nitride (Ni-gC₃N₄) with different loadings of Ni, and (f) hydrolysis of AB using Ni/g-CN with Ni particle size of 3.2 nm under dark environment, reproduced with permission from [200].

solution. It was also shown that the catalytic activity can be elevated to 246.8 H₂ mol metal⁻¹ min⁻¹ by using an alloy of Pd with Nickel (Ni). The porous structure of carbon nitride provided a good platform for a higher mass transfer and the interfacial interactions between metal nanoparticles and MCN led to improved catalytic efficiency.

Nickel alone could also be supported by carbon nitride for the hydrolysis of AB. For example, Ni nanoparticles of two different particle sizes (3.2 and 7.4 nm) were deposited on carbon nitride via a self-assembled route and used for hydrolysis of AB in both light and dark environments [200]. In both environments, the Ni/g-C₃N₄ with a smaller particle size of Ni

(3.2 nm) delivers efficient hydrolysis of AB with the evolution of H_2 (Figure 18(e,f)).

Another feasible approach to designing efficient carbon nitride-based catalysts for the hydrolysis of AB is to modify it with quantum dots. For instance, g- C_3N_4 prepared via thermal polymerization of melamine was treated with ruthenium chloride ($RuCl_3$) and sodium hypophosphite (NaH_2PO_2) in an *in-situ* phosphorization approach to form ruthenium phosphide/carbon nitride (RuP/CN) as a photocatalyst for hydrolysis of AB under visible illumination [202]. The catalysis data suggested that the light mode is faster and more effective than the dark environment for hydrolysis (Figure 19(a,b)). The higher temperature gave a better performance for both light and dark environments (Figure 19(c,d)).

Similar instances of the modification of carbon nitride with different metals and non-metal species for improved hydrolysis of ammonia borane have been reported [203,204]. Overall, the carbon nitride-based materials are promising for the hydrolysis of AB, and further research on increasing their light absorption ability in the visible region with reduced recombination of charge carriers and their prolonged time can be carried out to reveal the full potential of these materials.

4.6.2. Hydrolysis of carbonyl sulfide (COS)

The hydrolysis of COS is an important base-catalyzed chemical reaction that finds use in several industries and can be represented as $COS + H_2O \rightarrow H_2S + CO_2$ [205]. COS, being a source of organic sulfur in the blast furnace gas, can deactivate the industrial catalysts and also cause equipment corrosion [206]. Hydrolysis of COS is a preferred method to eliminate COS from the blast gas stream due to its advantages in terms of good efficiency and mild reaction conditions [207]. Similarly, various types of solid catalysts can also be employed for the hydrolysis of COS; however, their drawbacks in terms of reduced active sites, selectivity, and separation create the need for a continuous search for new and advanced materials that could defy these limitations. For example, a standard alumina Claus catalyst cannot perform 100% conversion of the COS using hydrolysis [208]. Carbon-based materials with a high surface area and compatible pore size are also good for the hydrolysis of COS [209]. For these reasons, carbon nitride is chosen as it is considered a fascinating material with intrinsic basic properties arising mainly from the presence of nitrogen in the ring. Nitrogen, being more electronegative than carbon, withdraws the bonded electrons that impart a negative character to carbon nitride. The nitrogen

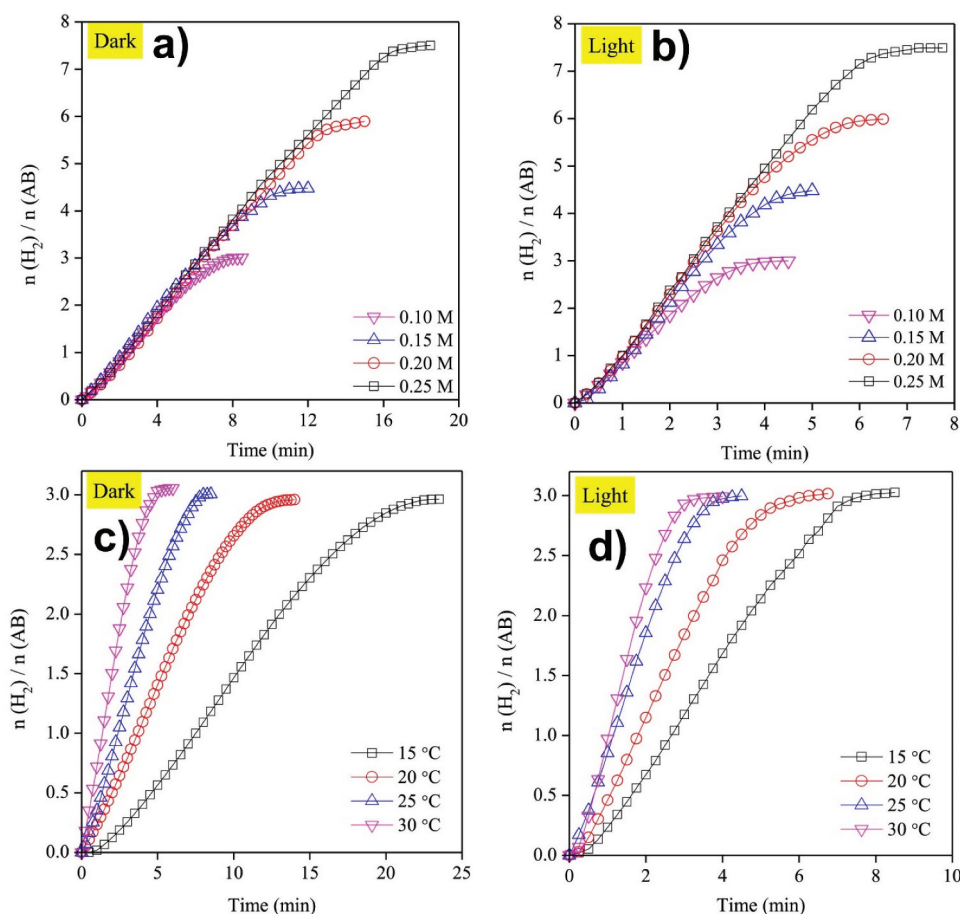


Figure 19. Hydrolysis of ammonia borane using RuP/CN at different concentrations of AB using (a) dark, and (b) light environments, and effect of temperature on the hydrolysis in (c) dark, and (d) and light environments, reproduced with permission from [202].

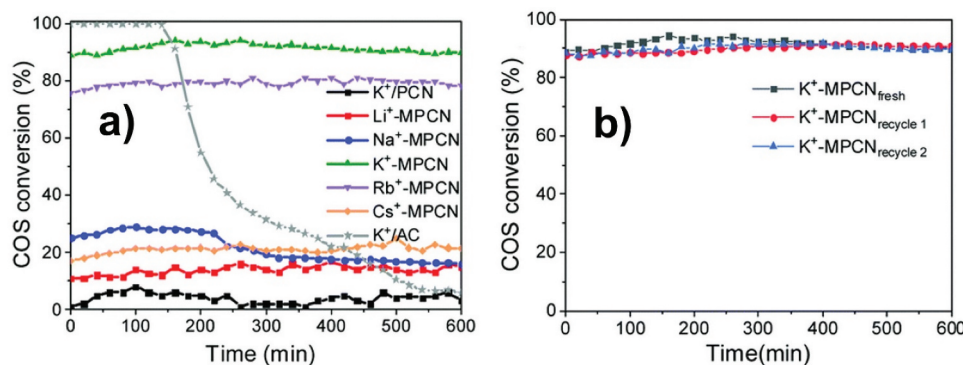


Figure 20. (a) COS conversion efficiency of the various metallated catalysts prepared using alkali metals and polymeric carbon nitride, and (b) long term and cyclic ability of potassium metallated polymeric carbon nitride, reproduced with permission from [210].

in the secondary amine groups can also be deprotonated to make it act as a Lewis base. Furthermore, the modifications of carbon nitride with other species including metal and non-metal make it an exciting material for base-catalyzed hydrolysis reactions including that of COS.

Metals, generally from group I and group II, can be combined with carbon nitride for enhancing their basicity for base-catalyzed hydrolysis. For example, lithium (Li⁺), sodium (Na⁺), potassium (K⁺), rubidium (Rb⁺), and cesium (Cs⁺) in their chloride form could be carbonized directly with PCN at 600°C for effective integration of alkali metals into the carbon nitride framework [210]. Out of all modified materials, it was observed that potassium imparts maximum basicity to carbon nitride and hence it was the most effective material (K⁺-MPCN) for the base-catalyzed hydrolysis of COS to H₂S. The COS conversion efficiency of K⁺-MPCN reaches >90% and it showed good long-term stability for over 600 min as compared to all other materials (Figure 20(a,b)). The recyclability studies suggested no loss in the COS hydrolysis efficiency of the catalyst over 3 cycles and the washing of the catalysts with water had very little impact on the leaching of K from the catalyst.

Potassium has also been reported as the most promising cation that can increase the efficiency of other types of catalysts such as γ -alumina [211]. Overall, the research on the hydrolysis of COS using carbon nitride is still in the initial stages. However, carbon nitrides in their mesoporous form with high surface area, large pore volume, and tunable pore size along with high basicity arising from nitrogen atoms are expected to be attractive for the hydrolysis of COS.

5. Conclusions and prospects

Carbon nitrides have emerged as front-running materials for several applications including organocatalysis owing to their exquisite features such as good thermal, chemical, and water stability, ease of porosity creation, high basicity due to nitrogen, tunable surface

functionalization, and modification with other species. Relentless efforts have been put into addressing their application for the field of organic catalysis which has led to noteworthy publications. Our group contributed to the field by the discovery of a new family of MCNs that contain high nitrogen content with the formulae C₃N₅, C₃N₆, and C₃N₇. These materials have since been explored for different applications.

In this review, we reviewed the carbon nitrides (g-C₃N₄), the N-rich carbon nitrides (C₃N₅, C₃N₆, and C₃N₇), PHI-based ionic CNs, and microporous CNs, extensively for their structure and properties and discussed how these materials are well suited for organocatalysis. Carbon nitrides work very well for non-metallic base catalysis and their soft basic character is ideally suited for typical base catalyses such as Knoevenagel condensation, and cycloaddition of CO₂ to epoxide with high selectivities. Carbon nitrides are also found to be excellent candidates for oxidation-type of organic reactions as these possess the ability to activate the oxidizing agents into radical oxygen species. For such reactions, carbon nitrides can either be used in the bare or metal functionalized form. The activities of these unique materials in organic catalysis can be enhanced with the suitable modification of their framework structure through deprotonation or acid functionalization with sulfonic acids or oxidation. Similarly, selective hydrogenation, esterification, and transesterification reactions can be achieved by anchoring the metal species onto the surface of carbon nitrides. In such cases, carbon nitrides offer ample opportunity for high and uniform dispersion of the metal particles without agglomeration, which leads to high catalytic activity. Carbon nitride is also a suitable porous platform for dispersing metal nanoparticles to enhance the efficiency of the hydrolysis of ammonia borane and carbonyl sulfide.

Overall, carbon nitride-based catalysts are low-cost, highly efficient, and eco-friendly which makes them suitable for organocatalysis, and more advanced research will bring out further incentives in the materials with enhanced efficiency.

Going forward, we believe that although the design and development of carbon nitrides is a hot topic in materials science with significant progress achieved so far, future research can still be improved by bringing innovations in their synthesis, sophistication in characterization, and deep insights into the mechanism of catalysis for various organic reactions.

- (1) Delving into the techniques such as advanced time-resolved spectroscopic techniques is crucial for a better understanding of the mechanistic details of CNs catalytic action through in-situ approach.
- (2) Materials development can focus on creating new materials with high N-contents and defects together for improving the properties for enhanced catalytic efficiency. Such vacancy defects and nitrogen content modulation have to be controlled for achieving the desired catalytic performance.
- (3) Multifunctional hybridization or modification of high nitrogen containing carbon nitrides with other species such as heteroatoms can bring out better catalytic actions for organic reactions.

Acknowledgments

One of the authors A. Vinu acknowledges the start-up funds provided by the University of Newcastle.

Disclosure statement

No potential conflict of interest was reported by the author(s).

Funding

This work was supported by the start-up funds provided by the University of Newcastle.

Notes on contributors



Sujanya Maria Ruban is a Ph.D. research scholar pursuing research under the guidance of Professor Ajayan Vinu. She completed her Bachelor's and Master's degrees in India. She carried out two years of research as a visiting student at the University of South Australia. She was mainly working on developing a new class of mesoporous carbon nitrides for the catalysis application, utilizing and converting the halloysites into multifunctional nanomaterials. Her current research is focused on the Synthesis of nanostructured transition metal phosphides and their applications in energy storage and conversion. She has published 9 articles in international journals, and her h-index is 8.



Kavitha Ramadass is a Research Fellow at the Global Innovative Centre for Advanced Nanomaterials (GICAN), The University of Newcastle. She received her Ph.D. degree from the Centre for Environmental Risk Assessment and Remediation at the University of South Australia. She worked as a postdoctoral research associate at Future Industries Institute, University of South Australia before moving to the University of Newcastle. Her research interests focus on the design of multifunctional nanoporous materials for energy and environmental applications. She has published around 60 articles in reputed scientific journals, and her H-index is 30.



Gurwinder Singh is a Research Fellow in the Global Innovative Centre for Advanced Nanomaterials at the University of Newcastle, Australia. He received his Ph.D. degree in materials sciences from the University of South Australia and his research primarily focuses on carbon capture using nanoporous materials. He has published 60 articles including review and research articles in high-quality materials science-based journals including Chemical Society Reviews and Advanced Materials which has fetched 3499 citations with an h-index of 31.



Siddulu Naidu Talapaneni is an ARC DECRA Fellow working at the School of Chemical Engineering, UNSW. He has completed his PhD in 2013 at the National Institute for Materials Science (NIMS), a number one materials institute in Japan in collaboration with Hokkaido University, Japan. He then worked as a CNRS postdoctoral fellow at the Laboratory of Catalysis and Spectrochimie (LCS), ENSICAEN, CNRS, France, followed by a BK 21 Plus postdoctoral stint at Korea Advanced Institute of Science and Technology (KAIST), South Korea, as a Research Associate and ARC DECRA Fellow at University of Newcastle, Newcastle, NSW, Australia.



Kamalakar Gunda has completed Undergraduate and Graduate studies at the Indian Institute of Technology (IIT) in Bombay and the Indian Institute of Chemical Technology (IICT), in India respectively. His research areas of interest include Heterogeneous Catalysis, Petrochemicals, Bio Energy, Nanomaterials, Adsorption, Microwave methodologies, and Industrially relevant chemical processes. He is the recipient of Alexander von Humboldt (AvH), Singapore Millennium Foundation, and JSPS Fellowships. He worked as a Research team lead at a Bioenergy company in Canada, Lead scientist at SABIC (KSA) and Shell Technology Centre (India). He has more than 25 research publications and 7 patents to his credit.



Chandrakanth Rajanna Gadipelly was born in 1986 in Mumbai (Maharashtra, India). He received his B.Sc. (2007) in Chemistry and M.Sc. (2009) in Organic Chemistry from Mumbai University. In 2017, he completed a Ph.D. Science degree in Chemistry from the Institute of Chemical Technology (formerly UDCT), Mumbai, under the

supervision of Professor Virendra K. Rathod. His work mainly focused on catalysis, materials development, and process intensification of wastewater treatment technologies. Before his graduation in 2016, he worked with Professor M. Lakshmi Kantam as a Postdoctoral research fellow in the J. C. Bose National Research grant for “Conversion of biomass to value-added chemicals.” He has also worked as a Research Scientist in the R&D division of Reliance Industries Limited for 2.5 years. Formerly, he worked as a postdoctoral research fellow at the Technion-Israel Institute of Chemical Technology and worked in cooperative catalysis. Currently, he is working as a Research Scientist in the Flow Chemistry division at Amar Equipment Pvt. Ltd. His research interests are processing chemistry and materials development for energy applications.



Lakshmi Kantam Mannepalli is currently Dr.B.P. Godrej Distinguished Chair Professor. She has been the Director of IICT Hyderabad during 2013-2015. She joined as a Scientist B in the Indian Institute of Chemical Technology, Hyderabad in the year 1984 and then became Director in 2013. She has guided 41 PhD students and 6 Ph.D students and 2 PDFs are presently working under her guidance. She has more than 350 research publications and 43 US patents to her credit. She has received many academic awards viz., Fellow of the World Academy of Sciences, National Academy of Sciences, India. BD Tilak Visiting Fellow, 2008, UICT, Mumbai; and RMIT Foundation Fellowship, RMIT University, Melbourne, Australia.



Yoshihiro Sugi received Ph.D. in Engineering from Tohoku University, Sendai in 1971. He worked at the National Institute of Advanced Industrial Science and Technology (AIST), Tsukuba as a Research Scientist from 1971–1995 and then, in the Faculty of Engineering, Gifu University as a Professor during 1995–2009. Currently, he is a Visiting Professor at the Global Innovation Centre for Advanced Nanomaterials (GICAN), The University of Newcastle, NSW, Australia. His research interests include zeolite catalysis in organic chemistry and energy.



Ajayan Vinu is a Professor and the Director of GICAN at the University of Newcastle. He was previously working as a full professor and ARC Future Fellow at the University of South Australia and the University of Queensland. Before coming to Australia, he had been working as a research group leader at the National Institute for Materials Science in Japan. His research is mainly focused on developing new approaches to create nanoporosity in carbon nitrides, conducting polymers, metal nitrides, metal silicates, graphenes, silicas, sulfides, fullerenes, and biomolecules with tunable structures and pore diameters and their potential applications in energy, environmental, biomedical and catalysis technology.

ORCID

Sujanya Maria Ruban <http://orcid.org/0009-0006-3575-9270>
 Kavitha Ramadass <http://orcid.org/0000-0003-4539-2442>
 Gurwinder Singh <http://orcid.org/0000-0001-6611-3567>
 Siddulu Naidu Talapaneni <http://orcid.org/0000-0002-7684-7529>
 Gunda Kamalakar <http://orcid.org/0009-0008-1176-4977>
 Chandrakanth Rajanna Gadipelly <http://orcid.org/0000-0003-1087-4695>
 Lakshmi Kantham Mannepalli <http://orcid.org/0000-0002-3914-412X>
 Yoshihiro Sugi <http://orcid.org/0000-0002-9928-7325>
 Ajayan Vinu <http://orcid.org/0000-0002-7508-251X>

Author contributions

SMR – Preparation and revision, KR – Reviewing and editing, GS, – Preparation, correction, and revision, reviewing and editing, SNT – Preparation, reviewing, and editing, GK, CRG, LKM – Preparation and correction, YS – Preparation, correction, and revision, reviewing and editing, AV – Supervision, correction, and revision, reviewing and editing.

References

- [1] Hattori H. Solid base catalysts: fundamentals and their applications in organic reactions. *Appl Catal A*. 2015;504:103–109.
- [2] Gong M, Wang D-Y, Chen C-C, et al. A mini review on nickel-based electrocatalysts for alkaline hydrogen evolution reaction. *Nano Res*. 2016;9(1):28–46.
- [3] Thomas A, Fischer A, Goettmann F, et al. Graphitic carbon nitride materials: variation of structure and morphology and their use as metal-free catalysts. *J Mater Chem*. 2008;18(41):4893–4908.
- [4] Hattori H, Ono Y. Catalysts and catalysis for acid-base reactions. In: Védrine JC, editor. *Metal oxides in heterogeneous catalysis*. Netherlands: Elsevier; 2018. p. 133–209.
- [5] Liu Z, Du Y, Zhang P, et al. Bringing catalytic order out of chaos with nitrogen-doped ordered mesoporous carbon. *Matters*. 2021;4(10):3161–3194.
- [6] Najam T, Ibraheem S, Nazir MA, et al. Partially oxidized cobalt species in nitrogen-doped carbon nanotubes: enhanced catalytic performance to water-splitting. *Int J Hydrogen Energy*. 2021;46(13):8864–8870.
- [7] Ewels C, Glerup M. Nitrogen doping in carbon nanotubes. *J Nanosci Nanotechnol*. 2005;5(9):1345–1363.
- [8] Vasseghian Y, Dragoi E-N, Almomani F. Graphene-based materials for metronidazole degradation: a comprehensive review. *Chemosphere*. 2022;286:131727.
- [9] Kumar P, Laishram D, Sharma RK, et al. Boosting photocatalytic activity using carbon nitride based 2D/2D van der Waals heterojunctions. *Chem Mater*. 2021;33(23):9012–9092.
- [10] Zhou Z, Zhang Y, Shen Y, et al. Molecular engineering of polymeric carbon nitride: advancing applications from photocatalysis to biosensing and more. *Chem Soc Rev*. 2018;47(7):2298–2321.

- [11] Bai Y, Zheng Y, Wang Z, et al. Metal-doped carbon nitrides: synthesis, structure and applications. *New J Chem.* **2021**;45(27):11876–11892.
- [12] Yang H, Wang Z, Liu S, et al. Molecular engineering of C_xN_y: topologies, electronic structures and multi-disciplinary applications. *Chin Chem Lett.* **2020**;31(12):3047–3054.
- [13] Wahono SK, Dwiatmoko AA, Cavallaro A, et al. Amine-functionalized natural zeolites prepared through plasma polymerization for enhanced carbon dioxide adsorption. *Plasma Process Polym.* **2021**;18(8):210028.
- [14] Lei Z, Lee JM, Singh G, et al. Recent advances of layered-transition metal oxides for energy-related applications. *Energy Storage Mater.* **2021**;36:514–550.
- [15] Falcaro P, Ricco R, Yazdi A, et al. Application of metal and metal oxide nanoparticles@ MOFs. *Coord Chem Rev.* **2016**;307:237–254.
- [16] Okechukwu OD, Joseph E, Nonso UC, et al. Improving heterogeneous catalysis for biodiesel production process. *Chem Eng Technol.* **2022**;3:100038.
- [17] Zhang T. Recent advances in heterogeneous catalysis for the nonoxidative conversion of methane. *Chem Sci.* **2021**;12(38):12529–12545.
- [18] Gong Y, Li M, Li H, et al. Graphitic carbon nitride polymers: promising catalysts or catalyst supports for heterogeneous oxidation and hydrogenation. *Green Chem.* **2015**;17(2):715–736.
- [19] Ong W-J, Tan L-L, Ng YH, et al. Graphitic carbon nitride (g-C₃N₄)-based photocatalysts for artificial photosynthesis and environmental remediation: are we a step closer to achieving sustainability? *Chem Rev.* **2016**;116(12):7159–7329.
- [20] Majdoub M, Anfar Z, Amedlous A. Emerging chemical functionalization of g-C₃N₄: covalent/noncovalent modifications and applications. *ACS Nano.* **2020**;14(10):12390–12469.
- [21] Zhu J, Xiao P, Li H, et al. Graphitic carbon nitride: synthesis, properties, and applications in catalysis. *ACS Appl Mater Interfaces.* **2014**;6(19):16449–16465.
- [22] Dandia A, Gupta SL, Saini P, et al. Structure couteure and appraisal of catalytic activity of carbon nitride (g-C₃N₄) based materials towards sustainability. *Curr Opin Green Sustain Chem.* **2020**;3:100039.
- [23] Su DS, Zhang J, Frank B, et al. Metal-free heterogeneous catalysis for sustainable chemistry. *ChemSuschem.* **2010**;3(2):169–180.
- [24] Talapaneni SN, Ramadass K, Ruban SJ, et al. 3D cubic mesoporous C₃N₄ with tunable pore diameters derived from KIT-6 and their application in base catalyzed Knoevenagel reaction. *Catal Today.* **2019**;324:33–38.
- [25] Sood SO, Churchill EF, Antin J. Automatic identification of personal insults on social news sites. *J Assoc Inf Sci Technol.* **2012**;63(2):270–285.
- [26] Talapaneni SN, Ramadass K, Benzigar MR, et al. Controlled synthesis of three dimensional mesoporous C₃N₄ with ordered porous structure for room temperature Suzuki coupling reaction. *Mol Catal.* **2019**;477:110548.
- [27] Xu J, Chen T, Jiang Q, et al. Utilization of environmentally benign dicyandiamide as a precursor for the synthesis of ordered mesoporous carbon nitride and its application in base-catalyzed reactions. *Chem Asian J.* **2014**;9(11):3269–3277.
- [28] Spinnato D, Schweitzer-chaput B, Goti G, et al. A photochemical organocatalytic strategy for the α -alkylation of ketones by using radicals. *Angew Chem.* **2020**;132(24):9572–9577.
- [29] Shaw MH, Twilton J, MacMillan DW. Photoredox catalysis in organic chemistry. *J Org Chem.* **2016**;81(16):6898–6926.
- [30] Hu D, Jiang X. Perspective for uranyl photo-redox catalysis. *Synlett.* **2021**;32(13): 1330–1342.
- [31] Khan I, Saeed K, Khan I. Nanoparticles: properties, applications and toxicities. *Arab J Chem.* **2019**;12(7):908–931.
- [32] Savateev A, Antonietti M. Heterogeneous organocatalysis for photoredox chemistry. *ACS Catal.* **2018**;8(10):9790–9808.
- [33] Akhundi A, Badiei A, Ziarani GM, et al. Graphitic carbon nitride-based photocatalysts: toward efficient organic transformation for value-added chemicals production. *Mol Catal.* **2020**;488:110902.
- [34] Qi M-Y, Conte M, Anpo M, et al. Cooperative coupling of oxidative organic synthesis and hydrogen production over semiconductor-based photocatalysts. *Chem Rev.* **2021**;121(21):13051–13085.
- [35] Ghosh I, Khamrai J, Savateev A, et al. Organic semiconductor photocatalyst can bifunctionalize arenes and heteroarenes. *Science.* **2019**;365(6451):360–366.
- [36] Chen K, Zhang P, Wang Y, et al. Metal-free allylic/benzylic oxidation strategies with molecular oxygen: recent advances and future prospects. *Green Chem.* **2014**;16(5):2344–2374.
- [37] Han Q, Chen N, Zhang J, et al. Graphene/Graphitic carbon nitride hybrids for catalysis. *Mater Horiz.* **2017**;4(5):832–850.
- [38] Wang A, Wang C, Fu L, et al. Recent advances of graphitic carbon nitride-based structures and applications in catalyst, sensing, imaging, and LEDs. *Micro Nano Lett.* **2017**;9(4):47.
- [39] Kumar P, Vahidzadeh E, Thakur UK, et al. C₃N₅: a low bandgap semiconductor containing an azo-linked carbon nitride framework for photocatalytic, photovoltaic and adsorbent applications. *J Am Chem Soc.* **2019**;141(13):5415–5436.
- [40] Navalón S, Ong W-J, Duan X. Sustainable catalytic processes driven by graphene-based materials. *Process.* **2020**;8(6):672.
- [41] Takht Ravanchi M, Fadaerayeni S, Rahimi Fard M. The effect of calcination temperature on physico-chemical properties of alumina as a support for acetylene selective hydrogenation catalyst. *Res Chem Intermed.* **2016**;42(5):4797–4811.
- [42] Wang J, Wang S. A critical review on graphitic carbon nitride (g-C₃N₄)-based materials: preparation, modification and environmental application. *Coord Chem Rev.* **2022**;453:214338.
- [43] Fernandes DM, Peixoto AF, Freire C. Nitrogen-doped metal-free carbon catalysts for (electro) chemical CO₂ conversion and valorisation. *Dalton Trans.* **2019**;48:36–13528.
- [44] Darkwah WK, Ao Y. Mini review on the structure and properties (photocatalysis), and preparation techniques of graphitic carbon nitride nano-based particle, and its applications. *Nanoscale Res Lett.* **2018**;13(1):1–15.
- [45] Shcherban N, Mäki-Arvela P, Aho A, et al. Melamine-derived graphitic carbon nitride as a new effective metal-free catalyst for Knoevenagel condensation of

- benzaldehyde with ethylcyanoacetate. *Catal Sci Technol.* **2018**;8(11):2928–2937.
- [46] Vidyasagar D, Bhojar T, Singh G, et al. Recent progress in polymorphs of carbon nitride: synthesis, properties, and their applications. *Macromol Rapid Commun.* **2021**;42(7):2000676.
- [47] Zhu B, Zhang L, Cheng B, et al. First-principle calculation study of tri-s-triazine-based g-C₃N₄: a review. *Appl Catal B.* **2018**;224:983–999.
- [48] Narkbuakaew T, Sujaridworakun P. Synthesis of Tri-S-Triazine based g-C₃N₄ photocatalyst for cationic rhodamine B degradation under visible light. *Top Catal.* **2020**;63(11):1086–1096.
- [49] Schwarzer A, Saplinova T, Kroke E. Tri-s-triazines (s-heptazines)—from a “mystery molecule” to industrially relevant carbon nitride materials. *Coord Chem Rev.* **2013**;257(13–14):2032–2062.
- [50] Zhang LH, Shi Y, Wang Y, et al. Nanocarbon catalysts: recent understanding regarding the active sites. *Adv Sci.* **2020**;7(5):1902126.
- [51] Ruban SM, Sathish CI, Ramadass K, et al. Ordered mesoporous carbon nitrides with tuneable nitrogen contents and basicity for Knoevenagel condensation. *ChemCatchem.* **2021**;13(1):468–474.
- [52] Ansari MB, Jin H, Parvin MN, et al. Mesoporous carbon nitride as a metal-free base catalyst in the microwave assisted Knoevenagel condensation of ethylcyanoacetate with aromatic aldehydes. *Catal Today.* **2012**;185(1):211–216.
- [53] Su F, Antonietti M, Wang X. Mpg-C₃N₄ as a solid base catalyst for Knoevenagel condensations and transesterification reactions. *Catal Sci Technol.* **2012**;2(5):1005–1009.
- [54] Choudhary P, Bahuguna A, Kumar A, et al. Oxidized graphitic carbon nitride as a sustainable metal-free catalyst for hydrogen transfer reactions under mild conditions. *Green Chem.* **2020**;22(15):5084–5095.
- [55] Gentile G, Rosso C, Criado A, et al. New insights into the exploitation of oxidized carbon nitrides as heterogeneous base catalysts. *Inorganica Chim Acta.* **2022**;531:120732.
- [56] Anandan S, Vinu A, Srinivasu P, Gokulakrishnan N, et al. Synthesis of nitrogen-doped mesoporous carbon using templating technique. *JP JP* 5294234. **2007**:125128.
- [57] Mane GP, Talapaneni SN, Lakhi KS, et al. Highly ordered nitrogen-rich mesoporous carbon nitrides and their superior performance for sensing and photocatalytic hydrogen generation. *Angew Chem Int Ed.* **2017**;56(29):8481–8485.
- [58] Kim IY, Kim S, Jin X, et al. Ordered mesoporous C₃N₅ with a combined triazole and triazine framework and its graphene hybrids for the oxygen reduction reaction (ORR). *Angew Chem Int Ed.* **2018**;57(52):17135–17140.
- [59] Park DH, Lakhi KS, Ramadass K, et al. Energy efficient synthesis of ordered mesoporous carbon nitrides with a high nitrogen content and enhanced CO₂. *Capture Capacity Chem Commun.* **2017**;23(45):10753–10757.
- [60] Talapaneni SN, Mane GP, Mano A, et al. Synthesis of nitrogen-rich mesoporous carbon nitride with tunable pores, band gaps and nitrogen content from a single aminoguanidine precursor. *ChemSuschem.* **2012**;5(4):700–708.
- [61] Luo L, Wang S, Wang H, et al. Molten-salt technology application for the synthesis of photocatalytic materials. *Energy Technol.* **2021**;9(2):2000945.
- [62] Lee T-G, Kang H-J, Kim J-H, et al. Eutectic iodide-based salt as a melem-to-PTI conversion stopping agent for all-in-one graphitic carbon nitride. *Appl Catal B.* **2021**;294:120222.
- [63] Ou H, Lin L, Zheng Y, et al. Tri-s-triazine-based crystalline carbon nitride nanosheets for an improved hydrogen evolution. *Adv Mater.* **2017**;29(22):1700008.
- [64] Savateev A, Antonietti M. Ionic carbon nitrides in solar hydrogen production and organic synthesis: exciting chemistry and economic advantages. *ChemCatchem.* **2019**;11(24):6166–6176.
- [65] Savateev A, Pronkin S, Epping JD, et al. Synthesis of an electronically modified carbon nitride from a processable semiconductor, 3-amino-1, 2, 4-triazole oligomer, via a topotactic-like phase transition. *J Mater Chem A.* **2017**;5(18):8394–8401.
- [66] Schlomberg H, Kröger J, Savasci G, et al. Structural insights into poly(Heptazine imides): a light-storing carbon nitride material for dark photocatalysis. *Chem Mater.* **2019**;31(18):7478–7486.
- [67] Markushyna Y, Lamagni P, Catalano J, et al. Advantages in using inexpensive CO₂ to favor photocatalytic oxidation of benzylamines. *ACS Catal.* **2020**;10(13):7336–7342.
- [68] Wu F, Du J, Liu N, et al. Potassium-doped carbon nitride supported on SBA-15 for enhanced catalytic Knoevenagel condensation under mild conditions. *Appl Catal A Gen.* **2022**;641:118677.
- [69] Srinivasu P, Vinu A, Hishita S, et al. Preparation and characterization of novel microporous carbon nitride with very high surface area via nanocasting technique. *Microporous Mesoporous Mater.* **2008**;108(1–3):340–344.
- [70] Xu J, Shen K, Xue B, et al. Microporous carbon nitride as an effective solid base catalyst for Knoevenagel condensation reactions. *J Mol Catal A Chem.* **2013**;372:105–113.
- [71] Stegmann N, Dai Y, Nürenberg E, et al. From 1D to 3D graphitic carbon nitride (melon): a bottom-up route via crystalline microporous templates. *Inorg Chem.* **2021**;60(24):18957–18963.
- [72] Sathish C, Premkumar S, Chu X, et al. Microporous carbon nitride (C₃N₅. 4) with tetrazine based molecular structure for efficient adsorption of CO₂ and water. *Angew Chem.* **2021**;133(39):21412–21419.
- [73] Ma J, Peng X, Zhou Z, et al. Extended conjugation tuning carbon nitride for non-sacrificial H₂O₂ photosynthesis and hypoxic tumor therapy. *Angew Chem Int Ed Engl.* **2022**;61(43):e202210856.
- [74] Yang H, Zhou Q, Fang Z, et al. Carbon nitride of five-membered rings with low optical bandgap for photoelectrochemical biosensing. *Chem.* **2021**;7(10):2708–2721.
- [75] Feng J, Li M. Large-scale synthesis of a new polymeric carbon nitride—c₃n₃ with good photoelectrochemical performance. *Adv Funct Mater.* **2020**;30(23):2001502.
- [76] Mahmood J, Lee EK, Jung M, et al. Nitrogenated holey two-dimensional structures. *Nat Commun.* **2015**;6(1):6486.
- [77] Mahmood J, Lee EK, Jung M, et al. Two-dimensional polyaniline (C₃N) from carbonized organic single crystals in solid state. *Proc Natl Acad Sci.* **2016**;113(27):7414–7419.

- [78] Zhou G, Shan Y, Hu Y, et al. Half-metallic carbon nitride nanosheets with micro grid mode resonance structure for efficient photocatalytic hydrogen evolution. *Nat Commun.* 2018;9(1):3366.
- [79] Cui Y, Ding Z, Liu P, et al. Metal-free activation of H₂ O₂ by g-C₃N₄ under visible light irradiation for the degradation of organic pollutants. *Phys Chem Chem.* 2012;14(4):1455–1462.
- [80] Wang TJ, Wollert KC, Larson MG, et al. Prognostic utility of novel biomarkers of cardiovascular stress: the Framingham heart study. *Circulation.* 2012;126(13):1596–1604.
- [81] Protti S, Fagnoni M. Photocatalytic C-H activation by hydrogen-atom transfer in synthesis. *ChemCatchem.* 2017;7:1516–1523.
- [82] Li G-X, Morales-Rivera CA, Gao F, et al. A unified photoredox-catalysis strategy for C (sp³)-H hydroxylation and amidation using hypervalent iodine. *Chem Sci.* 2017;8(10):7180–7185.
- [83] Liu G, Tang R, Wang Z. Metal-free allylic oxidation with molecular oxygen catalyzed by g-C₃N₄ and N-hydroxyphthalimide. *Catal Lett.* 2014;144(4):717–722.
- [84] Appaturi JN, Ratti R, Phoon BL, et al. A review of the recent progress on heterogeneous catalysts for Knoevenagel condensation. *J Chem Soc.* 2021;50(13):4445–4469.
- [85] Ájustin Thomas K. Rose bengal photocatalyzed Knoevenagel condensation of aldehydes and ketones in aqueous medium. *Green Chem.* 2022;24(12):4952–4957.
- [86] Kumari K, Choudhary P, Sharma D, et al. Amine functionalized graphitic carbon nitride as sustainable, metal-free catalyst for Knoevenagel condensation. *Ind Eng Chem Res.* 2022;62(1):158–168.
- [87] Johari S, Johan MR, Khaligh NG. An overview of metal-free sustainable nitrogen-based catalytic Knoevenagel condensation reaction. *Org Biomol Chem.* 2022;20(11):2164–2186.
- [88] Elamathi P, Chandrasekar G, Muthuraman S, et al. Pore size engineering of hexagonal mesoporous carbon nitride (HMCN) for high catalytic performance in the synthesis of α , β -unsaturated acid and its derivatives. *Appl Surf Sci.* 2019;463:481–491.
- [89] Zhang L, Wang H, Qin Z, et al. Synthesis of two-dimensional mesoporous carbon nitride under different carbonization temperatures and investigation of its catalytic properties in Knoevenagel condensations. *RSC Adv.* 2015;5(29):22838–22846.
- [90] Deng Q, Li Q. Facile preparation of Mg-doped graphitic carbon nitride composites as a solid base catalyst for Knoevenagel condensations. *J Mater Sci.* 2017;53(1):506–515.
- [91] Liu N, Wu F, Xu J, et al. Metal-free Knoevenagel condensation catalyzed by mesoporous and nitrogen-distribution-tunable supported carbon nitride. *Res Chem Intermed.* 2022;48:1989–2006.
- [92] Xu J, Wang Y, Shang J-K, et al. Synthesis of mesoporous carbon nitride via a novel detemplation method and its superior performance in base-catalyzed reactions. *Catal Sci Technol.* 2016;6(12):4192–4200.
- [93] Xu J, Shen K, Xue B, et al. Synthesis of three-dimensional mesostructured graphitic carbon nitride materials and their application as heterogeneous catalysts for Knoevenagel condensation reactions. *Catal Lett.* 2013;143(6):600–609.
- [94] Xu J, Wang Y, Shang J-K, et al. Preparation of mesoporous carbon nitride materials using urea and formaldehyde as precursors and catalytic application as solid bases. *Appl Catal A Gen.* 2017;538:221–229.
- [95] Xu J, Chen T, Jiang Q, et al. Utilization of environmentally benign dicyandiamide as a precursor for the synthesis of ordered mesoporous carbon nitride and its application in base-catalyzed reactions. *Chem Asian J.* 2014;9(11):3269–3277.
- [96] Bahuguna A, Kumar A, Chhabra T, et al. Potassium-functionalized graphitic carbon nitride supported on reduced graphene oxide as a sustainable catalyst for Knoevenagel condensation. *ACS Appl Nano Mater.* 2018;1(12):6711–6723.
- [97] Bahuguna A, Choudhary P, Chhabra T, et al. Ammonia-doped polyaniline-graphitic carbon nitride nanocomposite as a heterogeneous green catalyst for synthesis of indole-substituted 4 H-chromenes. *ACS Omega.* 2018;3(9):12163–12178.
- [98] Ghafuri H, Jafari G, Rashidizadeh A, et al. Co²⁺ immobilized on highly ordered mesoporous graphitic carbon nitride (ompg-C₃N₄/Co²⁺) as an efficient and recyclable heterogeneous catalyst for one-pot tandem selective photo-oxidation/knoevenagel condensation. *Mol Catal.* 2019;475:110491.
- [99] Nie R, Chen M, Pei Y, et al. Room-temperature tandem condensation-hydrogenation catalyzed by porous C₃N₄ nanosheet-supported pd nanoparticles. *ACS Sustain Chem Eng.* 2018;7(3):3356–3363.
- [100] Zhang L, Wang H, Shen W, et al. Controlled synthesis of graphitic carbon nitride and its catalytic properties in Knoevenagel condensations. *J Catal.* 2016;344:293–302.
- [101] Sharma P, Sasson Y. Highly active g-C₃N₄ as a solid base catalyst for Knoevenagel condensation reaction under phase transfer conditions. *RSC Adv.* 2017;7(41):25589–25596.
- [102] Sharma P, Patel DK, Kancharlapalli S, et al. Facile combined experimental and computational study: g-C₃N₄@ PDMS-Assisted Knoevenagel condensation reaction under phase transfer conditions. *ACS Sustain Chem Eng.* 2019;8(6):2350–2360.
- [103] Choudhary P, Sen A, Kumar A, et al. Sulfonic acid functionalized graphitic carbon nitride as solid acid-base bifunctional catalyst for Knoevenagel condensation and multicomponent tandem reactions. *Mater Chem Front.* 2021;5(16):6265–6278.
- [104] Sadjadi S, Koohestani F, Heravi M. Biochar-based graphitic carbon nitride adorned with ionic liquid containing acidic polymer: a versatile, non-metallic catalyst for acid catalyzed reaction. *Molecules.* 2020;25(24):5958.
- [105] Wei J, Shen W, Zhao J, et al. Boron doped g-C₃N₄ as an effective metal-free solid base catalyst in Knoevenagel condensation. *Catal Today.* 2018;316:199–205.
- [106] Li X, Lin B, Li H, et al. Carbon doped hexagonal BN as a highly efficient metal-free base catalyst for Knoevenagel condensation reaction. *Appl Catal B Environ.* 2018;239:254–259.
- [107] Wu J, Hua W, Yue Y, et al. A highly efficient bifunctional catalyst CoO x/tri-g-C₃N₄ for one-pot aerobic oxidation-Knoevenagel Condensation Reaction. *Catal.* 2020;10(6):712.
- [108] Wang D-Y, Xi G-H, Ma J-J, et al. Condensation reactions of aromatic aldehydes with active methylene compounds catalyzed by alkaline ionic liquid. *Synth Commun.* 2011;41(20):3060–3065.

- [109] van Beurden K, de Koning S, Molendijk D, et al. The Knoevenagel reaction: a review of the unfinished treasure map to forming carbon–carbon bonds. *Green Chem Lett Rev.* 2020;13(4):4–364.
- [110] Chênevert R, Lemieux EJ, Voyer N. The use of 18-crown-6 as phase transfer catalyst in the reinsert reaction. *Synth Commun.* 1983;13:1095–1101.
- [111] Ahmad A, Ali M, Al-Sehemi AG, et al. Carbon-integrated semiconductor photocatalysts for removal of volatile organic compounds in indoor environments. *J Chem Eng.* 2022;452:139436.
- [112] Lima MJ, Silva AM, Silva CG, et al. Graphitic carbon nitride modified by thermal, chemical and mechanical processes as metal-free photocatalyst for the selective synthesis of benzaldehyde from benzyl alcohol. *J Catal.* 2017;353:44–53.
- [113] Dong F, Zhao Z, Xiong T, et al. In situ construction of g-C₃N₄/g-C₃N₄ metal-free heterojunction for enhanced visible-light photocatalysis. *ACS Appl Mater Interfaces.* 2013;5(21):11392–11401.
- [114] Ansari MB, Min B-H, Mo Y-H, et al. CO₂ activation and promotional effect in the oxidation of cyclic olefins over mesoporous carbon nitrides. *Green Chem.* 2011;13(6):1416–1421.
- [115] Ren J, Liu X, Zhang L, et al. Thermal oxidative etching method derived graphitic C₃N₄: highly efficient metal-free catalyst in the selective epoxidation of styrene. *RSC Adv.* 2017;7(9):5340–5348.
- [116] Shcherban ND, Diyuk OA, Zazhigalov VA, et al. Graphitic carbon nitride as a sustainable catalyst for selective ethanol oxidation. *ACS Sustain Chem Eng.* 2021;9(14):5128–5137.
- [117] Zheng Z, Zhou X. Metal-free oxidation of α -hydroxy ketones to 1, 2-diketones catalyzed by mesoporous carbon nitride with visible light. *Chin J Chem.* 2012;30(8):1683–1686.
- [118] Wang Y, Li H, Yao J, et al. Synthesis of boron doped polymeric carbon nitride solids and their use as metal-free catalysts for aliphatic C–H bond oxidation. *Chem Sci.* 2011;2(3):446–450.
- [119] Li X-H, Wang X, Antonietti M. Solvent-free and metal-free oxidation of toluene using O₂ and g-C₃N₄ with nanopores: nanostructure boosts the catalytic selectivity. *ACS Catal.* 2012;2(10):2082–2086.
- [120] Wang Y, Zhang J, Wang X, et al. Boron-and fluorine-containing mesoporous carbon nitride polymers: metal-free catalysts for cyclohexane oxidation. *Angew Chem Int Ed.* 2010;49(19):3356–3359.
- [121] Wang R, Zhou C, Huang X, et al. Phenylphenothiazine-based porous organic polymers as visible-light heterogeneous photocatalysts for switchable bromoalkylation and cyclopropanation of unactivated terminal alkenes. *ACS Sustain Chem Eng.* 2022;10(14):4650–4659.
- [122] Geng P, Tang Y, Pan G, et al. AgC₃N₄-based heterogeneous photocatalyst for visible light mediated aerobic benzylic C–H oxygenations. *Green Chem.* 2019;21(22):6116–6122.
- [123] Mazzanti S, Manfredi G, Barker AJ, et al. Carbon nitride thin films as all-in-one technology for photocatalysis. *ACS Catal.* 2021;11(17):11109–11116.
- [124] Song T, Zhou B, Peng GW, et al. Aerobic oxidative coupling of resveratrol and its analogues by visible light using mesoporous graphitic carbon nitride (mpg-C₃N₄) as a bioinspired catalyst. *Chem Eur J.* 2014;20(3):678–682.
- [125] Zhang Y, Song Y, Shen Y, et al. Water molecule-triggered anisotropic deformation of carbon nitride nanoribbons enabling contactless respiratory inspection. *CCS Chemistry.* 2021;3(6):1615–1625.
- [126] Zhang Y, Zhou Z, Shen Y, et al. Reversible assembly of graphitic carbon nitride 3D network for highly selective dyes absorption and regeneration. *ACS Nano.* 2016;10(9):9036–9043.
- [127] Zhou Z, Shen Y, Li Y, et al. Chemical cleavage of layered carbon nitride with enhanced photoluminescent performances and photoconduction. *ACS Nano.* 2015;9(12):12480–12487.
- [128] Zhang J, Zhang M, Lin L, et al. Sol processing of conjugated carbon nitride powders for thin-film fabrication. *Angew Chem.* 2015;127(21):6395–6399.
- [129] Wang X, Maeda K, Thomas A, et al. A metal-free polymeric photocatalyst for hydrogen production from water under visible light. *Nat Mater.* 2009;8(1):76–80.
- [130] Lotsch BV, Schnick W. New light on an old story: formation of melam during thermal condensation of melamine. *Chem Eur J.* 2007;13(17):4956–4968.
- [131] Shcherban N, Mäki-Arvela P, Aho A, et al. Preparation of betulone via betulin oxidation over Ru nanoparticles deposited on graphitic carbon nitride. *Catal Lett.* 2019;149:723–732.
- [132] Veith C-TCVA, Unocic GKKALPLTA. Influence of periodic nitrogen functionality on the selective oxidation of alcohols. *Asian J Chem Sci.* 2012;7:387–393.
- [133] Zou H, Xiao G, Chen K, et al. Noble metal-free V₂O₅/g-C₃N₄ composites for selective oxidation of olefins using hydrogen peroxide as an oxidant. *J Chem Soc.* 2018;47(38):13565–13572.
- [134] Zhang W, Xu C, Kobayashi T, et al. Hydrazone-linked heptazine polymeric carbon nitrides for synergistic visible-light-driven catalysis. *Chem Eur J.* 2020;26(33):7358–7364.
- [135] Verma S, Nasir Baig R, Nadagouda MN, et al. Photocatalytic C–H activation of hydrocarbons over VO@ g-C₃N₄. *ACS Sustain Chem Eng.* 2016;4(4):2333–2336.
- [136] Rafiee M, Wang F, Hruszkewycz DP, et al. N-hydroxyphthalimide-mediated electrochemical iodination of methylarenes and comparison to electron-transfer-initiated C–H functionalization. *J Am Chem Soc.* 2018;140(1):22–25.
- [137] Liu T, Xue F, Chen Z, et al. Bi₄O₅Br₂ catalyzed selective oxidative of C=C double bonds to ketones with molecular oxygen under visible-light irradiation. *J Catal.* 2022;414:76–83.
- [138] Meyer AU, Lau VWH, König B, et al. Photocatalytic oxidation of sulfinates to vinyl sulfones with cyanamide-functionalised carbon nitride. *Eur J Org Chem.* 2017;2017(15):2179–2185.
- [139] Rashidizadeh A, Ghafuri H, Goodarzi N, et al. Tandem oxidative amidation of alcohols catalyzed by copper modified well-ordered mesoporous graphitic carbon nitride. *Solid State Sci.* 2020;109:106427.
- [140] Chevala NT, Kumar L, Veetilvalappil V, et al. Nanoporous and nano thickness film-forming bioactive composition for biomedical applications. *Sci Rep.* 2022;12(1):1–19.
- [141] Mao J, Yin J, Pei J, et al. Single atom alloy: an emerging atomic site material for catalytic applications. *Nano Today.* 2020;34:100917.
- [142] Han H, Ding G, Wu T, et al. Cu and boron doped carbon nitride for highly selective oxidation of

- toluene to benzaldehyde. *Molecules*. 2015;20(7):12686–12697.
- [143] Chen Y, Zhang J, Zhang M, et al. Molecular and textural engineering of conjugated carbon nitride catalysts for selective oxidation of alcohols with visible light. *Chem Sci*. 2013;4(8):3244–3248.
- [144] Krivtsov I, Ilkaeva M, García-lópez EI, et al. Effect of substituents on partial photocatalytic oxidation of aromatic alcohols assisted by polymeric C_3N_4 . *ChemCatChem*. 2019;11(11):2713–2724.
- [145] Zhang W, Bariotaki A, Smonou I, et al. Visible-light-driven photooxidation of alcohols using surface-doped graphitic carbon nitride. *Green Chem*. 2017;19(9):2096–2100.
- [146] García-López EI, Abbasi Z, Di Franco F, et al. Selective oxidation of aromatic alcohols in the presence of C_3N_4 photocatalysts derived from the polycondensation of melamine, cyanuric and barbituric acids. *Res Chem Intermed*. 2021;47(1):131–156.
- [147] Bellardita M, García-López EI, Marci G, et al. Selective photocatalytic oxidation of aromatic alcohols in water by using P-doped $g-C_3N_4$. *Appl Catal B Environ*. 2018;220:222–233.
- [148] Huang W, Ma BC, Lu H, et al. Visible-light-promoted selective oxidation of alcohols using a covalent triazine framework. *ACS Catal*. 2017;7(8):5438–5442.
- [149] Shvalagin V, Kompanets M, Kutsenko O, et al. Photocatalytic Activity of $g-C_3N_4$ in the Partial Oxidation of Benzyl Alcohol Under Visible Light. *Theor Exp Chem*. 2020;56(2):111–116.
- [150] Wu J, Hua W, Yue Y, et al. $g-C_3N_4$ modified Co_3O_4 as efficient catalysts for aerobic oxidation of benzyl alcohol. *React Kinet Mech Catal*. 2019;128(1):109–120.
- [151] Pahari D, Puravankara S. Greener, safer, and sustainable batteries: an insight into aqueous electrolytes for sodium-ion batteries. *ACS Sustain Chem Eng*. 2020;8(29):10613–10625.
- [152] Zhang F, Li J, Wang H, et al. Realizing synergistic effect of electronic modulation and nanostructure engineering over graphitic carbon nitride for highly efficient visible-light H_2 production coupled with benzyl alcohol oxidation. *Appl Catal B Environ*. 2020;269:118772.
- [153] Gu Q, Jiang P, Shen Y, et al. Synthesis of coralloid carbon nitride polymers and photocatalytic selective oxidation of benzyl alcohol. *Nanotechnology*. 2021;32(23):235602.
- [154] Lima MJ, Pastrana-martínez LM, Sampaio MJ, et al. Selective Production of Benzaldehyde Using Metal-Free Reduced Graphene Oxide/Carbon Nitride Hybrid Photocatalysts. *ChemistrySelect*. 2018;3(28):8070–8081.
- [155] Fernandes RA, Sampaio MJ, Faria JL, et al. Aqueous solution photocatalytic synthesis of p-anisaldehyde by using graphite-like carbon nitride photocatalysts obtained via the hard-templating route. *RSC Adv*. 2020;10(33):19431–19442.
- [156] Long B, Ding Z, Wang X. Carbon nitride for the selective oxidation of aromatic alcohols in water under visible light. *ChemSusChem*. 2013;6(11):2074–2078.
- [157] Ding J, Xu W, Wan H, et al. Nitrogen vacancy engineered graphitic C_3N_4 -based polymers for photocatalytic oxidation of aromatic alcohols to aldehydes. *Appl Catal B Environ*. 2018;221:626–634.
- [158] Zhang P, Yue C, Fan M, et al. The selective oxidation of glycerol over metal-free photocatalysts: insights into the solvent effect on catalytic efficiency and product distribution. *Catal Sci Technol*. 2021;11(10):3385–3392.
- [159] Dodangeh F, Rashidi A, Aghaie H, et al. Synthesis of Ni Supported Mesoporous Carbon Nitride Nanocatalyst for Selective Hydrogenation of Acetylene to Ethylene. *J Nanostruc*. 2021;11(3):432–445.
- [160] Montalbetti CA, Falque V. Amide bond formation and peptide coupling. *Tetrahedron*. 2005;61(46):10827–10852.
- [161] Wang Y, Yao J, Li H, et al. Highly selective hydrogenation of phenol and derivatives over a Pd@ carbon nitride catalyst in aqueous media. *J Am Chem Soc*. 2011;133(8):2362–2365.
- [162] Zhao Z, Yang H. Ni-W₂C/mpg- C_3N_4 as a promising catalyst for selective hydrogenation of nitroarenes to corresponding aryl amines in the presence of Lewis acid. *J Mol Catal A Chem*. 2015;398:268–274.
- [163] Gong L-H, Cai Y-Y, Li X-H, et al. Room-temperature transfer hydrogenation and fast separation of unsaturated compounds over heterogeneous catalysts in an aqueous solution of formic acid. *Green Chem*. 2014;16(8):3746–3751.
- [164] Coulson B, Lari L, Isaacs M, et al. Carbon nitride as a ligand: selective hydrogenation of terminal alkenes using $[(\eta^5-C_5Me_5)IrCl(g-C_3N_4-\kappa_2N)]$. *Chem Eur J*. 2020;26(30):6862–6868.
- [165] Gong Y, Zhang P, Xu X, et al. A novel catalyst Pd@ ompg- C_3N_4 for highly chemoselective hydrogenation of quinoline under mild conditions. *J Catal*. 2013;297:272–280.
- [166] Hoydonckx HE, De Vos DE, Chavan SA, et al. Esterification and transesterification of renewable chemicals. *Top Catal*. 2004;27(1):83–96.
- [167] Samanta S, Srivastava R. Graphitic carbon nitride for organic transformation. In: Pandikumar A, Murugan C, Vinoth S, editors. *Nanoscale Graphitic Carbon Nitride*. Netherlands: Elsevier; 2022. p. 393–456.
- [168] Georgakilas V, Perman JA, Tucek J, et al. Broad family of carbon nanoallotropes: classification, chemistry, and applications of fullerenes, carbon dots, nanotubes, graphene, nanodiamonds, and combined superstructures. *Chem Rev*. 2015;115(11):4744–4822.
- [169] Jiang L, Yuan X, Pan Y, et al. Doping of graphitic carbon nitride for photocatalysis: a review. *Appl Catal B*. 2017;217:388–406.
- [170] Cleland WW, Andrews TJ, Gutteridge S, et al. Mechanism of Rubisco: the carbamate as general base. *Chem Rev*. 1998;98(2):549–562.
- [171] Verma S, Baig RN, Nadagouda M, et al. Selective oxidation of alcohols using photoactive VO@g- C_3N_4 . *ACS sustain*. *ACS Sustain Chem Eng*. 2016;4(3):2333–2336.
- [172] Nasirábai R. Oxidative esterification via photocatalytic C–H activation. *Green Chem*. 2016;18(1):251–254.
- [173] Dong F, Wu L, Sun Y, et al. Efficient synthesis of polymeric $g-C_3N_4$ layered materials as novel efficient visible light driven photocatalysts. *J Mater Chem*. 2011;21(39):15171–15174.
- [174] Zhang G, Li G, Lan ZA, et al. Optimizing optical absorption, exciton dissociation, and charge transfer of a polymeric carbon nitride with ultrahigh solar hydrogen production activity. *Angew Chem*. 2017;129(43):13630–13634.

- [175] Pieber B, Malik JA, Cavedon C, et al. Semi-heterogeneous dual nickel/photocatalysis using carbon nitrides: esterification of carboxylic acids with aryl halides. *Angew Chem Int Ed*. 2019;58(28):9575–9580.
- [176] Samanta S, Srivastava R. A novel method to introduce acidic and basic bi-functional sites in graphitic carbon nitride for sustainable catalysis: cycloaddition, esterification, and transesterification reactions. *Sustain. Energy Fuels*. 2017;1(6):1390–1404.
- [177] Xu J, Long K-Z, Chen T, et al. Mesoporous graphitic carbon nitride as a new base catalyst for the efficient synthesis of dimethyl carbonate by transesterification. *Catal. Sci Technol*. 2013;3(12):3192–3199.
- [178] de Medeiros TV, Macina A, Naccache R. Graphitic carbon nitrides: Efficient heterogeneous catalysts for biodiesel production. *Nano Energy*. 2020;78:105306.
- [179] Anand C, Priya SV, Lawrence G, et al. Transesterification of ethylacetate catalysed by metal free mesoporous carbon nitride. *Catal Today*. 2013;204:164–169.
- [180] Jin X, Balasubramanian VV, Selvan ST, et al. Highly ordered mesoporous carbon nitride nanoparticles with high nitrogen content: a metal-free basic catalyst. *Angew Chem Int Ed Engl*. 2009;48(42):7884–7887.
- [181] Xu J, Chen T, Shang J-K, et al. Facile preparation of SBA-15-supported carbon nitride materials for high-performance base catalysis. *Microporous Mesoporous Mater*. 2015;211:105–112.
- [182] Baig R, Verma S, Nadagouda MN, et al. Room temperature synthesis of biodiesel using sulfonated graphitic carbon nitride. *Sci Rep*. 2016;6(1):1–6.
- [183] Salaheldeen M, Mariod AA, Aroua MK, et al. Current state and perspectives on transesterification of triglycerides for biodiesel production. *Catal*. 2021;11(9):1121.
- [184] Peng Y, Qian H, Zhao N, et al. Synthesis of a novel 1D/2D Bi₂O₂CO₃-BiOI heterostructure and its enhanced photocatalytic activity. *Catal*. 2021;11(11):1284.
- [185] Tu W, Zhou Y, Zou Z. Photocatalytic conversion of CO₂ into renewable hydrocarbon fuels: state-of-the-art accomplishment, challenges, and prospects. *Adv Mater*. 2014;26(27):4607–4626.
- [186] Huang Z, Li F, Chen B, et al. Well-dispersed g-C₃N₄ nanophases in mesoporous silica channels and their catalytic activity for carbon dioxide activation and conversion. *Appl Catal B Environ*. 2013;136:269–277.
- [187] Su Q, Sun J, Wang J, et al. Urea-derived graphitic carbon nitride as an efficient heterogeneous catalyst for CO₂ conversion into cyclic carbonates. *Catal Sci Technol*. 2014;4(6):1556–1562.
- [188] Zhu J, Diao T, Wang W, et al. Boron doped graphitic carbon nitride with acid-base duality for cycloaddition of carbon dioxide to epoxide under solvent-free condition. *Appl Catal B Environ*. 2017;219:92–100.
- [189] Xu J, Wu F, Jiang Q, et al. Mesoporous carbon nitride grafted with n-bromobutane: a high-performance heterogeneous catalyst for the solvent-free cycloaddition of CO₂ to propylene carbonate. *Catal Sci Technol*. 2015;5(1):447–454.
- [190] Zhao Z, Sun Y, Dong F. Graphitic carbon nitride based nanocomposites: a review. *Nanoscale*. 2015;7(1):15–37.
- [191] Ren Y, Chen J, Qi C, et al. A new type of Lewis acid–base bifunctional M (salphen)(M= Zn, Cu and Ni) catalysts for CO₂ fixation. *ChemCatChem*. 2015;7(10):1535–1538.
- [192] Zhang Y, Mori T, Ye J, et al. Phosphorus-doped carbon nitride solid: enhanced electrical conductivity and photocurrent generation. *J Am Chem Soc*. 2010;132(18):6294–6295.
- [193] Ma TY, Ran J, Dai S, et al. Phosphorus-doped graphitic carbon nitrides grown in situ on carbon-fiber paper: flexible and reversible oxygen electrodes. *Angew Chem*. 2015;127(15):4729–4733.
- [194] Lan D-H, Wang H-T, Chen L, et al. Phosphorous-modified bulk graphitic carbon nitride: Facile preparation and application as an acid-base bifunctional and efficient catalyst for CO₂ cycloaddition with epoxides. *Carbon*. 2016;100:81–89.
- [195] Huang Z, Li F, Chen B, et al. Cycloaddition of CO₂ and epoxide catalyzed by amino-and hydroxyl-rich graphitic carbon nitride. *Catal. Sci Technol*. 2016;6(9):2942–2948.
- [196] Samanta S, Srivastava R. Catalytic conversion of CO₂ to chemicals and fuels: the collective thermocatalytic/photocatalytic/electrocatalytic approach with graphitic carbon nitride. *Adv Mater*. 2020;1(6):1506–1545.
- [197] Biswas T, Mahalingam V. g-C₃N₄ and tetrabutylammonium bromide catalyzed efficient conversion of epoxide to cyclic carbonate under ambient conditions. *New J Chem*. 2017;41(24):14839–14842.
- [198] Jiang H-L, Xu Q. Catalytic hydrolysis of ammonia borane for chemical hydrogen storage. *Catal Today*. 2011;170(1):56–63.
- [199] Aksoy M, Metin Ö. Pt nanoparticles supported on mesoporous graphitic carbon nitride as catalysts for hydrolytic dehydrogenation of ammonia borane. *ACS Appl Nano Mater*. 2020;3(7):6836–6846.
- [200] Gao M, Yu Y, Yang W, et al. Ni nanoparticles supported on graphitic carbon nitride as visible light catalysts for hydrolytic dehydrogenation of ammonia borane. *Nanoscale*. 2019;11(8):3506–3513.
- [201] Wang W, Lu Z-H, Luo Y, et al. Mesoporous carbon nitride supported Pd and Pd-Ni nanoparticles as highly efficient catalyst for catalytic hydrolysis of NH₃BH₃. *ChemCatChem*. 2018;10(7):1620–1626.
- [202] Wei L, Yang Y, Yu Y-N, et al. Visible-light-enhanced catalytic hydrolysis of ammonia borane using RuP₂ quantum dots supported by graphitic carbon nitride. *Int J Hydrogen Energy*. 2021;46(5):3811–3820.
- [203] Zhang H, Gu X, Song J. Co, Ni-based nanoparticles supported on graphitic carbon nitride nanosheets as catalysts for hydrogen generation from the hydrolysis of ammonia borane under broad-spectrum light irradiation. *Int J Hydrogen Energy*. 2020;45(41):21273–21286.
- [204] Jia H, Chen X, Song X, et al. Graphitic carbon nitride-chitosan composites-anchored palladium nanoparticles as high-performance catalyst for ammonia borane hydrolysis. *Int J Energy Res*. 2019;43(1):535–543.
- [205] Yi H, He D, Tang X, et al. Effects of preparation conditions for active carbon-based catalyst on catalytic hydrolysis of carbon disulfide. *J Fuels*. 2012;97:337–343.
- [206] Zhao S, Kang D, Liu Y, et al. Spontaneous formation of asymmetric oxygen vacancies in transition-metal-doped CeO₂ nanorods with improved activity for

- carbonyl sulfide hydrolysis. *ACS Catal.* **2020**;10(20):11739–11750.
- [207] Cao R, Ning P, Wang X, et al. Low-temperature hydrolysis of carbonyl sulfide in blast furnace gas using Al₂O₃-based catalysts with high oxidation resistance. *J Fuels.* **2022**;310:122295.
- [208] Rhodes C, Riddell SA, West J, et al. The low-temperature hydrolysis of carbonyl sulfide and carbon disulfide: a review. *Catal Today.* **2000**;59(3):443–464.
- [209] Yi H, Li K, Tang X, et al. Simultaneous catalytic hydrolysis of low concentration of carbonyl sulfide and carbon disulfide by impregnated microwave activated carbon at low temperatures. *J Chem Eng.* **2013**;230:220–226.
- [210] Guo F, Li S, Hou Y, et al. Metalated carbon nitrides as base catalysts for efficient catalytic hydrolysis of carbonyl sulfide. *Chem Commun.* **2019**;55(75):11259–11262.
- [211] Thomas B, Williams BP, Young N, et al. Ambient Temperature hydrolysis of carbonyl sulfide using γ -alumina catalysts: effect of calcination temperature and alkali doping. *Catal Lett.* **2003**;86(4):201–205.